Acta Universitatis Agriculturae Sueciae

Doctoral Thesis No. 2025:75
Faculty of Forest Sciences

Quantitative imaging and mechanics of single plant cell adhesion

Léa Bogdziewiez

Quantitative imaging and mechanics of single plant cell adhesion

Léa Bogdziewiez
Faculty of Forest Science
Department of Forest Genetics and Plant Physiology
Umeå

SLU
SWEDISH UNIVERSITY
OF AGRICULTURAL
SCIENCES

DOCTORAL THESIS
Umeå 2025

Acta Universitatis Agriculturae Sueciae
2025:75

Cover: Detaching cells (drawing and pictures, Léa Bogdziewiez)

ISSN 1652-6880
ISBN (print version) 978-91-8124-059-7
ISBN (electronic version) 978-91-8124-105-1
https://doi.org/10.54612/a.5uu0ccufug
 https://orcid.org/0000-0002-2085-1246
Swedish University of Agricultural Sciences, Department of Forest Genetics and Plant Physiology , Umeå, Sweden

Print: CityPrint i Norr AB, Umeå 2025

Quantitative imaging and mechanics of single plant cell adhesion

Abstract

Cell adhesion is fundamental for multicellular integrity. In plants, cell-cell adhesion is mediated by the cell wall, a polysaccharide-protein matrix constantly remodelled to enable growth. Adhesion and communication between cells and between the plasma membrane, and the cell wall are essential to respond to mechanical constraints. Despite its well-established importance, plant adhesion remains poorly understood due to limited tools for measuring the forces involved. This thesis focuses on developing novel methods to study plant cell adhesion at both single-cell and tissue levels, providing new tools to advance our fundamental understanding.

Single cells offer a simplified model for investigating cell-cell adhesion. Protoplasts are widely used in plant research, industry and breeding. However, they are not considered “true” plant cells as they lack a cell wall. Since reliable wall recovery is challenging, we created a fluorescence-microscopy pipeline to quantitatively assess wall recovery post-protoplasting, streamlining culture optimization. Using this workflow, we optimize our protoplast culture conditions to promote cell wall recovery and produce single plant cells. We showed the pipeline reproducibility and versatility in collaborative studies.

Adapting animal-cell methods, we tested adhesion assays and implemented two complementary approaches: microfluidic shear assays and optical-tweezer force measurements. These quantified interactions between the plasma membrane and wall components, revealing new phenomena such as time dependent adhesion strengthening, tether formation, and cycles of detachment/reattachment.

At the tissue level, we established an imaging workflow to detect adhesion defects in Arabidopsis seedling hypocotyls, enabling phenotypic comparisons.

Collectively, these contributions provide a versatile toolbox for probing plant cell adhesion from subcellular to organ levels, laying groundwork for future studies of plant tissue adhesion mechanisms.

Keywords: Cell adhesion, cell wall, protoplasts, cell wall recovery, method development, quantification, imaging-based pipeline.

Kvantitativ avbildning och mekanik för adhesion av enskilda växtceller

Sammanfattning

Celladhesion är grundläggande för multicellulär integritet. I växter medieras cell-celladhesion av cellväggen, en polysackarid-proteinmatris som ständigt omformas för att möjliggöra tillväxt. Adhesion och kommunikation mellan celler och mellan plasmamembranet och cellväggen är avgörande för att kunna reagera på mekaniska påfrestningar. Trots dess välkända betydelse är växtadhesion fortfarande dåligt förstådd på grund av begränsade verktyg för att mäta de krafter som är inblandade. Denna avhandling fokuserar på att utveckla nya metoder för att studera växtcelladhesion på både encells- och vävnadsnivå, vilket ger nya verktyg för att främja vår grundläggande förståelse.

Enskilda celler erbjuder en förenklad modell för att undersöka cell-cell-adhesion. Protoplaster används ofta inom växtforskning, industri och förädling. De anses dock inte vara ”äkta” växtceller eftersom de saknar cellvägg. Eftersom det är svårt att återställa cellväggen på ett tillförlitligt sätt har vi skapat en fluorescensmikroskopipipeline för att kvantitativt bedöma återställningen av cellväggen efter protoplastisering, vilket effektiviserar optimeringen av odlingen. Med hjälp av detta arbetsflöde optimerar vi våra protoplastodlingsförhållanden för att främja återställning av cellväggar och producera enskilda växtceller. Vi har visat pipeline-metodens reproducerbarhet och mångsidighet i samarbetsstudier. Genom att anpassa metoder för djurceller testade vi adhesionsanalyser och implementerade två kompletterande metoder: mikrofluidiska skjuvningsanalyser och optiska pincettkraftsmätningar. Dessa kvantifierade interaktioner mellan plasmamembranet och väggkomponenterna avslöjade nya fenomen såsom tidsberoende adhesionsförstärkning, tetherbildning och cykler av lossning/återfästning. På vävnadsnivå etablerade vi ett bildbehandlingsflöde för att upptäcka adhesionsdefekter i Arabidopsis-plantors hypokotyl, vilket möjliggjorde fenotypiska jämförelser. Sammantaget utgör dessa bidrag en mångsidig verktygslåda för att undersöka växtcellers adhesion från subcellulär till organnivå, vilket lägger grunden för framtida studier av växtvävnaders adhesionsmekanismer.

Nyckelord: Celladhesion, cellvägg, protoplaster, cellväggsåterhämtning, metodutveckling, kvantifiering, bildbaserad pipeline.

Preface

Establishing methods is fundamental to scientific progress. Advancement is often driven by the introduction of novel toolsets that allow researchers to push the limits of what we know. Technique development is often based on interdisciplinarity cooperation, mixing physics, computer sciences, chemistry, engineering and biology. Because this thesis' work is centred on methodological development, a special attention has been given to the Methods section.

“Patience et longueur de temps font plus que force ni que rage”
Le Lion et le Rat, Jean de la Fontaine (1668)

Contents

List of publications 11

List of figures 13

Abbreviations 15

1. Introduction 19
   - 1.1 Cell-cell adhesion 19
     - 1.1.1 Primary CW and middle lamella composition 20
     - 1.1.2 CW adhesion in other organisms 23
   - 1.2 Plasma membrane to extracellular matrix adhesion 24
     - 1.2.1 In other organisms 25
     - 1.2.2 In plants 25
   - 1.3 Physics of cell adhesion 35

2. Research aims and objectives 37

3. Methods 39
   - 3.1 Methods to study cell-cell adhesion (**Paper I**) 39
     - 3.1.1 Tissue scale adhesion 39
     - 3.1.2 Large scale cell-substrate adhesion 41
     - 3.1.3 Single cell adhesion assays 43
   - 3.2 Isolated plant cells and protoplasts 46
     - 3.2.1 Protoplast extraction 48
     - 3.2.2 CW recovery 49
   - 3.3 Light microscopy and image analysis 53
     - 3.3.1 Light microscopy 54
     - 3.3.2 Quantitative imaging 56
   - 3.4 FACS 57
   - 3.5 Microfluidics 58
     - 3.5.1 U-shaped chips 60
     - 3.5.2 Channel chips 60
   - 3.6 AFM 61
   - 3.7 Optical tweezers 62
   - 3.8 Open science 64
     - 3.8.1 3D printing 64

3.8.2 Open-source live imaging 66

4. Results and discussion 71
4.1 The Q-Warg pipeline: a robust and versatile workflow for quantitative analysis of protoplast culture conditions (**Paper II**) 71
4.2 Plasma membrane to cell wall adhesion assays in plants reveals emergent adhesion dynamics behaviours (**paper III**) 75
4.3 RRQuant: High-throughput quantification of seedling's epidermal integrity (paper IV) 78

5. Conclusion and perspectives 83
5.1 Protoplasts and CW regeneration 84
5.2 Image analysis workflows 85
5.3 DIY 86
5.4 Single cell adhesion quantification methods 87

References 89

Popular science summary 107

Populärvetenskaplig sammanfattning 109

Acknowledgements 113

List of publications

This thesis is based on the work contained in the following papers, referred to by Roman numerals in the text:

I. Asal Atakhani, **Léa Bogdziewiez**, Stéphane Verger (2022). Characterising the mechanics of cell-cell adhesion in plants. Quantitative Plant Biology, volume: 3, article number: e2. https://doi.org/10.1017/qpb.2021.16

II. **Léa Bogdziewiez**, Rik Froeling, Patricia Schöppl, Jeanne Juquel, Ioanna Antoniadi, Vladimìr Skalický, Ambroise Mathey, Jacques Fattaccioli, Joris Sprakel, Stéphane Verger (2025). The Q-Warg Pipeline: A Robust and Versatile Workflow for Quantitative Analysis of Protoplast Culture Conditions. Plant Direct, volume 9, (issue 7) e70090. https://doi.org/10.1002/pld3.70090

III. **Léa Bogdziewiez**, Rubén Casanova-Sáez, Stéphane Verger. Plasma membrane to cell wall adhesion assays in plants reveals emergent adhesion dynamics behaviours (manuscript)

IV. **Léa Bogdziewiez**, Lucija Lisica, Abu Imran Baba, Özer Erguvan, Adrien Heymans, Asal Atakhani, Stéphane Verger. RRQuant: High-throughput quantification of seedling's epidermal integrity. (manuscript)

All published papers are published in open access.

The contribution of Léa Bogdziewiez to the papers included in this thesis was as follows:

I. LB participated in literature review and wrote the manuscript together with the other authors.

II. LB designed and conducted experiments, performed the literature review, analysed data and wrote the manuscript together with the other authors.

III. LB designed and conducted experiments, analysed data and wrote the manuscript together with the other authors.

IV. LB analysed data and wrote the manuscript together with the other authors.

List of figures

Figure 1: Plant and cell wall structure.....20

Figure 2: Protoplasts present PM structures resembling to animal filopods.....26

Figure 3: Cell surface receptors 29

Figure 4: Tissue scale adhesion quantification 41

Figure 5: Large scale cell substrate adhesion quantification.....42

Figure 6: Single cell adhesion assay using micromanipulation.....44

Figure 7: OpenFlexure microscope.....68

Abbreviations

AFM	Atomic Force Microscopy
AGPs	Arabinogalactan Proteins
CAMs	Cell-adhesion molecules
CESA	Cellulose synthase A
CrLRKs	*Catharanthus roseus* Receptor Like Kinases
CSCs	Cellulose Synthase Complexes
CW	Cell Wall
DAP	Dual Aspiration Pipettes
DIY	Do-It-Yourself
ECM	Extra Cellular Matrix
ER	Endoplasmic Reticulum
FACS	Fluorescence Activated Cell Sorting
FDM	Fused Deposition Modelling
FER	Feronia
FLA	Fasciclin-like AGPs
FluidFM	Fluidic Force Microscopy
FSC	Forward scattering
GalAs	Galacturonic acids
GIPC	Glycosyl Inositol Phospho Ceramides
GPI	Glycophosphatidyl inositol
HGs	Homogalacturonans
HRGPs	Hydroxyproline-Rich Glycoproteins
LecRKs	Lectin Receptor Kinases
LLG	LRE-like GPI-ap

LRE	Lorelei
LRXs	Leucin-rich repeat extensins
NDR1	Non-race specific disease resistance
PDMS	Poly(dimethylsiloxane)
PERKs	Proline-rich Extensin-like Receptor Kinases
PLL	Poly-lysine
PM	Plasma membrane
Q-Warg	Quantitative cell wall regeneration
RGI, RGII	Rhamnogalagturonans I, II
RALFs	Rapid Alkalinization Factors
REMs	Remorins
RemCA	C-terminal anchor of REMs
RGD	Arg-Gly-Asp
ROS	Reaxtive oxygen species
SLA	Stereolithography
STM	Scanning tunnelling microscopy
SPCs	Single plant cells
SSC	Side scattering
WAKs	Wall-associated kinases

1. Introduction

1.1 Cell-cell adhesion

Plants are multicellular organisms that develop from a single cell, which can give rise to exceptional individuals like *Pando*, a clonal aspen (*Populus tremuloides*). Covering up to 43 ha and weighing roughly 6 000 t, this organism appears as multiple stems, yet all of them are connected through a common root system (Kemperman and Barnes, 1976). This striking example highlights the importance of cell adhesion that binds cells together, enabling the existence of such massive organisms.

However, cells are not merely passively stuck together; dynamic control and maintenance of adhesion are key to plant growth and development. Both tightening and loosening of adhesion are required to preserve tissue integrity and cohesion (Baba and Verger, 2024). While strong cell-cell adhesion is essential, certain physiological processes, such as intrusive cell growth for fibre elongation in wood (Gorshkova *et al.*, 2012; Marsollier and Ingram, 2018), require localized wall loosening. Thus, the cell wall must combine mechanical strength with elasticity, a regulation that can occur within seconds (Cosgrove, 2024). The leaf structure also reflects the diversity of cell-cell adhesion tightening in a same tissue (Figure 1). Large intercellular air spaces are crucial for gas exchange in photosynthetic cells (Whitewoods, 2021), whereas the epidermis must retain strong adhesion to prevent dehydration, block pathogen entry, and provide mechanical support (Galletti *et al.*, 2016).

Because plants are sessile, they must resist constraints imposed by their environment, such as wind or soil compaction. Internally, plant cells maintain a high turgor pressure that is balanced by the cortical tension generated by their surrounding cell wall (CW). When cell-cell adhesion is defective, the tension tends to pull cells apart. Hence, cell-cell adhesion is essential for preserving the organism's integrity. The plant CW is also the stiffest, stress-bearing component of plant tissues, making it crucial for maintaining mechanical integrity.

Consequently, the CW is a hotspot for sensing and transmitting mechanical signals (Fruleux, Verger and Boudaoud, 2019).

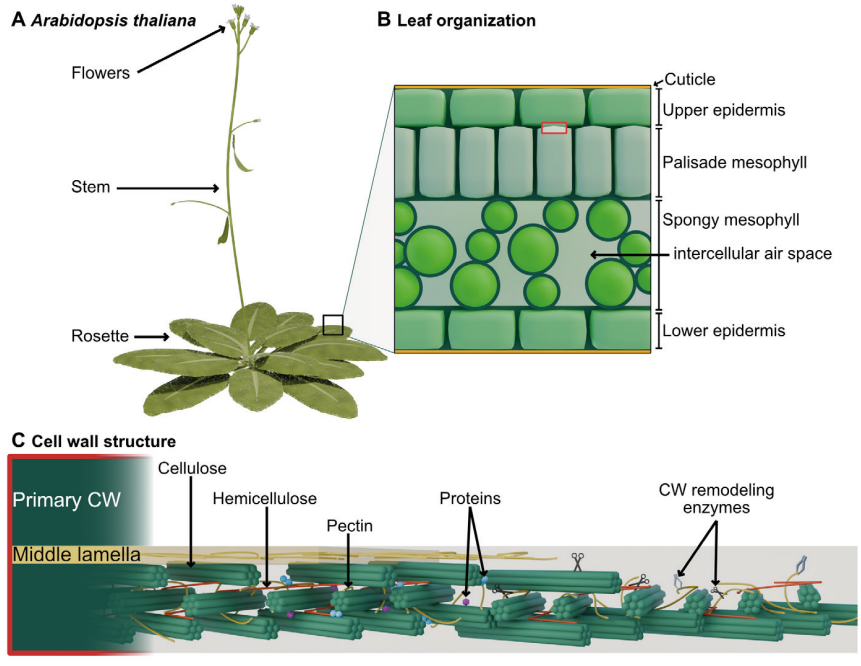

Figure 1: Plant and cell wall structure

(A) *Arabidopsis thaliana* adult plant. **(B)** Transversal view of leaf. Several cell types are associated to form the leaf tissue. Epidermal cells are tightly attached together and covered by a cuticle, while cell-cell adhesion is looser in between photosynthetic mesophyll cells. **(C)** Cell wall overview. The CW is mainly composed by polysaccharides, such as cellulose, hemicellulose and pectins. It also contains structural and signalling proteins, and CW remodelling enzymes. Primary CWs of two adjacent cells are connected by the middle lamella rich in pectins.

1.1.1 Primary CW and middle lamella composition

Plant cells are adhering to each other via their cell wall. Adhesion between cells is established during cell division by the two daughter cells secreting cellulose, hemicelluloses and pectins to form their own CW (Anderson and Kieber, 2020). The polysaccharides cross-linking creates a continuous network that ensures cell-cell adhesion. The central layer of the cell wall that lies between two adjacent cells, namely the middle lamella, is rich in pectins and is considered the

main determinant of cell-cell adhesion in the early stages of growth and development (Zamil and Geitmann, 2017). The exact composition of the cell wall can differ widely, depending on the tissue, the specific cell type, and even the face of the cell. The primary wall is dynamic and is remodelled during plant growth. By contrast, the secondary CW is inextensible. Built in between the primary wall and the PM, it is highly present in wood tissues and plays a role as structural support (Cosgrove, 2024).

Polysaccharides

The structural backbone of the primary cell wall is composed by different polysaccharides, providing both rigidity and flexibility to support growth and protect the plant cell. Cellulose serves as the main load-bearing scaffold to build the CW. It consists of long chains of β-1,4-linked D-glucose units assembled by cellulose synthase A (CESA) enzymes. CESAs polymerize glucose into parallel β-1,4-glucan strands which bundle together to form microfibrils. These proteins operate as part of larger, multimeric cellulose synthase complexes (CSCs). CSCs are guided by cortical microtubules and travel along the plasma membrane as they synthesize cellulose. The resulting microfibrils are highly ordered, granting them high mechanical strength. Hemicelluloses increase the loadbearing capacity of the CW by associating non-covalently with cellulose and pectins. Xyloglucan represents the most abundant hemicellulose in the primary CW.

Pectins are the main contributor to cell adhesion via the middle lamella and represent about 50% of the constituents of the primary CW. Pectins also have an important role in cell expansion mechanisms and participate in plant development and defence. They form a group of various polysaccharides: homogalacturonans (HGs), rhamnogalacturonans I and II (RGI, RGII; (Anderson, 2019)). HGs are linear chains of galacturonic acids (GalAs) synthesized in a highly methyl esterified form. They can be de-esterified after secretion to the CW by pectin methylesterases (Hocq, Pelloux and Lefebvre, 2017). The de-esterification process leaves negatively charged residues on GalAs allowing the formation of calcium mediated bridges with other

de-esterified HGs forming an egg-box conformation. This can in principle binds effectively HG chains coming from adjacent cells (Liners *et al.*, 1989; Jarvis and Apperley, 1995; Huxham *et al.*, 1999; Willats *et al.*, 2001). Similarly, RGII monomers dimerize through borate ester bonds (O'Neill *et al.*, 2001). This boron-mediated dimerization creates a robust network that reinforces the pectic matrix and contributes to cell-cell adhesion (O'Neill *et al.*, 1996; Begum and Fry, 2022). Cross-linking mechanisms importance has been highlighted via cell-cell adhesion deficient mutant characterization (Bonin *et al.*, 1997; Pabst *et al.*, 2013; Baba *et al.*, 2024). In Arabidopsis, mutants with modification of genes involved in HG synthesis, remodelling or degradation show adhesion defects, either through loss of adhesion or incapacity to separate (source papers are cited in (Atakhani, Bogdziewiez and Verger, 2022; Baba and Verger, 2024)).

Callose is another important constituent of the plant cell wall. It consists of β-1,3-glucan chains synthesized by callose synthases embedded in the plasma membrane. During cytokinesis, callose forms an early, transient layer of the primary wall that separates the newly formed daughter cells. It also accumulates around plasmodesmata and is rapidly deposited in response to various stresses. Because callose has a high turnover, it is considered one of the most dynamic wall polymers (Ellinger and Voigt, 2014; Anderson and Kieber, 2020).

Proteins / enzymes

The primary CW contains various proteins that either participate in the structural framework of the CW, in the signalling or act as remodelling enzymes. Since the CW is a dynamic structure, it must be reshaped over time to support plant growth and developmental events like cell abscission for instance (Baba and Verger, 2024). CW remodelling and degrading enzymes like pectin methyl esterases (PMEs), polygalacturonases (PGs) and pectate lyases (PLs) act on the pectins. For instance, HGs de-methyl-esterification by PMEs enables their crosslinking by calcium leading to the rigidification of the CW (Anderson and Kieber, 2020) while PLs and PGs degrade pectins. Beyond pectin modifications, endoglucanases hydrolyse ß-1,4-glucan

bonds in cellulose and hemicelluloses, while α-expansins act on hydrogen bonds (Cosgrove, 2024). Hemicelluloses can also be remodelled by xyloglucan endotransglycosylases/hydrolases (XTHs) (Zhang *et al.*, 2025).

Other CW proteins interact with transmembrane receptor-like-kinases (RLKs) or receptor-like-proteins (RLPs), triggering intracellular signalling cascades. For example, Rapid Alkalinization Factors (RALFs) bind RLKs to regulate plant developmental processes as well as plant immune defence (Pratyusha and Sarada, 2025). The superfamily of hydroxyproline-rich glycoproteins (HGRPs) is abundant in the CW and includes extensins and arabinogalactan proteins. Leucin-rich repeat extensins (LRXs) are tightly associated with the CW and participate in the CW sensing (Herger *et al.*, 2019). LRXs are, for example, involved in cell expansion (Dünser *et al.*, 2019). LRXs and RALFs can cooperate to interact with *Catharanthus roseus* Receptor Like Kinases (CrRLKs) such as FERONIA to monitor CW integrity sensing.

Arabinogalactan proteins (AGPs) form a superfamily of glycoproteins present in the CW of plants and algae. Each AGP possesses a N-terminal signal sequence to be directed to the endoplasmic reticulum for post-translational glycosylation before secretion to the CW. In *Arabidopsis*, some AGPs can be covalently bound to RG-I maintaining the wall structure through pectin crosslinking (Tan *et al.*, 2013; Cosgrove, 2024). Beyond their structural role, AGPs are involved in signaling by either changing CW properties or acting as co-receptor for RLPs and/or RLKs (Ma and Johnson, 2023).

1.1.2 CW adhesion in other organisms

The preceding CW description focuses mainly on flowering plants (angiosperms), because they are studied extensively and especially using *Arabidopsis thaliana* as a model organism. Nonetheless, the composition and ratio of polysaccharides differ in other clades. Further away from land plants, algae, fungi and bacteria can also possess a CW. Despite the variability in composition existing between

organisms, CWs share common features: they are dynamic carbohydrate-based structures playing an essential role in organism morphogenesis, cell viability and immune defence (Fuertes-Rabanal *et al.*, 2025). From prokaryotes to multicellular eukaryotes, the coating of choice contains glycans associated to various extents with proteins. The basic organisation of CWs is also conserved: a partially crystalline structure, namely cellulose, chitin and peptidoglycans, serves as scaffold for the rest of CW constituents (Fuertes-Rabanal *et al.*, 2025).

As reviewed briefly in paper I, plants might share cell-cell adhesion mechanisms with microorganisms and algae. Typically, bacteria adhesion is established in two stages. First, a passive adhesion phase driven by Van-der-Waals forces (hydrophobic and electrostatic interactions and hydrogen bonds). Then, an active adhesion stage, during which, a glue-like substance is secreted by cells to enhance their adherence, which resemble to CW deposition at the cell membrane in plants (Jones, 1994; Razatos *et al.*, 1998; Lebret, Thabard and Hellio, 2009).

Understanding how microorganisms can attach to a substrate is essential for health-related research and applications. Consequently, methods and techniques have been developed to investigate and measure the strength of interaction between bacteria or fungi and their substrate (Ashkin and Dziedzic, 1987; Razatos *et al.*, 1998; Alam, Kumar and Varadarajan, 2019). Insights from these studies can guide future development of tools to quantify plant cell adhesion.

1.2 Plasma membrane to extracellular matrix adhesion

While cell-cell adhesion is essential for holding plant cells together, cell attachment to and communication with its own cell wall is also fundamental. This interaction shapes cell morphology as well as drives proliferation and differentiation through mechano-sensing and chemical feedback, helping the plant respond to both biotic and abiotic stresses. In many ways, plant cells use biological process that are similar to those of animal cells, a parallel discussed in detail in this chapter.

1.2.1 In other organisms

In animals, cells are in contact with each other directly through their plasma membrane (PM) and do not have a CW. They can also interact with the extra-cellular matrix (ECM). This adhesion is mediated by a group of proteins called Cell-Adhesion Molecules (CAMs) (Juliano, 2002; Weber, Bjerke and DeSimone, 2011). Two major classes of CAMs dominate: Cadherins, which are mostly involved in cell-cell contact, and Integrins, which mediate cell-substrate adhesion. Both families serve as a link between the extracellular space and the cytoskeleton through the PM (Weber, Bjerke and DeSimone, 2011).

Integrins are one of the most studied protein family, they are involved in a wide array of processes such as cell migration, proliferation and immune defence (Langhans *et al.*, 2017). Eighteen integrin subunits have been described with 2 different forms: α and β assembling into 24 known heterodimers (Hynes, 2002). Each functional integrin consists of a short intracellular tail that transduces signals and a long extracellular domain that binds ECM components, thereby bridging the matrix to the cytoskeleton (Langhans *et al.*, 2017). More specifically, integrins can bind proteins or peptides containing the so-called RGD motif: a tripeptide containing arginine, glycine and aspartate (Kanchanawong and Calderwood, 2023). Through this bridge, animal cells are able to sense chemical or mechanical changes in the ECM and trigger signalling cascades. Specific regions of the PM regroup specialized adhesion molecules forming focal adhesion points, which act as mechanosensors. Mechanical cues are captured at these sites and transmitted to the intracellular space to activate cytoskeletal remodelling and/or downstream signalling responses (Katsumi *et al.*, 2004).

1.2.2 In plants

Similarly to animal cells, a physical bond can be observed between the protoplast and its surrounding CW. It becomes especially apparent during osmotic changes and especially plasmolysis. When a cell is placed in a hyper-osmotic medium, the protoplast releases water and shrinks inside its rigid wall. Even as it contracts, the protoplast remains anchored to the wall by thin membrane tethers called Hechtian strands

(Hecht 1912; Domozych *et al.*, 2003; Yoneda *et al.*, 2020; Arico *et al.*, 2023). Interestingly, protoplasts extracted from a tissue show structures resembling to animal filopodia (Figure 2; (Dickmann *et al.*, 2024)). When cultured into microwells protoplasts form membrane tethers that attach to the well´s walls, creating a small "foot" at the adhesion region (Dickmann *et al.*, 2024). This is reminiscent of animal cells' focal adhesion points and filopods used during cell migration. The study by (Dickmann *et al.*, 2024) highlights unexpected similarities between animal and plant cells in the organization and communication of PM–ECM attachments. Yet, no true integrins nor cadherins have been found in plant cells. Nevertheless, various molecules involved in PM to CW interaction present an animal integrin-analogous structure; present an RGD-like motif or ability to bind to it; share similar function, and mode of activation, by forming heterodimers. Thus, these plant proteins are often referred to as integrin-like proteins. Associated to these molecules, other receptor-like proteins are thought to participate in PM-CW interaction and will be presented in this chapter.

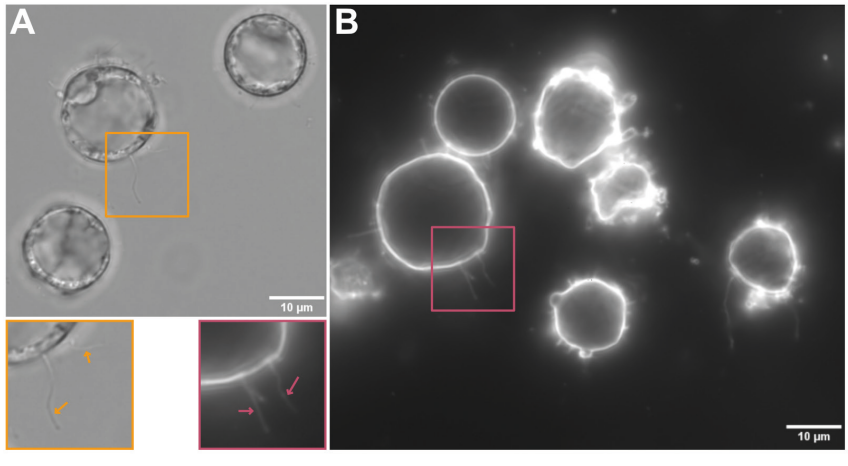

Figure 2: Protoplasts present PM structures resembling to animal filopods

(A) Brightfield image of protoplast suspension **(B)** Protoplast suspension imaged with PM fluorescence staining (FM4-64). Close up images show filopods (arrows).

Hechtian strands

Plasmolysis is a standard technique in plant biology for confirming plasma-membrane protein localisation and studying PM-CW attachment sites. When cells are placed in a hyper-osmotic solution, the protoplast pulls away from the rigid wall but remains tethered by thin, tense structures called Hechtian strands**,** which closely resemble the animal cells filopodia (Hecht, 1912; Arico *et al.*, 2023). These structures have been observed in various photosynthetic organisms ranging from vascular plants (Yoneda *et al.*, 2020), to moss (Harant and Lang, 2020) or unicellular algae (Domozych *et al.*, 2003) as well as in other walled organisms like oomycetes and ascomycete (Bachewich and Heath, 1997).

In the review by (Arico *et al.*, 2023), the authors propose the term Hechtian structure instead of Hechtian strands to denote a more complex organisation. The Hechtian structure regroups:

- the Hechtian attachment site: cortical regions of connection between the PM and the CW (Pont-Lezica, McNally and Pickard, 1993).
- the Hechtian reticulum: branched network of membranes under the CW observed in plasmolyzed cells (Hecht, 1912).
- the Hechtian strand: thin PM tube going through the space between the PM and the CW, also called the periplasm. It joins the protoplast to its CW via the Hechtian reticulum and the Hechtian attachment sites. Some Hechtian strands are plasmodesmata-related and thus maintain a continuity with the neighbouring cells during plasmolysis (Hecht, 1912).

Some studies showed the presence of cytoplasm in Hechtian structures (Drake, Carr and Anderson, 1978; Attree and Sheffield, 1985; Chang *et al.*, 1996) as well as endoplasmic reticulum in Hechtian reticulum and some Hechtian strands (Oparka, 1994; Lang-Pauluzzi and Gunning, 2000; Cheng *et al.*, 2017). The involvement of the cytoskeleton is difficult to study because of the microtubule depolymerisation during the plasmolysis as well as the reorganisation of actin filaments to fit the new protoplast shape. Moreover, the use of anti-cytoskeletal drugs like oryzalin and latrunculin B do not seem to affect the formation and shape of Hechtian strands (Lang-Pauluzzi and

Gunning, 2000). Yet, a later study showed the presence of both actin filaments and microtubules associated with endoplasmic reticulum in the Hechtian strands of tobacco and Arabidopsis cells (Cheng *et al.*, 2017). It is thought that Hechtian strands are reincorporated into the PM during de-plasmolysis (Lang-Pauluzzi and Gunning, 2000).

Hechtian structure's roles are not yet fully defined. They may be involved in cell polarity and response to cold stress (Pont-Lezica, McNally and Pickard, 1993; Domozych *et al.*, 2003). Their main role is probably PM-CW signalling. Some studies highlight the role of Hechtian structures in sensing cell-wall integrity. During plasmolysis, new wall material is deposited precisely at the sites where Hechtian strands remain attached to the original wall. If those structures are disrupted, CW synthesis occurs uniformly over the entire protoplast surface (Schindler, Meiners and Cheresh, 1989; Yoneda *et al.*, 2020). Those structures might as well be participating in pathogen defence. Interestingly, impaired Hechtian strands with RGD-peptides in Pea or Cowpea cells lead to decreased ROS production and callose deposition and an increased penetration efficiency by fungi (Mellersh *et al.*, 2002). This suggests the importance of CW sensing molecules in Hechtian structures leading to defence responses.

PM/CW interaction molecules

Plasmolysis sheds light on Hechtian structures, simultaneously revealing hotspots of PM-CW adhesion. This experimental system is also used to track protein mobility at the PM and to identify which proteins are anchored to the cell wall. The transmembrane proteins that may mediate PM-CW adhesion can be sorted in two groups based on their structure and function: integrin-like proteins and receptor like kinases (RLKs), even though, certain integrin-like proteins are also classified as RLKs (Figure 3).

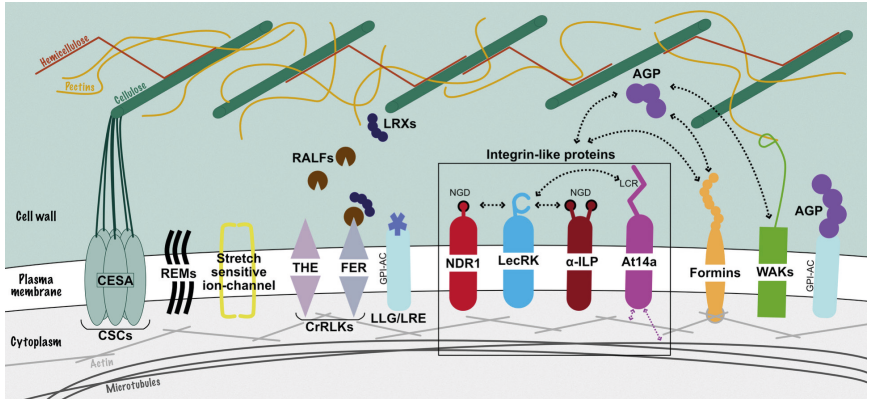

Figure 3: Cell surface receptors

Cellulose synthases A (CESAs) are organised in cellulose synthase complexes (CSCs) and polymerize glucose into cellulose microfibrils. PM nanodomains are organised by remorins (REMs) participating in the transmission of CW strain to the PM leading to the opening of stretch sensitive ion-channels. Catharanthus roseus Receptor Like Kinases (CrRLKs), like THESEUS (THE) and FERONIA (FER), are interacting with rapid alkanisation factors (RALFs) in association with leucin-rich repeat extensins (LRXs) and/or glycosylphosphatidylinositol (GPI) anchored proteins from the LORELEI (LRE)-like GPI-ap/LRE family (LLG/LRE) and pectins. CrRLKs trigger intracellular cascades in response to CW signalling. Integrin-like proteins regroup the putative adhesion molecules non-race specific disease resistance gene (NDR1) and α-Integrin like protein (α-ILP) and At14a. NDR1 and α-ILP are thought to interact with lectin receptor kinases (LecRKs) via their RGD-like motif (NGD). At14a contains an extracellular low complexity region (LCR) that may interact with other cell surface receptors and has an impact on cytoskeleton organization. Formins are anchors of the cytoskeleton to the CW and can initiate actin nucleation. Wall associated kinases (WAKs) bind to the CW and transmit signalling internally via their kinase. Arabinogalactan proteins (AGPs) can be exclusively in the CW or anchored to the PM via a GPI-ac. They have both structural, by linking pectins, and a signalling role by interacting with cell surface receptors.

Integrin-like

Although no direct homologues of animal integrins have been discovered in plants, several PM proteins play analogous structural and functional roles (Knepper, Savory and Day, 2011a; Lü *et al.*, 2012; Langhans *et al.*, 2017). Those proteins present an intracellular domain capable of triggering a signalling cascade, a transmembrane domain and an extracellular domain binding to CW polysaccharides or, most often, to other transmembrane or CW proteins (Gouget *et al.*, 2006; Langhans *et al.*, 2017). This organisation in heterodimers is another

similarity with animal integrins which become active when 2 different subunits associate. The structural similarity is often based on the presence of an RGD-like motif or peptide: NGD (Knepper, Savory and Day, 2011a, 2011b). During plasmolysis, addition of exogenous RGD peptides in the medium could disrupt the bond between certain transmembrane proteins and their partner (Canut *et al.*, 1998; García-Gómez *et al.*, 2000; Senchou *et al.*, 2004).

Three putative PM-CW adhesion protein are described as integrin-like proteins: At14a, non-race specific disease resistance gene (NDR1) and α-Integrin like protein (α-ILP). At14a is described as the most prominent integrin-like protein. It is a regulator of CW and cytoskeleton organization and thus, is involved in cell shape (Lü *et al.*, 2012; Wang *et al.*, 2015). Even if it lacks an extracellular RGD motif, it contains a low complexity region (LCR), which often serves as flexible interaction platforms. At14a could then bind with different transmembrane or CW proteins without the integrin binding motif (Coletta *et al.*, 2010). NDR1 shares specific protein motifs that suggest a functional homology with animal integrins (Langhans *et al.*, 2017). It contains an NGD motif, RGD-like motif of integrins (Knepper, Savory and Day, 2011a). NDR1 is also involved in plant immunity via pathogen recognition and defence signalling (Coppinger *et al.*, 2004; Knepper, Savory and Day, 2011b). The third putative PM-CW protein is α-ILP, which presents 2 NGD sites in its extracellular domain. The intracellular tail of α-ILP shows sequence homology with mammalian proteins that are linked to the actin cytoskeleton (Langhans *et al.*, 2017). Altogether, both extracellular features and potential ability to bind the cytoskeleton of these three proteins make them excellent candidate for forming heterodimeric integrin-like adhesion complexes.

In addition, (Gouget *et al.*, 2006) identified the lectin-receptor kinase LecRK-I.9 as capable of binding RGD motifs, highlighting its role as a structural analogue of integrin-like proteins. LecRK receptors may have both a role in adhesion and signalling (Senchou *et al.*, 2004; Gouget *et al.*, 2006; Bouwmeester *et al.*, 2014; Langhans *et al.*, 2017). Further evidence of the importance of LecRKs in PM-CW interactions comes from the observation of increased number of Hechtian strands

in LecRKI.9 overexpression lines during plasmolysis (Arico *et al.*, 2023). A recent study investigating the role of LecRK-I.9 showed the importance of its lectin domain as anchor to the CW and more specifically building stiff hotspots linking the PM to the CW (Arico *et al.*, 2025). LecRKs could be potential partners to the putative PM-CW adhesion proteins via their RGD-like motifs, acting as anchors for these proteins to the cell wall.

Other wall-binding cell surface receptors and proteins

Receptor like kinases (RLKs) regroup transmembrane proteins containing an extracellular signal perception domain and an intracellular kinase (Wolf, 2017; Dievart *et al.*, 2020). Major RLKs subfamilies involved in CW signalling are *Catharanthus roseus* Receptor Like Kinases (CrRLKs), Wall associated kinases (WAKs), Proline-rich Extensin-like Receptor Kinases (PERKs) and leucin-rich-repeats RLKs (LRR-RLKs) (Dievart *et al.*, 2020).

Among this large family, FERONIA (FER) is a key CrRLK member for CW sensing (Cheung and Wu, 2025). It is a malectin-domain receptor kinase that is part of the CrLRK1-like family. FER associates with a GPI-anchored protein (GPI-ap) and intracellular signalling proteins forming a core FER signalling module (Cheung and Wu, 2025). FER interacting GPI-ap are thought to be members of the LORELEI (LRE)-like GPI-ap/LRE family (LLG/LRE) (Dünser *et al.*, 2019; Cheung and Wu, 2025). Rapid alkanisation factor 1 (RALF1) is an extracellular soluble protein that can bind the complex taking part in the pectin dynamics (Haruta *et al.*, 2014; Murphy and De Smet, 2014; Dünser *et al.*, 2019). FER is also able to interact directly with de-esterified pectins as well as with oligogalacturonans derived from pectin fragmentation (Cheung and Wu, 2025).

Another member of the CrLRK family is THESEUS which also interacts with a RALF peptide (Gonneau *et al.*, 2018). It is involved in cellulose alteration sensing and triggers growth inhibition in case of alterations (Hématy *et al.*, 2007; Engelsdorf *et al.*, 2018).

WAKs are a distinct family among RLKs, whose extracellular domains vary among isoforms but consistently bind pectins in the cell wall (Kohorn, 2001, 2016). Their structure, a variable extracellular region coupled to a cytoplasmic kinase, suggests that they not only have a structural role but also a signalling role at the interface of the CW, the PM and intracellular space (Kohorn, 2001).

Although, no evidence proves their implication in PM-CW adhesion, PERKs and LRR-RLKs are interesting candidates. PERKs are sharing sequence similarities with WAKs (Silva and Goring, 2002) and are thought to possess a similar function, but their exact implication is unknown (Nakhamchik *et al.*, 2004; Kesawat *et al.*, 2023). LRR-RLKs regroup many kinases, which function is uncharacterized. The LRR units serve as receptor generally for peptide or hormonal ligand (Dievart *et al.*, 2020). Both subfamilies may at least be involved in CW sensing and/or biotic and abiotic stress.

Most of the potential PM-CW adhesion proteins possess both intracellular and extracellular domains, yet they rarely function on their own. Like animal integrins, which act as heterodimers, many plant adhesion proteins require a partner to form an operational complex.

Arabinogalactan proteins (AGPs) are key players in PM to CW adhesion, although no known AGPs have a RGD motif (Langhans *et al.*, 2017), and are thought to associate with an integrin-like protein to form together a functional complex creating a bridge between the CW and the cytoskeleton. AGPs can bind to pectins and arabinoxylans and may also interact with transmembrane proteins involved in CW-PM adhesion such as WAKs, Formins or LecRK (Kohorn, 2001; Baluska *et al.*, 2003; Gouget *et al.*, 2006). A subset of AGPs can be directly linked to the membrane through a GPI-anchor serving as direct link between the PM and the CW (Showalter and Basu, 2016). AGPs are involved in multiple signalling mechanisms that are summed up in comprehensive reviews (Showalter, 2001; Langhans *et al.*, 2017; Ma and Johnson, 2023).

A potential partner to AGPs is AtFH1, a transmembrane protein from the Formin family anchored to the CW via its long extracellular

N-terminal domain. The cytoplasmic domain of AtFH1 binds the cortical actin cytoskeleton and initiates new actin filament formation (Showalter, 2001; Martinière *et al.*, 2012; Tolmie *et al.*, 2017; Ma and Johnson, 2023). AtFH1 could participate in signal transmission from the CW to remodel actin cytoskeleton in association with AGPs (Martinière *et al.*, 2011).

Additionally, the PM is organized into nanodomains, which can be specifically enriched in certain molecules (McKenna *et al.*, 2019; Hdedeh *et al.*, 2025) like a class of lipids called Glycosyl Inositol Phospho Ceramides (GIPC) forming PM-CW anchors by interacting with pectin RGII in presence of boron (Voxeur and Fry, 2014). This binding creates a direct molecular link between the PM and CW pectins. Remorins (REMs) are a protein family known to organize into nanodomains in plants (Gouguet *et al.*, 2021). *In-vitro* studies suggest that REMs can bind both different constituents of pectins and the cortical cytoskeleton. They are organizing PM nanodomains and could play the role of scaffold proteins (Gronnier *et al.*, 2017). Recently, (Rui *et al.*, 2025) presented evidence that different nanodomains are important for PM-CW attachments during hyperosmotic stress: Cellulose synthases complexes (CSCs) and REMs. Both nanodomains are antagonists as REMs recruit inhibitors of CSCs exocytosis. CSCs might as well directly be involved in PM-CW adhesion as they are physically linked to cellulose microfibrils during their synthesis (Somerville, 2006).

Mechano-sensing

Plants are constantly submitted to various extra and intra-organism physical stimuli and need to adjust to these mechanical forces like the wind or cell compression for example. The high turgor pressure that inflates the cell puts the CW under tension, driving expansion in growing tissues (Sapala *et al.*, 2018). Because the CW is very dynamic and in constant remodelling in developing tissues, any modification must be sensed and transmitted inside the cells. Among the forementioned PM-CW adhesion proteins, some of them are thought to act as mechanosensors. Hydroxyproline-Rich Glycoproteins (HRGPs), namely AGPs and extensins, are linked covalently via their

glucan groups to other CW constituents. They might be involved in mechano-sensing via changes in their conformation or affinity for CW components (Tan *et al.*, 2013; Showalter and Basu, 2016). Additionally, the affinity of CW remodelling enzymes might depend on mechanical properties of the CW and thus on its deformation (Fruleux, Verger and Boudaoud, 2019). Rapid Alkalinization Factors (RALFs) interact with CW molecules with an affinity which varies depending on stress or strain applied onto them (Haruta *et al.*, 2014; Murphy and De Smet, 2014).

PM stretch-sensitive ion channels are also main contributors of mechano-sensing. They are formed by protein complexes which are closed when the PM is under low tension. When the tension increases the pore is opened by protein rearrangement leading to entry of ions in the cytosol. Yet, the PM being considerably softer than the CW and thus bearing only a fraction of the mechanical load brings the question of the effective participation of these channels to mechanosensing. The prevailing view is that mechanical stress generated in the CW is transmitted to the PM through trans-membrane adhesion proteins such as WAKs, LecRKs, CrRLKs and PERKs (Wolf, 2017). CW strain could also be transmitted via GIPC and remorins nanodomains. By anchoring the PM to the CW, these proteins transmit wall mechanical deformation to the membrane, thereby increasing local tension and opening the stretch-activated channels (Wolf, 2017).

Mechano-sensing could also involve endocytosis and exocytosis as they are dependent on the membrane tension (Gauthier, Masters and Sheetz, 2012; Fruleux, Verger and Boudaoud, 2019). If the membrane is too tensed, it is maintained flat preventing the formation of vesicles by membrane bending. Additionally, Hechtian structures could also be an important player in the transduction of mechanical signals. During plasmolysis, the Hechtian strands are maintained while the protoplast retracts. The high attachment of the PM to the CW at the Hechtian attachment sites might allow the transmission of mechanical signals from the CW to the cytoplasm via ion channels or cytoskeleton (Arico *et al.*, 2023).

In conclusion, PM-CW adhesion is a though nut to crack. Many actors are involved either directly, forming a physical link between the cytoskeleton and CW polysaccharides for example, or indirectly, like CSCs which function consequently maintains a bond between PM and CW. Nevertheless, a lot of work is still needed to decipher the adhesion mechanisms and new methods are required to study the various molecular players and understand their specific role.

1.3 Physics of cell adhesion

Adhesion between cells or between the PM and the CW is constantly challenged by mechanical forces both intrinsic, generated by plant growth, or extrinsic, imposed by environmental conditions. To unravel the underlying adhesion mechanisms and identify the molecular players involved, we must measure these forces and quantitatively characterize the interactions.

The physics of adhesion is described by different parameters. It is frequent to use the term adhesion "strength", but adhesion "work" and "energy" should also be considered (paper I – Figure 1). To explain the physics of adhesion, certain physical parameters must be described beforehand (Fruleux, Verger and Boudaoud, 2019):

- The force expressed in newtons (N) is represented by a vector and quantifies the capacity to give motion in absence of opposite force. However, if there is an opposite force, it will describe the capacity to deform the object.
- The stress is the equivalent of the force but integrating the area of the deformed object and is expressed in N/m^2 or pascals (Pa).
- The strain is the deformation of the object due to stress. It does not have physical units as it gives a relative change in size.

Although the importance of cell adhesion is widely recognized, the literature contains very little information on cell adhesion mechanics in plants. This knowledge gap largely originates from the lack of established methods for quantifying the adhesive strength between cells, a limitation that delays the identification of the actual molecular

players and the ability to decipher their specific roles in cell adhesion. Nevertheless, cell adhesion mechanisms are well studied using other model organisms such as bacteria, fungi or animal cells. Common experiments to measure adhesion between cells infer the separation of two cells or a tissue using pulling forces. This gives a value of de-adhesion from which adhesion mechanics can then be indirectly computed. The amount of force applied, and the cell deformation can be measured leading to the generation of a stress-strain force curve. From this curve, mechanical parameters can be calculated:

- De-adhesion strength is the maximal stress value applied to separate the cells.
- De-adhesion work is the energy transferred to the sample during stretching and can be computed via the area under the stress-strain curve.

However, the adhesion energy cannot be measured accurately with a simple pulling experiment (Maître and Heisenberg, 2011; Sackmann and Smith, 2014; Winklbauer, 2015). It reflects the sum of all molecular bonds that form between adjacent cells. When the sample is stretched, part of the input energy is stored in elastic deformation, which is reversible, while another portion is lost to plastic deformation, which is permanent. Because the measured force includes both the reversible elastic response and the irreversible plastic dissipation, it is difficult to isolate the true adhesion energy from the overall stress-dissipation signal.

Plant cell adhesion is a cornerstone of tissue integrity, yet its mechanical characterization remains limited by the absence of reliable quantitative assays. By establishing robust, quantitative tools researchers will be able to identify the key molecular players mediating adhesion, clarify how mechanical cues are translated into biochemical signals, and ultimately integrate cell-adhesion mechanics into our broader understanding of plant development as well as plant stress adaptation.

2. Research aims and objectives

This thesis work focused on developing a range of techniques to study cell adhesion in plants. In **paper I**, we reviewed the existing adhesion quantification methods originally designed for animal cells or microorganisms. Based on this, the aim was to test different assays and adapt them to meet the specific requirements of plant cells. The work has been divided in 3 main parts.

First, we aimed at studying cell-cell adhesion at the single cell level using single plant cells in suspension: protoplasts with a regenerated CW. However, obtaining the biological material to develop the adhesion assays was more challenging than anticipated. Indeed, CW recovery after protoplasting requires a lot of optimization steps and depends on many factors to be successful. A new unexpected objective was drawn to facilitate the optimization of CW recovery protocols. In **paper II**, we established a quantitative method based on fluorescence microscopy imaging to compare CW recovery after protoplast extraction.

Second, we tested different adhesion quantification assays to determine which ones would be the most appropriate for plant cells. In **paper III**, we implemented two complementary approaches, using microfluidics and optical tweezers, to measure the strength of adhesion between PM and CW.

Finally, in **paper IV**, in parallel with the single-cell work, we established an imaging-based workflow to compare cell-cell adhesion defects in seedlings' hypocotyls.

Taken together, this thesis contributes to the development of tools to study plant cell adhesion at different scales, opening new possibilities for gaining a fundamental understanding of how adhesion operates in plants.

3. Methods

3.1 Methods to study cell-cell adhesion (**Paper I**)

Cell adhesion quantification typically relies on methods where a sample is stretched until a detachment occurs. Most adhesion assays focus on single cells, because measuring mechanical properties at the tissue level make interpretations more complex as many cell types and extracellular-matrix (ECM) components contribute to overall tissue mechanics. Single-cell assays can probe two distinct mechanisms: cell-cell adhesion and cell-substrate (e.g., ECM) adhesion. Techniques designed for cell-substrate interactions often employ large-scale quantification, monitoring thousands of cells simultaneously. In contrast, cell-cell interaction assays require more precise manipulation and thus focuses on only two cells at a time.

These complementary approaches allow researchers to explore adhesion mechanisms at different scales. A comprehensive review of adhesion methods is presented in **paper I** of this thesis; the following sections summarize that review.

3.1.1 Tissue scale adhesion

In plants methods developed to quantify adhesion are mostly tissue based. One example is the “vortex-induced” cell separation assay (Figure 4A), which was used to study the differences in adhesion in *Arabidopsis* microcalli cultures at different developmental stages (Parker and Waldron, 1995; Leboeuf, Thoiron and Lahaye, 2004). This method consists in measuring the size of calli in suspension before and after vortexing using a particle size analyser (spectrophotometer). The more cells detach, the smaller the particle size are, indicating weaker adhesion. Although this method can give a first hint of the adhesion strength in between the cells, it is unprecise as the calli will be different in size as they are growing and thus the force applied on the cells is variable. Also, cell damages might be very important leading fragmentation by tissue fracture instead of cell detachment.

Tensile tests are the principal method used to quantify cell adhesion at the tissue level (Figure 4B). They have been especially developed to study cell-adhesion establishment after grafting (Lindsay, Yeoman and Brown, 1974; Moore, 1984; Kawakatsu *et al.*, 2020; Notaguchi *et al.*, 2020). In a typical assay, a force gauge applies a pulling force onto the sample until it breaks. Based on the shape of the sample and the force applied, a stress-strain curve can be generated and the de-adhesion force calculated. Yet, a major limitation is that it cannot distinguish whether the break happens because of cell-cell detachment or rupture of the cells themselves. To address this, microscale extensometers have been developed. The sample is placed on two arms that will stretch it, while the force used is precisely monitored with a load cell and cell deformations and detachments are visually followed using a microscope (Melnyk, 2017). From their experiments on grafted seedlings, Melnyk et al, showed that cells were not separating but merely breaking suggesting that the CW from cell junction perpendicular to the pulling force are stronger than the cell cortex. Tensile tests have been performed at the CW level using onion epidermal CW and showed a similar result (Zamil, Yi and Puri, 2014; Bidhendi *et al.*, 2023).

In our lab, we developed the use of extensometer to quantify cell-cell adhesion in hypocotyl of various cell adhesion-deficient mutants. Interestingly, in the case of mutants presenting reduced adhesion, cells separate rather than rupture, providing a clear indicator of weakened cell-cell connections (Erguvan *et al.*, 2025). We also developed a tool based on microscopy imaging to quantify the uptake of a dye, ruthenium red, in hypocotyls (**Paper IV**). With short staining time, the dye can only penetrate hypocotyls of plants with cell adhesion or cuticle defects. This approach does not produce quantitative data about the adhesion strength but gives a comparable baseline to find and investigate cell adhesion.

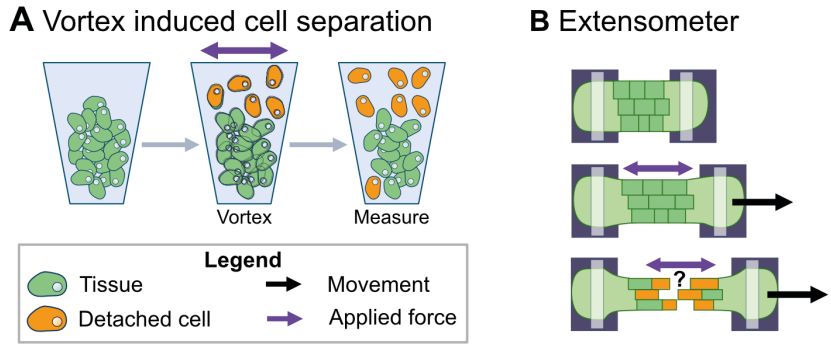

Figure 4: Tissue scale adhesion quantification

(A) A calli or tissue is vortexed and cluster size is measured using a spectrophotometer. **(B)** A tissue is stretched until it breaks. The question mark represents the lack of knowledge about how the tissue may break: cell separation or rupture. Figure from paper I with modifications.

Even though the results of such experiments can be harder to interpret, tissue-scale studies provide more physiological insights compared to single-cell approaches, which are artificial systems. They are therefore valuable tools that could be used in parallel to single-cell approaches.

3.1.2 Large scale cell-substrate adhesion

Historically, most of the adhesion measurements have been developed to study for cell-substrate interactions. Most of these methods are using hydrodynamic shear stress to detach cells. The earliest procedure is the plate and wash assay (Figure 5A; (Klebe, 1974)). In this assay, cells in suspension are put in contact with a substrate and allowed to interact for a defined pause time. Afterwards, the medium is removed and replaced by washing with a pipette. Cells that have not adhered are washed away, and the number of cells before and after washing provides a relative quantification of adhesion. Although simple, the plate and wash method is semi-quantitative and does not provide a direct measure of the adhesion strength (Alam, Kumar and Varadarajan, 2019). Nevertheless, the same basic strategy is used in other hydrodynamic adhesion assays, such as centrifugation assay, radial flow chamber, spinning disc or parallel plate assay

(Figure 5BC; Paper I (van Kooten *et al.*, 1992; García, Ducheyne and Boettiger, 1997; Ungai-Salánki *et al.*, 2019), and do permit quantitative measurements by applying controlled shear forces on the cells.

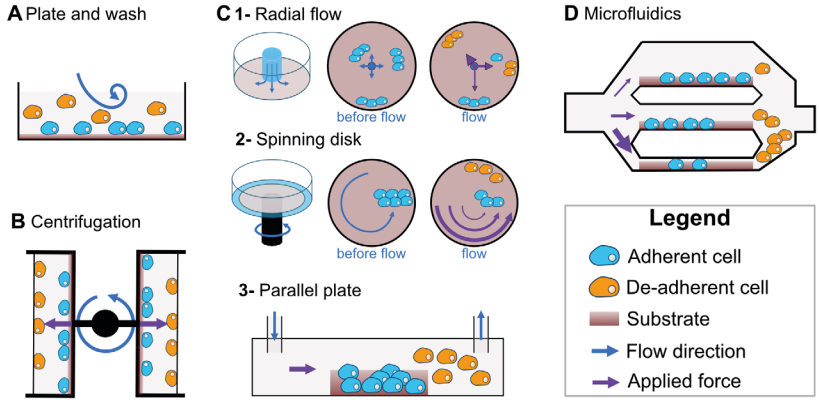

Figure 5: Large scale cell substrate adhesion quantification

The flow of liquid, e.g. of medium, is used to break the interaction of the cells with a substrate. The differences between the methods hold in the direction of the flow as well as the precision of the amount of pressure applied (**A** less precise; **D** most precise). Figure from paper I.

Following preliminary tests using plate and wash assays, we turned to microfluidic adhesion assays for plant cells as detailed in **paper III**. Indeed, more recently, the use of microfluidics has replaced the use of traditional flow chambers (Figure 5D). Microfluidic devices present several advantages in relation with their small size, the possibility to maintain a laminar flow that can be precisely controlled and a wide range of flow pressure and thus, shear stress that can be applied (Lu *et al.*, 2004; Christ *et al.*, 2010). Moreover, microfluidic chips are compatible with live-cell microscopy allowing simultaneous observation of the cell morphology and deformation under shear stress. Overall, large-scale microfluidic adhesion assays enable direct comparison of different cell populations, such as distinct cell types or mutant lines, at the single-cell level. Multiple distinct populations can be introduced in the same channel, ensuring identical shear stress condition is being applied.

However, because large-scale assays average the responses of heterogeneous cells and cannot resolve the mechanics of individual cell adhesion, complementary single-cell assays remain essential for dissecting the precise forces and molecular mechanisms underlying adhesion.

3.1.3 Single cell adhesion assays

Single cell adhesion assays use micromanipulation to bring a cell in contact with a substrate (or another cell) for a defined adhesion time, then separate them while continuously recording the force (Figure 6). The cell can either be held on a surface (Optical tweezers, atomic force microscopy (AFM)), a cantilever (AFM, FluidFM), with micro-aspiration pipette (Dual Aspiration Pipette (DAP), FluidFM) or directly with a laser trap (Optical tweezers). The substrate may be a coated surface, a functionalized bead, or a cantilever; alternatively, a second cell can serve as the substrate in DAP, FluidFM, or AFM configurations. Single-cell force spectroscopy (SCFS) is a specific AFM-based technique that quantifies the adhesion between a cell and a substrate. A functionalized AFM tip contacts the cell, and the detachment force is measured (Benoit *et al.*, 2000).

In every configuration, the micromanipulator is coupled to a force sensor that provides real-time readouts, yielding a force-vs-displacement curve. By combining the measured force with the known geometry and displacement, the curve can be transformed into a stress-strain relationship. From this relationship several quantitative parameters can be extracted (Paper I Figure 1BC). The maximum stress sustained before detachment defines the de-adhesion strength. Integrating the area under the stress-strain curve gives the de-adhesion work, which comprises both the dissipated stress (elastic and/or plastic deformation) and the adhesive energy arising from molecular bonds between the interacting cells or cell and substrate (Arroyo and Trepat, 2017).

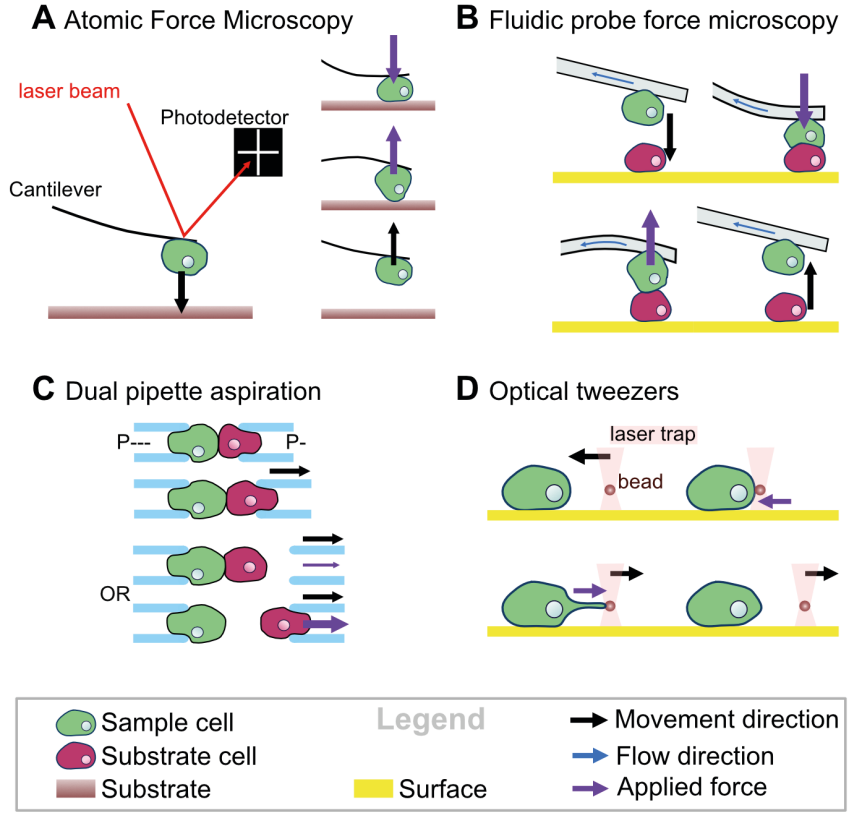

Figure 6: Single cell adhesion assay using micromanipulation

(A) AFM - a cell attached to a cantilever is placed in contact with a substrate. The interaction is measured by the cantilever bending, which reflects a laser beam, read by a detector and translated as a force curve. **(B)** FluidFM - a cell is maintained by a micro aspiration inside a cantilever pipette. The cell is put in contact with another cell and the interaction is measured by the cantilever bending. **(C)** DAP - a doublet of cell is held by two pipettes. To detach them, the negative pressure inside the pipettes must be stronger than the strength of adhesion between the cells. **(D)** Optical tweezers - a cell is immobilized on a surface, and a bead is coated with a substrate of interest. The bead and the cell are brought in contact and pulled away from each other.Figure from paper I with modifications

In plants, single-cell adhesion assays have previously been developed, but are limited to the study of pollen and its adhesion to a substrate or the stigma, using similar technique to the plate and wash

assay (Jauh *et al.*, 1997) but also higher precision approach resembling SCFS (Zinkl *et al.*, 1999).

In **paper III**, we established a protocol to perform mechanobiology experiments on plant cells using optical tweezers through the C-Trap system (LUMICKS, see 3.7).

During my PhD studies, I also attempted to put in place DAP system for single plant cells to investigate cell-cell adhesion (Figure 6C). Two isolated cells, each surrounded by their CW, were captured by suction in opposite pipettes and brought in contact so that they could interact and potentially attach. Preliminary experiments revealed several limitations to the adaptation of DAP to plant cells. First, when I tried to separate cell doublets obtained from a suspension culture (Pesquet *et al.*, 2010), the pressure generated inside the pipettes was insufficient to break the doublet, either in between the cells or within a cell directly. Indeed, cells doublets extracted from cell culture result from cell division instead of aggregation as the adhesion in plant is set up when the two daughter cells are dividing. The force required to break this bond is likely exceeding the one reachable with our system. Although another factor likely contributed to the problem: plant cells have rigid, non-flexible CWs unlike the highly deformable membranes of animal cells, which are entirely drawn into the pipette tip during aspiration. Because the plant cells did not fully occupy the pipette aperture, the effective contact area was reduced, limiting the maximal suction pressure that could be applied to the doublet and thus the pulling force.

To contravene this limitation, we then used single plant cells. We trapped two individual cells, positioned the pair of cells in direct contact, and monitored how they adhered. However, in this setup we discovered another issue: CW-mediated adhesion between the cells can require a prolonged incubation period to be established. To form a bond detectable by our system, plant cells would need to remain sucked in the pipettes for several minutes or even hours. Prolonged suction can compromise cell viability and trigger mechanosensory signalling, because the applied pressure may exceed the weak forces initially present at the cell-cell interface. Additionally, the

experimental throughput would be very low if each measurement requires an hour or more. To bypass this limitation, we could pre-form cell doublets by placing them by pair in narrow wells that would force them to touch each other. Each cell could then be captured with a pipette and directly pulled away from each other, reducing the experimental time. Nevertheless, more experiments are necessary to conclude on the feasibility of such experiments with single plant cells. Even if DAP devices are unsuitable for plant cell-cell adhesion assays, the technique could be still quite useful to probe PM to CW interactions which are generally weaker. It could also be a complementary approach to optical tweezers methods to avoid the potential effect of the laser on the cell.

3.2 Isolated plant cells and protoplasts

Plant cells are very rarely isolated under physiological conditions, only specialized cell types, such as pollen, can function autonomously for their specific purpose. Yet, in the lab, we can single out cells by digesting enzymatically the CW surrounding protoplasts freeing them from a tissue or an entire organism. Although the protoplast cannot survive outside of adequate conditions, they provide a great system to investigate plant cell biological processes including CW recovery. Another advantage of using protoplasts extracted using full CW digestion is the homogeneity of the cell suspension in terms of CW composition facilitating comparative analysis and downstream experiments. Indeed, we expect a more uniform CW composition than within intact tissues, where different cell types, tissue layers, or even distinct faces of a single cell can possess markedly different wall chemistry and mechanical properties. From a mechanical point of view, their spherical shape greatly simplifies the analysis of forces involved in potential interactions with other cells or substrate.

In 1879, Hanstein described for the first time the protoplast as the “living matter” inside the CW (Hanstein, 1879). In 1892, Klercker isolated protoplasts by using microsurgery on plasmolyzed cells (*Klercker*, 1892). Later, in 1960, Cocking isolated protoplasts using enzymatic digestion of the CW (Cocking, 1960). Since then, protoplasts are still widely used to study various processes of plant cell

biology like cell signalling, dedifferentiation and CW recovery (Yoo, Cho and Sheen, 2007; Xu *et al.*, 2022; Jayachandran *et al.*, 2023; Huh *et al.*, 2025; Mukundan, Satyamoorthy and Babu, 2025). The absence of a CW makes transformation possible without using Agrobacterium or biolistic (bombardment) transformation (Levengood, Zhou and Zhang, 2024). This offered the possibility of transient expression and quick gene functional analysis without integrating biological vector. Consequently, protoplasts are also widely used in biotechnology applications more specifically for new plant breeding technologies using CRISPR/Cas9 (Reed and Bargmann, 2021; He, E and Li, 2025; Mukundan, Satyamoorthy and Babu, 2025).

The primary goal of my work was to study cell-cell adhesion, therefore CW to CW interactions, based on the different methods developed for animal cells. We therefore needed isolated plant cells, single cells surrounded with a CW, that we could manipulate, i.e. in suspension. Across the literature, it is rare to find two publications with the same protocol for protoplast extraction and CW recovery. I tested several of them without success (Schirawski, Planchais and Haenni, 2000; Yoo, Cho and Sheen, 2007; Wu *et al.*, 2009; Kuki *et al.*, 2017; Pasternak, Paponov and Kondratenko, 2021; Jayachandran *et al.*, 2023). Although I often could extract protoplasts, I did not observe a similar ratio of cells with a recovered CW to the ones reported in those papers. Additionally, many protocols used protoplast embedding to facilitate the CW recovery (e.g: (Masson and Paszkowski, 1992; Jeong *et al.*, 2021; Sakamoto *et al.*, 2022)). That approach was unsuitable for our experiments because we needed to be able to manipulate the cells and study their CW, which would have be potentially contaminated by the embedding material.

I first focused on protocols presenting the same biological material I intended to use. To be able to work with the readily available *Arabidopsis* mutant and reporter lines presenting cell-cell adhesion defects, I began extracting mesophyll protoplasts from leaves of Arabidopsis rosettes grown in soil. I then tried different protocols from the literature, starting from the ones that appeared “simpler” to set up: protocols requiring fewer homemade solutions versus those

demanding more complex media (Pasternak, Paponov and Kondratenko, 2021).

My first challenge was to obtain enough protoplasts to reach the concentration recommended in protocols, which proved relatively easy to reach once I acquired enough practice. The second challenge was keeping the protoplasts alive in suspension long enough to observe CW recovery. This step was more difficult to reach, the extraction yield was not high enough to test various conditions simultaneously, and the heterogeneity of plants, tissues and cells used increased the difficulty of establishing a reproducible protocol for CW recovery. Additionally, contamination problems arose as the plants were not grown in sterile conditions. Therefore, to limit the biological material heterogeneity and contaminations, I switched to protoplasts extracted from a cell suspension culture originally derived from root of *Arabidopsis thaliana* Col-0 (Pesquet *et al.*, 2010). This cell culture is habituated and hence does not require hormone supply to grow. Starting from an established protoplast extraction protocol at UPSC (adapted from (Yoo, Cho and Sheen, 2007)), I optimized some steps to suit the cell culture for improved CW recovery. In parallel, we developed the quantitative cell wall regeneration (Q-Warg) pipeline to facilitate the comparison between the different extraction protocols and CW recovery conditions tested (**Paper II**).

3.2.1 Protoplast extraction

A healthy tissue is essential for the success of the protoplast extraction and the following regeneration process (Masson and Paszkowski, 1992). The material should be relatively young and have been grown under optimal conditions, e.g.: adequate watering, light, etc (Jeong *et al.*, 2021; Chen *et al.*, 2023; Stajič, 2023). In the case of cell culture, cells should be utilized during the growth phase. After enzymatic digestion, protoplasts must be resuspended with a certain density (Kang, Naing and Kim, 2020; Jeong *et al.*, 2021). From own experience, too few protoplasts per mL would lead to their death, indicating that a certain form of communication might be required to promote CW recovery in suspension. On the contrary, an excessive protoplasts concentration might lead to later issues, such as cell

aggregation and fast nutrient depletion. Although, cell aggregation might not be a problem depending on the final aim of the experiment.

The composition of the extraction medium also influence the protoplast viability and regeneration (Mathur, Koncz and Szabados, 1995; Pasternak, Paponov and Kondratenko, 2021). As with the growing medium, osmolarity balance must be respected to avoid cell bursting or plasmolysis. Although the CW digestion enzymes Cellulase and Macerozyme are quite commonly used across the different protocols, their concentration varies.

In summary, successful protoplast extraction relies on various parameters, starting from the tissue growth conditions to the protoplasting enzyme concentration. Optimizing those factors builds the foundation for protoplast long term viability and CW recovery.

3.2.2 CW recovery

Theory

From a protoplast, a whole plant can be regenerated as demonstrated for several plant species (Damm 1988, Meyer 2009, siemens 1993). Before it can divide, the protoplast must first recover its CW, however, little is known about the regeneration process. Innovative systems have been developed to follow primary CW recovery of single cells such as an impedance-coupled microfluidic device (Chen *et al.*, 2020). The electrical properties of a cell change depending on the CW presence and its thickness. Such non-invasive platform could be an interesting tool to follow CW recovery and link the electrical fingerprint to the CW composition to perform high-throughput analysis of protoplast suspension. Historically, most studies about CW recovery used fluorescent dyes and especially Calcofluor white to stain cellulose (Nagata 1970). Indeed, cellulose staining is often used to follow the CW recovery. Additionally, gas chromatography-mass spectrometry of polysaccharides extracted from 24-h-old protoplasts confirmed that cellulose dominates the newly synthesized wall (Huh *et al.*, 2025).

Sakai et al. (2017) followed the growth of moss protoplasts in micro-fluidic chips using time-lapse confocal microscopy and

reported that cellulose became detectable about 100 min after the start of culture. In a recent study, live cell time lapse fluorescence imaging was used to investigate the cellulose biosynthesis in Arabidopsis (Huh *et al.*, 2025). In this study, the authors propose a model for cellulose biosynthesis starting from short fibrils synthesized by CSCs that diffuse and bind to each other forming a primordial network. While less mobile, the assembly of fibrils continues to grow, forming a reticulated mesh surrounding the protoplast that solidifies to become a compact and stable network. In Huh's study, the earliest cellulose fragments were visible as soon as one hour after protoplasting, while a continuous network began to appear around 10 h post-isolation.

In *Arabidopsis* protoplasts, CW recovery begins almost immediately after culture initiation and can already be visualized with cellulose-specific stains as early as 1 h post-extraction. Depending on the protocols, the CW is recognized as fully recovered in 12 hours (Shafi *et al.*, 2019) to 48h (Kuki *et al.*, 2017). However, the definition of a recovered CW is not precise, reflecting the fact that CW recovery is a multistage process. Hence, several questions remained unanswered regarding the definition of a recovered CW: Is it based on a CW staining visible all around the protoplasts? On the capacity of the cell to sustain its own turgor pressure in hypotonic medium? Or else on the capacity of the cell to divide?

Embedding

CW recovery is in practice more difficult to achieve than it appears. Moreover, only a ratio of cells recover their CW in suspension (Kuki *et al.*, 2017). To increase this ratio, many of the existing protocols propose to embed protoplasts in a gel (Damm and Willmitzer, 1988; Jeong *et al.*, 2021; Sakamoto *et al.*, 2022). The literature shows that embedded protoplasts can regenerate a cell wall, after which the cells or calli are liberated from the matrix by depolymerisation and transferred to agar plates for plant growth. One hypothesis explaining the success of embedded protoplasts, is that CW components are secreted outside of the cell and, in the absence of any CW, would not be retained at the membrane proximity. Using embedding would

therefore force the secreted polysaccharides to accumulate at the cell periphery.

Similarly, a first layer of artificial CW could be added with coating of the protoplast with a polymer or extra-cellular polysaccharides like HGs. However, embedding or coating of protoplasts may "pollute" the newly formed CW, which would be the result of a mix of exogenous and endogenous molecules. This approach might therefore not be ideal for CW composition or physical properties studies. Alternatively, an encapsulation of protoplasts could help the CW recovery step. Protoplasts would be individually trapped inside an oil droplet containing medium using a microfluidic chip (Zheng *et al.*, 2021). The droplet can be burst after CW recovery, freeing cells to be used in later experiments avoiding CW contamination by gelling or coating agent.

Another hypothesis is that the cell requires a mechanical signal to secrete new CW components, which is absent in a suspension. Hence culturing protoplasts under pressure could potentially give insights to the CW recovery mechanisms.

When struggling with CW recovery of protoplasts, we explored other ways to obtain single plant cells without extracting protoplasts. In a cell culture, some cells might detach from a callus and remain as individual cells until division. By filtering the cell suspension, it is possible to isolate them. However, this method had two major drawbacks. First, it would require a large volume of cell culture for very few isolated cells as divided plant cells stay attached together via their newly synthesized CW. Second, the isolated cells may be a biased sub-population, differing physiologically from the bulk of the culture.

To increase the yield of such approach, we tried to vortex the cell suspension to detach weakly adherent cells. Adhesion can be further reduced by treating the culture with CW-degrading enzymes that target pectins to weaken the middle lamella before vortexing. Using this method, I extracted cells from leaves without entirely removing their CW. After extraction, they generally conserved their initial shape. which is undesirable for our goal of measuring adhesion

strength: irregular shapes complicate image-analysis pipelines, whereas spherical cells would provide a much cleaner model system. While using this kind of approach to get single plant cells, it is important to keep in mind that isolated cells obtained are probably keeping their tissue identity unlike protoplasts that dedifferentiate (Jiang, Zhu and Liu, 2013). It might thus be more difficult to regenerate a full organism from such a cell. Also, vortex would probably cause damages that would be difficult to assess and could alter the cells viability.

After those experiments, it appeared clearly that to study cell-cell adhesion using isolated cells, we needed protoplasts with a regenerated CW cultured in suspension.

Practice

Various parameters influence the quality of a protoplast suspension and its ability to regenerate a CW (**Paper II**). The most obvious factor is the composition of the medium in which the protoplasts are resuspended and cultured (Pasternak, Paponov and Kondratenko, 2021). After extraction, by definition, protoplasts are not surrounded and protected by their CW anymore making them highly sensitive to their environment. An iso-osmotic pressure in the medium must be maintained to avoid any cell bursting or plasmolysis. The presence of damaged cells in the medium can also trigger the death of healthy protoplasts. They might also require salts, sugars and hormones. Not only the culture medium must be optimized but also the physical conditions like temperature, light, or agitation. Here again, sources differ. For some, the culture must be placed in the dark (Masson and Paszkowski, 1992; Planchais, Camborde and Jupin, 2023), while others incubate their protoplasts under continuous light (Kuki *et al.*, 2020; Pasternak, Paponov and Kondratenko, 2021). The labware can also be optimised, e.g. to reduce pressure on the protoplasts while manipulation (Pasteur pipettes instead of classical pipettes) or to ensure correct oxygenation during growth (6 well-plate instead of erlenmeyer). Considering all the above parameters, the number of possible condition combinations for optimal CW recovery grows exponentially, making exhaustive testing of all parameters practically impossible. This is why in a lab, optimization steps must be taken with

the idea of getting the best result for the specific application but keeping in mind that improvement of the protocol is always possible and might be needed for another biological question or to study another cell line.

The establishment of a protocol would benefit from a statistical approach to reduce the number of conditions to be tested and to direct the optimisation steps that should be taken. Using a multivariate analysis to review existing protocols and results could predict what are the best parameters considering the specie, the final aim of the experiment and the local conditions. Such a computing approach taken before starting experiments would reduce again the number of optimization steps and therefore focus on the question of interest. To increase the efficiency of such method, reporting the list of optimization steps taken such as the different media and conditions tested, and the different outcomes, positive and negative, would greatly help narrowing down the crucial parameters to test.

Extracting protoplasts and having the CW regenerated is still the most promising method to get a homogeneous isolated cell suspension. Starting from a cell culture or a calli can increase even more the homogeneity of protoplasts. One big advantage is also their shape. Without their CW, protoplasts adopt a spherical shape, minimizing the energy required to maintain their integrity while keeping minimal tension for the PM and cytoskeleton. Additionally, when the CW is regenerated around the isolated protoplast, the cell keeps its spherical shape in the absence of external mechanical constraints (Colin *et al.*, 2020).

3.3 Light microscopy and image analysis

From the observation of cork cells by Hooke and living cells and bacteria by Leeuwenhoek with elementary microscopes in the XVII century, to recent technology advances allowing fast 4D confocal imaging, microscopy has evolved and diversified to fulfil the desire to always observe smaller things. Microscopes are becoming increasingly powerful. Yet, an image can be interpreted in many ways and without the proper analysis can lead to false information.

Consequently, even though the imaging process is the foundation of microscopy experiments, image processing and analysis are at least as essential to obtain the correct data.

3.3.1 Light microscopy

Microscopes

Across the different projects presented in this thesis, a variety of microscopy techniques were used. Starting from the macro-scale with the use of stereomicroscope equipped with a fluorescence system and an automated stage (Leica M205 FA). This equipment fits perfectly for the observation of Arabidopsis seedlings. This fully automated microscope allowed rapid acquisition of large field of views using the Navigator function that stiches several images together into one. The stereomicroscope was used for **paper IV**, to image Ruthenium red stained seedlings and the resulting images served as basis for the analysis.

Going to the microscale, my personal favourite, mostly because I relied on it a lot during my thesis, was an epifluorescence widefield microscope (Leica DMi8). This system is also fully automated and can acquire large fields of view by assembling several images into one. By switching LED excitation sources, it can image multiple fluorescent markers or dyes. The images taken with this microscope were the basis for the Q-Warg pipeline (**Paper II**).

To monitor CW recovery, I also employed confocal microscopy (Zeiss LSM780, LSM800 and LSM880 CLSM). In a confocal system a pinhole placed in front of the detector blocks out-of-focus light from adjacent planes, yielding superior resolution compared with wide-field modalities.

Dyes

For the different techniques, several dyes were used depending on our aim.

To study cell adhesion at the tissue scale, we used a dye penetration assay (**Paper IV**). Ruthenium Red (RR) is a colorimetric stain that

penetrates in tissues only if they present cell-cell adhesion, cuticle defects, damaged or dead cells and binds the carboxyl groups of pectic polysaccharides in the CW (Piccinini, Nirina Ramamonjy and Ursache, 2024).

When working with protoplasts and single plant cells, we wanted to quantify cell viability and CW recovery (paper II). To assess cell viability, we employed fluorescein diacetate (FDA)**.** FDA is a non-fluorescent, lipophilic compound that readily crosses intact plasma membranes. Once inside the cytosol of a metabolically active (i.e., living) cell, intracellular esterases hydrolyse the acetate groups, converting FDA into fluorescent fluorescein marking viable cells (Rotman, Zderic and Edelstein, 1963).

I used different stains across the different projects to check CW recovery after protoplast extraction. Calcofluor White was the primary dye I used because it binds specifically to ß-linked polysaccharides, notably to cellulose (Piccinini, Nirina Ramamonjy and Ursache, 2024). Its rapidity to stain and ease of visualisation, made Calcofluor White the staining of choice to follow CW recovery and for the comparative study of protoplast culture conditions (**Paper II**). However, this stain has proved to be toxic for the cells and was therefore not indicated for long term observation of single cells. To overcome this limitation, I also tested and used CarboTag and Carbotrace to visualize the CW. CarboTag is built around a pyridine-boronic acid motif, which mimics the natural CW cross-linker boric acid used by plants, and is associated with AlexaFluor488 for visualisation (Besten *et al.*, 2024). Carbotrace is available commercially in several variants that bind to repetitive motifs in carbohydrates and proteins. It can be used to visualize cellulose and xyloglucans (Choong *et al.*, 2019; Ferrara *et al.*, 2024). We used CarboTrace680 for FACS studies as our violet laser became deficient and prevented us to use Calcofluor White but also to limit the dye toxicity for sorted cells (**Paper II**).

For RR staining the sample is examined with bright-field illumination, and the signal is quantified from the colour intensity (i.e., the absorbance) of the stained region. In contrast, fluorescent dyes are

measured by the intensity of the emitted light: a higher fluorescence signal reflects a larger number of excited fluorophores, which in turn emit more photons as they relax to the ground state.

3.3.2 Quantitative imaging

Microscopy is a wonderful world. It is also a tricky technic and a subtle change in settings or conditions might have a big impact on the result. Quantitative imaging aims to eliminate bias by standardization of the sample preparation procedure, image acquisition and the automation of image analysis. To compare different samples with each other, the protocol must be the same from the sample preparation to the analysis. Even though it is not possible to eliminate all human error for sample processing, using a computing workflow to analyse the images is very beneficial. Automated processing is essential for tasks that are impractical or even infeasible to perform manually, such as quantifying signal intensity or extracting morphometric parameters, tracking individual cells over time, handling large-scale data sets or integrating multiple 2D acquisitions into coherent 3D or 4D reconstructions.

Additionally, using such workflows increases the efficiency, reproducibility and shareability of methods. Although the time gained might not be directly visible when establishing and testing a pipeline, the overall benefit is totally worth it.

During my PhD, I used different software or packages freely available. First Fiji (Fiji is just ImageJ) an open-source software specialized in image processing and analysis (Schindelin *et al.*, 2012). The large community surrounding Fiji and ImageJ helps to develop new tools, make them accessible to non-developer users while keeping the possibility for more advanced users to dig into programming. For the three results papers presented in this thesis, Fiji was used to batch process and extract data from the microscopy images using automated or semi-automated scripts (macros). Once numerical data were extracted from the images in form of .csv data tables, I wrote R scripts to manipulate, analyse and represent the data (https://posit.co/download/rstudio-desktop/ (Wickham *et al.*, 2019; Nolan [aut *et al.*, 2023; Ooms [aut and cre, 2024)). Using the Shiny

package (Chang *et al.*, 2024), I developed applications to facilitate the user input for data verification (Q-Warg, **Paper II**) and data visualisation (RRQuant, **Paper IV**).

To analyse images, we needed to separate the sample from the background using segmentation. We incorporated a deep-learning strategy into the RRQuant pipeline to segment hypocotyls automatically (paper IV). Deep learning constructs multilayer neural networks that learn hierarchical features directly from raw images, eliminating the need for hand-crafted descriptors (Zhang, Zhao and LeCun, 2016). To create a reliable model, we used the RootPainter platform (Smith *et al.*, 2022), assembling a diverse training set including both wild-type and mutant lines. After iterative annotation and training, the resulting network accurately distinguishes hypocotyl tissue from background and other tissues across genotypes, enabling high-throughput, reproducible quantification. In papers II and III, I used CellPose, a generalist deep-learning based segmentation tool (Stringer *et al.*, 2021), combined with a denoising algorithm, model cyto3 (Stringer and Pachitariu, 2024).

Overall, reducing the experimenter bias by automating image processing and analysis, is framed within the FAIR principles (Findability, Accessibility, Interoperability and Reusability) of the data. With open access to the analysis workflow and a precise description of the protocols, future experiments, in the original lab or elsewhere, should be easier to reproduce and confirmed.

3.4 FACS

Fluorescence activated cell sorting (FACS) development was initiated in the late 60's by Leonard Herzenberg and colleagues (Herzenberg and Herzenberg, 2004; Dangl and Lanier, 2013). Working in the immunology field with a poor eyesight and a lot of microscopy observations to do, it became evident for Herzenberg that he and his team needed a high-throughput and quantitative technique to classify cells. Based on advances in flow sorting technology for particles associated with oscillatory ink-jet printing techniques (Cram and Arndt-Jovin, 2005), Herzenberg and a team of engineers and

physicists developed the first FACS machine able to identify and sort cells.

Nowadays, FACS is a powerful method widely used to observe particles, cells, one by one and sort them based on their morphological properties and fluorescent markers. A suspension of particle is going through a nozzle and separated in drops. Each drop passes in front of a laser, and several signals are read by different detectors. The forward scattering (FSC) provides information about the size of the particle while the side scattering (SSC) gives an indication of the particle complexity/granularity. Size sorting with FSC facilitates the classification of particles of interest. SSC can be useful to detect dead or dying cells for instance, as their cytoplasm is often full of apoptotic bodies, increasing the cell granularity. Other detectors capture the fluorescence signals, allowing multiple dyes or reporters to be measured simultaneously.

In **paper II** (Q-Warg), we sorted single plant cells (SPCs), meaning living isolated cells with a recovered CW. First, the sorting was based on cell size to remove all dead particles or cell aggregates. Then the viability fluorescence signal and the CW staining had to be positive to classify the cells as SPCs. Cells meeting all 3 conditions were sorted in a well plate for cultivation or experiments. In our case, the SSC was not a good option to determine the viability of cells as the CW can also scatter the light, we would therefore eliminate our cells of interest. FACS was very promising to select SPCs. Yet, the quite low yield led us to prefer another method to quantify CW recovery after protoplasting. Moreover, cells selected by the FACS as SPCs were experiencing a very high stress during sorting and quickly presented signs of cell death. Therefore, sorted cells could not be used in adhesion experiments.

3.5 Microfluidics

A microfluidic device is a system designed to manipulate very small volumes of fluid. It typically contains a network of microchannels guiding the fluid along a defined path. By reducing reagent consumption, it enables micro-scale experiments and

high-throughput screening. For our aim, studying cell adhesion, the main advantage of this technique is the ability to precisely control and tune the flow, allowing cells to be subjected to a controlled shear stress.

The work considered to be the origin of microfluidics dates from the early 80's: a miniature gas chromatograph integrated on a silicon wafer (Terry, Jerman and Angell, 1979; Delaquilla, 2021). Originally, lab-on-chip derives from microelectronics and molecular analysis. The parallel work on both fields led to the development of soft lithography to pattern the chip (Xia and Whitesides, 1998). With this method, an elastomeric mould is used to transfer the pattern on a wide range of materials. Silicon and glass were used to build the first microfluidic chips. However, silicon chips were inconvenient for biology. Indeed, silicon has a low permeability to gas, is opaque, which makes it unsuitable for optical microscopy, and, to top it all off, is expensive. Therefore, other materials were needed to adapt microfluidics to biological systems. Polydimethylsiloxane (PDMS) became a key material for microfluidic chips and is still used today (Duffy *et al.*, 1998). PDMS is transparent, gas permeable and biocompatible, hence its use opened the field for biological applications (Folch *et al.*, 1999). From then, the interest and use of microfluidics continue to increase, and many biology fields are using this technology.

In plant biology, the first plant on chip was reported in 2010 (Meier, Lucchetta and Ismagilov, 2010; Yanagisawa *et al.*, 2021). This study focused on roots and their stimulation with auxin. They could control the roots environment and observed the fluorescent signal from DR5::GFP (auxin response regulator DR5). In 2011, a study about pollen tube guidance by isolated ovules in micro-chips was published (Yetisen *et al.*, 2011). Since then, the number of publications in plant science using microfluidic devices continued to increase (Yanagisawa *et al.*, 2021).

Microfluidic chips are greatly versatile. Various shapes or patterns can be used. The simplest one is a straight channel as we used for adhesion assays. Using soft lithography to prepare moulds and PDMS

as material, it is possible to make a chip with a microscale precision. The different procedures leading to chip fabrication must be conducted in very clean environments like under fume hoods or in a clean room in which the number of particles is very low (NanoLab class 100 / ISO 5, 100 particles per cubic foot) to avoid any contamination to the chip leading to unexpected shapes and therefore unpredictable flow patterns.

3.5.1 U-shaped chips

In this thesis, microfluidic devices have been used for different applications. First, chips produced by Sakai et al., (2019), originally developed to study the growth of the moss *Physcomistrella patens* over time. The pattern is composed of U-shaped traps that let the flow go through even when a cell is caught, allowing permanent perfusion of medium. Cells are trapped without requiring chemical coating and only the flux inside the chip maintain them in the trap (at least for single cells). A constant medium flow feed the cells in a sterile environment. It is then possible to keep plant cells alive over a long period of time. The PDMS chip being optically compatible with microscopy it allowed us to perform long term observation experiments. The U-chips were used in an attempt to follow the CW recovery after protoplasting. However, no CW staining was observed even after several days. It was probably linked to the forementioned secretion of CW components outside of the cell without being retained around it and being carried away with the flow or the absence of secretion.

The same chips were used for osmotic shock experiments. Using the precise flow control, the osmolarity of the medium was decreased while acquiring time lapse images with an epifluorescence microscope (Paper II Figure3).

3.5.2 Channel chips

Microfluidic adhesion assays were performed in **paper III**, using channel chips. The channels were coated with PLL and cellulose nanofibers (Svagan *et al.*, 2014). Coating involved sequential steps following a layer-by-layer approach: a PLL base layer followed by

cellulose layers, each applied using a DIY syringe pump (Baas and Saggiomo, 2021). The protoplast suspension was introduced in the coated channels and after a settling time, the flow was increased gradually to detach the protoplasts. During the adhesion assay, a pressure pump was used to increase the precision and control over the flow (Sensapex). The detachment of the cells could be followed and imaged over time. The images were then analysed to determine the force applied on the cells when the adhesion was disrupted.

Microfluidics offer a large range of possibilities to study isolated plant cells, from adhesion to cell development. Unfortunately, the various challenges encountered during my studies, prevented me to explore more deeply the technique and some 3D plans for new chips remained only drawings.

3.6 AFM

In 1982, the atomic resolution was reached by Binning and Rohrer who developed Scanning Tunnelling Microscopy (STM, (Binnig *et al.*, 1982)) for which they received the Nobel prize in 1986. STM was the first step towards probe microscopes: physical scanning of the sample using a probe that is in contact with the sample (Habibullah, 2020). While STM uses an electric current to scan the surface of the sample, which must be electrically conductive, Atomic Force Microscopy (AFM) can be used both on conductive and non-conductive surfaces. It uses a tip carried by a cantilever to scan physically the surface of a sample. A laser is reflected on the back of the cantilever, and its movement is read by a detector. The topology of the sample can be acquired as well as its mechanical properties such as elasticity, stiffness, charge but also adhesion.

I took part in a project aiming to characterize mechanical properties of microalgae. We compared different strains and analysed their elasticity and stiffness (unpublished data). The main challenge was to keep mechanically stable the cells on a glass slide. To solve this, I began to use Poly-lysin (PLL) to coat glass slides. PLL is a polymer widely used in animal research to stick the cells to a surface. Later, I

used PLL coating for various experiments, especially in microfluidic and optical tweezers adhesion assays as detailed in **paper III**.

For my primary project, developing methods to study cell-cell adhesion in plants using single plant cells, I did not employ AFM. We chose instead to focus on the optimisation of other novel methods using optical tweezers (C-Trap). Yet, AFM could be used to complement our work by providing precise measurements of the mechanical properties of CW regenerated single plant cells, or by enabling adhesion tests with tips coated in CW components or even with a whole cell attached directly to the cantilever. Compared with AFM, C-Trap offers higher throughput: many cells can be examined simultaneously in the presence of numerous beads, whereas AFM typically requires swapping the tip for each measurement, particularly when the tip itself is functionalised. Another drawback of AFM is the fragility of protoplasts; excessive pressure on their surface can easily cause bursting, demanding extensive optimisation.

Despite these challenges, AFM remains a strong candidate for characterising the CW mechanics of individual plant cells and for comparing mutant lines with cell-cell adhesion defects.

3.7 Optical tweezers

Originally developed for trapping and cooling of atoms by Ashkin and colleagues in 1986 (Ashkin *et al.*, 1986), optical tweezers were soon recognized as a powerful tool to study bacteria, viruses and single cells (Ashkin and Dziedzic, 1987; Ashkin, Dziedzic and Yamane, 1987). Since then, multiple biopolymers have been studied using optical tweezers like DNA, cytoskeleton constituents or bacteria's filopodia dynamics (Koch and Shaevitz, 2017).

Optical tweezers are using a focused laser light to trap small objects in a non-invasive manner (Koch and Shaevitz, 2017). Although it is possible to trap single cells within a laser trap, it may be damaging for the cells as photons are transferring energy to the object leading to heating and potentially to photodamage (Favre-Bulle and Scott, 2022). The damages caused vary greatly depending on wavelength and power

of the laser used. Therefore, most of optical tweezer's experiments use beads as polymers carriers. Beads can be coated with various polymers and serve as substrate for cells or for biomolecules of interest.

The C-Trap (LUMICKS) is an optical tweezer system associated with a microfluidic system and a confocal microscope. It allows simultaneous manipulation and visualisation of single molecules with computing of the force involved in molecular interactions in real time.

With C-Trap experiments, we wanted to compare the adhesion strength between the protoplasts PM and CW components as substrates. Beads were therefore coated with CW constituents like cellulose and pectins. I established a protocol to coat the beads using a layer-by-layer approach based on the electric charge of the different polymers and the bead itself. Polystyrene beads are negatively charged as pectins and cellulose nanofibrils (obtained by TEMPO oxidation, (Svagan *et al.*, 2014)). To get CW-coated beads, we used a first layer of PLL surrounding the bead and in a second step added a cellulose or pectin solution. To check the coating efficiency, we then turned to the chemical properties of the coating solution. We measured the electrical potential at the surface of the bead, expecting it to be different depending on the composition of the last deposited layer. Additionally, the bead size was measured further confirming the layer addition obtained by the different coating steps (see results in Paper III Figure 3).

As for AFM, to conduct mechanobiology experiments with optical tweezers, the cell must be mechanically stable. From previous experiments, I had tested the interaction of PLL with the protoplast and the bond seemed to be strong enough to perform AFM measurements on the cells. Therefore, we also used PLL for C-Trap measurements. We then had to adapt the custom chamber developed for animal cells to plant cells. The custom chamber is composed of two coverslips separated by a layer of microfluidic tape. We had to increase the internal volume of the chamber to alleviate the pressure put on the protoplasts and fit their larger dimensions compared to animal cells. The third optimization step that was taken regards the protoplast medium. The medium osmolarity needed to be kept

avoiding protoplast bursting but its density needed to be low enough to have the protoplasts sinking and attaching to the PLL-coated glass slide. We thus used W5 solution (washing solution after protoplasting) to perform experiments on fresh protoplasts. Building on these optimization steps, we established a protocol to measure PM to CW components interaction. The experiment was automatized using a Python script reducing human intervention and increasing precision.

The C-Trap platform combines optical tweezers with microfluidics and both wide-field and confocal imaging. It opens the path for new mechanobiology experiments on plant cells. To our knowledge, the work reported in **paper III** represents the first demonstration of these capabilities applied to plant protoplasts.

3.8 Open science

Across this thesis, numerous state-of-the-art techniques were described. Most of them require advanced machines and potentially specific premises, which increase the cost and reduce the availability of such equipment. Yet, it is nowadays possible to take detour paths to build high-performing apparatus.

3.8.1 3D printing

3D printing, also known as additive manufacturing, is a revolutionary technology where digital designs are brought to life by building new or customized objects layer upon layer. Initially used by industries, 3D printing is increasingly accessible and used both in households and in the professional sector. In a lab, it allows a huge creativity to develop solutions, repair equipment and reduce costs. Various objects can be built with the help of 3D printing, from simple goods like tube holders to more intricate and specialized devices like microscopes.

There are two main types of 3D printing methods:

- Fused deposition modelling (FDM): a plastic filament is heated up until it reaches its melting point and deposited following a specific pattern.

- Stereolithography (SLA): a photosensitive resin is exposed to light and cured in a specific pattern.

Both methods build objects layer by layer and they have their specific advantages and downsides. FDM is very cheap. The cost of the machine varies between 200 and 3000€. With a "home" 3D printer, reliable equipment can be purchase for less than 1000€ (e.g.: Prusa MK4S – 819€ in kit). The printing size is quite large (about 20*20*25cm for most common machines), enabling the construction of diverse parts. The XY resolution of such a printer is limited by the nozzle size, which is often 0.4mm but can be smaller (0.2mm). In Z, the resolution is dictated by the layer size that can be about 50µm (Prusa MK4S). FDM printing is very user friendly and accessible to beginners.

With SLA printers, the costs can be higher as the resin is more expensive than filaments. It also requires more safety precautions as the resin is a dangerous chemical and needs to be handled in well-ventilated areas with gloves, mask, lab coat and the waste must be discarded following the applicable rules. With SLA printing high resolution prints can be achieved (XY 22µm, Z down to 10µm for Phrozen Mini 8K) depending on the resin and the light used to polymerize it.

I designed and printed various parts to make my lab life easier during my PhD, from specific tube holders to microscopy stage adaptor with FDM printing. I also used SLA printing in an attempt to make microfluidic chips moulds. While promising, more optimisation was required to obtain chips for cell studies.

Beyond the technique, 3D printer users' community is quite large, and members are prompt to exchange tips on how to get the best results, how to learn how to use or repair the equipment. In science, using 3D printing allows to reduce drastically the cost of some objects but also to repair lab equipment that are not supported by companies anymore. For instance, we could replace easily a piece from a centrifuge that was perfectly functional, but the manufacturer was not selling the needed part anymore.

3.8.2 Open-source live imaging

3D printing is part of a larger world that regroups DIY (do-it-yourself) and open-source communities, fostering innovation, collaboration, and accessible technology development. It encourages another way of thinking and solving problems as well as independence with regard to companies that must sell products for the larger number of labs but can rarely provide customized solutions. Moreover, tedious tasks can be automatized by inventive solutions. For example, monitoring the growth of plant seedlings over several days traditionally requires frequent trips to the microscope. It is an approach that consumes considerable labour time and disturbs the plants by removing them from their growth chamber. Open-source devices like the Smart Plate Imaging Robot (SPIRO, (Ohlsson *et al.*, 2024)), represent an affordable and accessible solution. The SPIRO can image up to 4 agar plates placed in a carrousel. It is driven by a Raspberry Pi, an open-source computer platform that controls the automatic rotation of the carrousel, illumination and imaging at precisely defined intervals. Its structure is built with aluminium profiles and 3D printed parts, keeping the building costs under 300€. This setup enables dark growth phenotypic characterization without perturbing the plants thanks to the green illumination and eliminates manual handling, ensure consistent acquisition parameters, and guarantee that no time points are missed. The SPIRO nicely demonstrates that a fully automated setup tailored to specific and advanced experimental needs can be built at an affordable cost and shared with the community.

3D printing democratizes scientific instrumentation by providing low-cost alternatives to very expensive equipment like microscopes. It is also a very good pedagogical object. Taking again the example of microscopes, various models of 3D printed microscopes have been developed (Del Rosario *et al.*, 2022). UC2 for instance is highly customizable. It consists in several cubes containing each a part of a microscope (Diederich *et al.*, 2020). Students or public can build and understand how a microscope works. In parallel, this is also made for scientists and lately, STORM (Stochastic Optical Reconstruction Microscopy) was implemented on the UC2 system and super-resolution images were taken (Zehrer *et al.*, 2023) showing that molecular resolution is achievable using DIY approaches.

During my PhD, I built and used the Openflexure microscope (Sharkey *et al.*, 2016; Collins *et al.*, 2020). Flexure hinges are built on the weakening of certain points in a structure by making them thin, this allows their reversible deformation under stress. The Openflexure microscope exploits the plastic compliance to those deformations enabling a precision at the nanometre scale in terms of stage movement. Several versions are available and are a trade-off between price or resolution and automation. The overall cost, even for the high-resolution microscope would largely be reduced compared to a regular microscope distributed by a company. The main costs are the objective and the camera but depending on the image quality wanted, the cost can be maintained under 200€. Even though the Openflexure has been designed for the Raspberry Pi module v2 camera, it is possible to use a different camera with various quality objectives to get a higher resolution. A complete automatization of the microscope is achievable by adding motors to the stage and focus screws. This can be controlled by a Raspberry Pi and a Sangaboard (https://gitlab.com/filipayazi/sangaboard-rp2040). A software has been developed to avoid the necessity of programming to use the system, and the microscope can be fully controlled from distance using Openflexure Connect. Nevertheless, it is also possible, and that is the option I chose, to control the microscope via a python script (https://github.com/LB0g/Code_BApp).

When I started to build my Openflexure microscope (Figure 7A), no application was available to image Z-stacks during time. Associated with the U-shaped microfluidic chips, we wanted to follow CW recovery and potentially the first cell divisions after protoplasting. To image more cells during one experiment, we wanted to first mark several traps containing cells and take Z-stacks of each marked position overtime. Therefore, I built a Python-based application corresponding to those needs (Figure 7B). However, because of the low precision of the motors controlling the stage and the plastic of the microscope itself, the positions were drifting overtime. In association with issues with protoplasting, this experimental goal was not reached using the Openflexure microscope at the time. Yet, a drift correction was implemented in more recent Openflexure Connect software as

well as the specialised Raspbian distribution solving the issues we had (see openflexure.org).

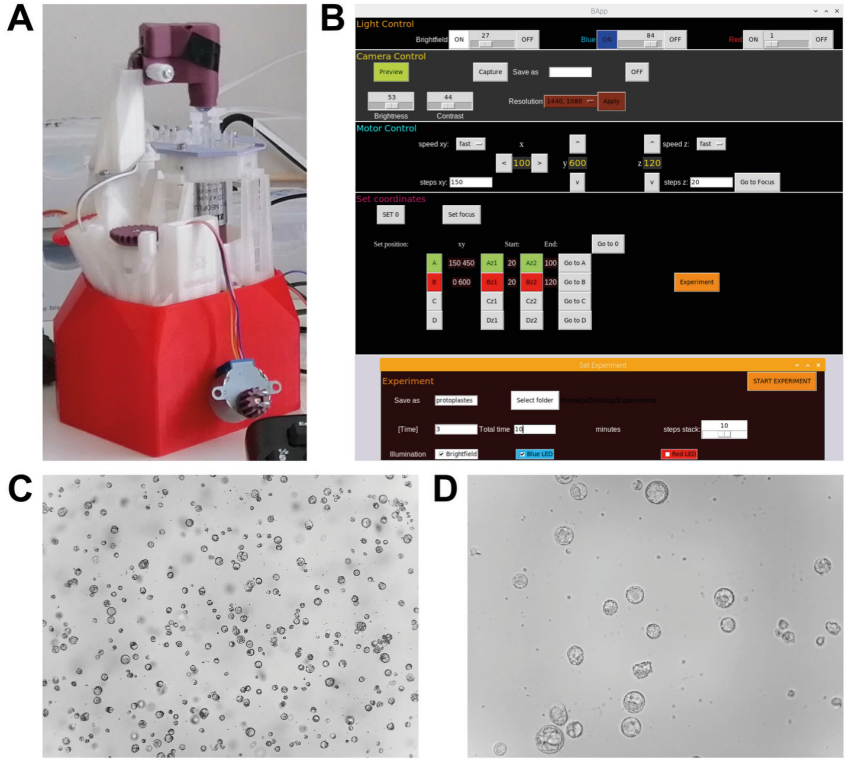

Figure 7: OpenFlexure microscope

(A) Openflexure microscope in use to observe a microfluidic chip. **(B)** Application programmed with Python to control the light and the motorized stage and focus. The app can also be used to set coordinates in XY and Z stack limits as well as the number of steps to acquire multiple Z stacks overtime. **(CD)** Protoplast suspension imaged with the Openflexure microscope. **(C)** 10x objective. **(D)** 40x objective.

One important benefit of this microscope is its size, as it is very small, it can fit in an incubator maintaining the best conditions for the samples. For me, the main advantage was also its availability: as I built my own microscope, I could use it for long periods without preventing other users to have access to a shared microscope. The main example

in this thesis is the timelapse of the protoplast suspension over 5 days (**Paper II** – Q-Warg Movie S1).

Another partly 3D printed device that was essential for many experiments, was the DIY-syringe pump. The syringe pump was built by first disassembling an Ender 3 3D printer and by adding 3D printed parts (Baas and Saggiomo, 2021). The flow that could be reached with this pump was from 5µL/min up to mL/min order. I used mostly this pump to coat microfluidic channels but also for the osmotic shock experiments (**Papers II and III**).

At a personal level, using 3D printing during my PhD taught me a bit of electronics, engineering and was my first step into programming. Most of all, it enlarged my way of thinking and how to apprehend problems in the lab from different angles.

4. Results and discussion

4.1 The Q-Warg pipeline: a robust and versatile workflow for quantitative analysis of protoplast culture conditions (**Paper II**)

Paper II presents the method, computing pipeline and proof of concept to optimize efficiently and rapidly the protocol for protoplast extraction, culture and CW recovery.

This paper was not originally planned in the research plan of this thesis. The project originated from the unexpected difficulty to get single plant cells (SPCs) in suspension. To study cell adhesion at the single cell scale, most methods developed in animal cells use single cells to monitor their adhesion with a substrate. To adapt those methods to plants and accurately quantify the interactions between a cell and its substrate, it was necessary to work with isolated plant cells. Single cells in suspension can be produced by enzymatically digesting their CW, separating cells and freeing protoplasts. However, protoplasts are not considered "true" plant cell as they lack a CW. We thus needed to make the cells regenerate their CW to have real plant cells. Moreover, our primary aim was to investigate cell-cell adhesion, therefore focusing on CW.

Although protoplasts have been used for a very long time in research, working with them remains quite challenging, particularly when it comes to finding the best conditions to keep them alive and especially to promote CW recovery. The literature contains a plethora of protocols for protoplast extraction, culture and plant regeneration. Strikingly, while the outlines are often similar, many parameters differ in between protocols. This variation may reflect the differences in equipment in the labs, variations in the biological material as well as habits of individual experimenters. The ultimate goal of the experiment can also significantly influence protocol selection. We also noticed that there was no easily accessible and straightforward method using quantitative criteria to compare CW recovery efficiency between protocols.

To compare results, fluorescence activated cell sorting (FACS) can be used to monitor the proportion of living cells with a regenerated CW in a cell suspension using fluorescent dyes. Cells corresponding to the selected parameters can be sorted and potentially utilized in downstream applications. During my PhD, we initially aimed to optimize a protocol using FACS to obtain a cell suspension containing only CW-regenerated living cells. Unfortunately, technical issues rendered the machine unusable for an extended period, forcing us to reconsider our strategy.

While FACS appeared promising, it also presented drawbacks. First the technique requires specialized material, not available in every plant lab, and specific skills. Additionally, we noticed that most cells were experiencing high stress during sorting causing cell death quickly afterwards. The proportion of cells corresponding to the requested parameters to be sorted was also very low under our condition. To address those issues, we changed method, using standard lab equipment, an epifluorescence microscope.

We thus developed a pipeline based on image analysis and quantification to efficiently identify the best conditions for CW recovery after protoplasting. The workflow uses large fluorescence images from the protoplast suspension with different markers for viability and CW recovery (Paper II Figure 1). Cells are segmented using a deep learning-based segmentation algorithm called CellPose (Stringer and Pachitariu, 2024). Data are then extracted from the original images using ImageJ to get information about fluorescence intensity but also morphometry like size or circularity of the cells (Schindelin *et al.*, 2012; Legland, Arganda-Carreras and Andrey, 2016). Data are treated with help of an R script from which plots are obtained to compare the effect of different parameters for every condition tested. We also developed a Shiny app programmed in R language to allow the user to easily check the results visually by linking the data values and the microscopy image ((Chang *et al.*, 2024); Paper II Figure 1M). In the app, the fluorescence intensity plots are displayed, either for viability or for CW staining. Those plots are interactive. Clicking on a data point reveals the corresponding microscopy images focused on the cell of interest. The different

channels can be checked as well as the segmentation. This allows the user to verify outliers and assess the segmentation parameter accuracy as well as the fluorescence intensity threshold used for viability. Although the pipeline requires the use of three different software which may prove difficult to apprehend for new users, one potential improvement could be the development of a master script to automate the workflow. However, the use of different scripts also offers advanced users the possibility to customize the pipeline to specific needs. Another upgrade could involve recoding the entire workflow in Python to build a standalone application. This approach would increase accessibility for novices while enabling advanced users to easily modify individual components of the pipeline. Nevertheless, the workflow is well-documented (user guide, tutorial videos available on GitHub: https://github.com/VergerLab/Q-Warg) for an independent experimenter to use the pipeline without additional help.

Using this pipeline, we tested 11 different media for CW recovery: six sugar compositions and three auxin sources and concentrations (one medium was common for sugars and hormones comparison, Paper II Figure 2, S1). After extraction, protoplasts were cultured for four days in each medium before imaging for quantification. Viability and CW recovery were quantified using fluorescence signal intensity of FDA and Calcofluor White respectively. Based on this medium screen, the impact of the sugar composition seemed to be higher than the hormones in the conditions tested. Indeed, for three of the media tested, the cell viability was very low. Using the pipeline, we identified one medium, that we named CRRUM (CW recovery root cells UPSC medium), yielding the highest number of living cells and the highest CW recovery.

To verify the reproducibility of the Q-Warg pipeline, we collaborated with Joris Sprakel, Patricia Schöppl and Rik Froeling from Wageningen. They monitored protoplast viability with different hormones concentrations as well as different media. With the pipeline, they rapidly determined which of the media were the most suited to keep their protoplasts alive (Protoplast regeneration medium, PRM (Chupeau *et al.*, 2013), Paper II Figure 4B). In addition, we demonstrated the workflow versatility by quantifying the proportion

of cells containing chloroplasts in a protoplast suspension extracted from entire seedlings (Paper II Figure 4CD).

In summary, we developed a new workflow to facilitate the optimization of protoplast extraction and culture protocols. Thanks to the Q-Warg pipeline, we at UPSC and in the Laboratory of Biochemistry, Wageningen, could efficiently and quantitatively compare CW recovery in several conditions to select the best fitted for our personal experimental aims. The reproducibility was also tested by performing the medium screen three times with the same result: the S4 medium was yielding the highest protoplast viability and promoting CW recovery (Paper II Figure 2). We showed the versatility of the pipeline by measuring the ratio of chloroplast-containing protoplasts. Indeed, although we first intended to develop the pipeline to optimize CW recovery, the workflow can be adapted for various research aims. For instance, if the focus is solely on cell viability or on morphological parameters such as circularity or diameter, this information is already implemented into the pipeline. It could for example be used to calculate the proportion of cells that divided. Since the workflow is based on microscopy images, any fluorescent reporter can be observed instead of CW and viability stain without changing the scripts. Moreover, the pipeline could also be used for protoplasts embedded in gel provided the cells can be segmented and stained or contain fluorescence markers.

Beyond specific protocol optimization, we envision that the Q-Warg workflow will be a powerful tool to investigate the fundamental processes underlying protoplast viability and CW recovery. By gathering data from different conditions used during protocol set up as well as re-analysing previously acquired images, patterns could arise. These could highlight consistent growth conditions and parameters that either promote or impair those processes, which will help us dissect how they are regulated. Quantitative data from Q-Warg could also be used to train deep learning models to predict optimization steps or optimal media for a specific question and biological material coming from different tissues or species.

Taken together, the multiple advantages of using such a pipeline including reproducibility, versatility and ease of use, will hopefully help many research groups to speed up the optimization process for protoplast extraction, CW recovery and potentially, plant regeneration freeing time for the research question of interest. Additionally, the workflow could be used in plant breeding industry to compare cell lines and their resistance to different conditions.

4.2 Plasma membrane to cell wall adhesion assays in plants reveals emergent adhesion dynamics behaviours (**paper III**)

In **paper III**, we adapted microfluidics and optical tweezers techniques to study PM to CW interaction. Starting from protocols developed for animal cells, we set up and optimized the methods to fit plant cells requirements. We then performed adhesion strength measurements. From the results obtained, we observed for the first time several PM-CW adhesion behaviours that were not previously described in plants such as the strengthening of adhesion over time, cell rolling on a substrate and membrane tether pulling.

In plants, cells are adhering to each other via their CW. The CW is dynamic and maintenance of the bond between the protoplast and its CW is essential for the correct development of the plant. More than just PM to CW bond, the cytoskeleton-PM-CW continuum is necessary to transmit both information from the extracellular compartment to the cytoplasm but also adjust the CW composition in response to intracellular stimuli. Even though the importance of PM to CW adhesion is well established, it is still not clear how this bond is set up and what are the different molecular actors in play. This lack of knowledge can be explained by the low number of tools available to measure and quantify these interactions. Methods have been developed for other organisms like animal cells or bacteria.

We took advantage of these existing methods to apply them to plant cells. The main principle is to put in contact a protoplast with a CW substrate for a selected time and then use different forces to detach the

cell from its substrate. From this de-adhesion force, it is possible to deduce the adhesion strength.

We used microfluidic adhesion assays to quantify cell adhesion strength at the population scale. In other words, interactions of many cells are monitored at the same time. Using this method, we tested the force needed to detach protoplasts from a non-coated surface (as negative control), polylysine (PLL, as a positive control) and cellulose. First, on the non-coated surface, no strong interaction was observed, and all protoplasts were detached/moved away using the lower pressure (0.2kPa) reachable with our system (Paper III Figure 3A). With coating, protoplasts stayed attached under higher pressure. On PLL coating, last protoplasts were detached at 2.2kPa and on cellulose at 0.7kPa (Paper III Figure 3B). Additionally, these experiments showed that the time given to interact have an impact on the adhesion strength: the longer the contact time was, the stronger the force to detach protoplasts (Paper III Figure 3). This indicates that PM-CW adhesion is an active process that strengthen over time. Additionally, we observed an unexpected detaching behaviour of the protoplasts. Indeed, we expected a binary situation: either the protoplast is attached or detached. Yet, some cells appeared to roll on the surface instead. This rolling could reflect the detachment and re-attachment of individual adhesion sites, or the involvement of multiple filopods that bind to the substrate and release sequentially. It may also show the presence of newly formed membrane tethers resembling artificial Hechtian strands.

We also used micromanipulation with an optical tweezer approach (C-Trap dymo 300 LUMICKS). With the C-trap, we studied the interaction between the PM and the CW at the single cell level using beads coated with CW constituents like cellulose and pectins. The protoplast is brought in contact with the bead and allowed to adhere for a selected time (Paper III Figure 5). Then the protoplast is moved away from the bead. The bead position in the laser trap is translated into a force curve from which we could extract different information. Then we extracted the maximal force sensed by the trap which correspond to the rupture of the bond between the PM and the bead. Three types of interaction were observed based on the interaction

strength (Paper III Figure 5DE). In the case of absence or weak interaction, the PM simply detaches from the bead while the protoplast is being pulled. When the interaction was stronger, we often observed a force curve exhibiting a sawtooth pattern. This may be due to the successive detachment of several adhesion points. We also observed an interaction strong enough to keep the bond between the PM and the substrate leading to the formation of a tether (Paper III Figure 7). In this case, the bead stays attached to the tether when it retracts. Additionally, the results showed a similar trend as for the microfluidic assays with a strengthening of the adhesion over time (Paper III Figure 6A, pluronic and PLL) and the samples, which showed a stronger interaction, were interacting with beads coated with cellulose and pectins (Paper III - Figure 6).

Taken together, those two methods enabled to shed light on undescribed adhesion mechanisms: strengthening of adhesion over time, tether formation and sawtooth detachment curve as well as sequential detachment and attachment of the PM to its substrate highlighted by the rolling behaviour in microfluidic assays. By their different observation scales, the methods are complementary and provide a promising toolset to explore and understand the fundamental mechanisms of cell adhesion and mechano-sensing in plants.

This study highlights two technically challenging methods that turn out to be highly effective for investigating cell adhesion and could help us in the future uncovering underlying mechanosensing mechanisms. This proof-of-concept paves the way for many experiments, involving using mutants presenting cell adhesion defects or chemicals treatments to help decipher the molecular actor of adhesion and their relative role in the scale of a cell. Although we used protoplasts to develop the different technics, such adhesion strength quantification methods could also be used to study more largely cell-cell adhesion using SPCs instead of protoplasts and shed light onto the mechanisms and molecular players of cell-cell adhesion bringing new insights on how cell adhesion is mediated and maintained in plants.

4.3 RRQuant: High-throughput quantification of seedling's epidermal integrity (paper IV)

The epidermis is the outermost cell layer of plant tissues. It plays an essential role in growth, development and adaptation to environmental conditions (Javelle *et al.*, 2011). It also acts as a protective layer of internal tissues, regulates exchanges with the environment (Samuels, Kunst and Jetter, 2008) and provides mechanical support to the plant (Galletti *et al.*, 2016). The plant epidermis is covered by a cuticle that helps control water loss and regulates gas exchange via stomata (Samuels, Kunst and Jetter, 2008). Mutants with impaired cuticle often become more permeable, showing abnormal organ fusions, and are less able to withstand environmental stresses (Ingram and Nawrath, 2017). While the processes regulating cell adhesion, cuticle deposition, and wall integrity are increasingly understood, many of the crucial regulatory factors involved are still unknown. Epidermal cells are continuously under high mechanical stress due to the differential growth of internal tissues (Kutschera and Niklas, 2007). The constant stretching requires a precise control of cell-cell adhesion and thus of their CW properties to avoid cell rupture or separation (Verger *et al.*, 2018; Asaoka *et al.*, 2021). Therefore, understanding the mechanisms maintaining epidermal integrity is a key question in plant developmental biology.

Phenotypically, it is quite clear for some mutants that they have cell-cell adhesion defects as they present gaps in between their cells or even curled cells (e.g.: *Quasimodo 2 (qua2)*; (Mouille *et al.*, 2007; Raggi *et al.*, 2015; Verger, Liu and Hamant, 2019)). Some mutants present less clear adhesion defects (e.g.: *actin-related protein2 (arp2)* (Li *et al.*, 2003; Mathur *et al.*, 2003; Basu *et al.*, 2005; Erguvan *et al.*, 2025)). This description is based on phenotypic observations of mutants that express strong phenotypes like cell bursting or loss of intercellular adhesion that can be visualized by microscopy (Buda *et al.*, 2009; Verger, Cerutti and Hamant, 2018). Weaker defects or cuticle impairment are more difficult to detect and require dye-penetration assays (Tanaka *et al.*, 2004). Nevertheless, quantifying the severity of the defects remains challenging.

To quantify the differences in cell-cell adhesion between samples, we developed a tool based on a dye-penetration assay using ruthenium red (RR) used to assess epidermal permeability (Kohorn *et al.*, 2021). This dye can penetrate tissues when there are defects in epithelial continuity, cell-cell adhesion and/or cuticle defects (Piccinini, Nirina Ramamonjy and Ursache, 2024). To develop this tool, we chose to work with dark-grown hypocotyls as they display the strongest epidermal adhesion defects (Verger *et al.*, 2018). Indeed, this tissue undergoes rapid anisotropic elongation leading to high epidermal tension, which amplifies the cell-cell adhesion defects and cell bursting (Verger *et al.*, 2018; Malivert *et al.*, 2021). Additionally, the dark-grown seedlings do not accumulate pigments as light-grown seedling, allowing clearer visualisation and greater sensitivity to detect epidermal defects.

RRQuant is a standardized, high-throughput workflow to quantify epidermal integrity defects in Arabidopsis seedlings. It integrates a protocol for controlled RR staining, sample preparation, imaging and semi-automated image analysis (available on GitHub: https://github.com/VergerLab/RRQuant).

Using RootPainter, a deep learning-based segmentation tool (Smith *et al.*, 2022), we built a robust, general-purpose segmentation model for dark-grown hypocotyls by assembling a varied training set that includes both wild-type and mutant plants, with stained and unstained samples. To minimize individual annotator bias, several people jointly labelled hypocotyl regions using RootPainter's correction interface, creating a consensus annotation set. This model now serves as a baseline segmentation model within the RRQuant workflow. Its performance can be improved further as more annotated data become available, because RootPainter allows incremental training. Users can therefore fine-tune the base model for their specific experimental conditions.

We developed a fully integrated image processing pipeline based on ImageJ macro enabling high-throughput, standardized, and reproducible quantification of epidermal integrity defects from RR-stained seedlings. First, large tile images containing multiple

genotypes and controls are processed with an ImageJ macro that lets users select regions of interest, assign genotype or condition labels, and automatically split the plates into individual files with a consistent naming scheme used for segmentation. After segmentation with RootPainter, the masks can be checked and potentially corrected if errors of segmentation arise. Then, hypocotyls features, like staining intensity and morphological traits, are quantified using the MorphoLibJ plugin (Legland, Arganda-Carreras and Andrey, 2016).

The data analysis pipeline based on R scripts utilizes the data tables generated by ImageJ quantification, combine and organise the information to perform statistical analysis. Additionally, I developed a Shiny app to facilitate data visualisation and representation (Chang et al., 2024). Data can be plotted following a customable organization and the samples to be displayed can be selected directly in the app. Additionally, interactive plots can be displayed to get additional information about the data points as well as verify the origin of outliers (real sample or segmentation error).

To test the accuracy of the workflow, we compared the mutant lines with different amplitude of adhesion defects. Two mutant lines, *arp2-1* (mild) and *qua2-1* (severe), and the wild-type Col-0 were stained for just 1 minute. With such a short staining time, the relative staining intensity of *arp2-1* was indistinguishable from Col-0, both visually and quantitatively via RRQuant (Paper IV Figure 3). In contrast, *qua2-1* displayed a clear staining pattern with a significant increase in relative intensity. Beyond staining intensity, the RRQuant workflow produces multiple morphometric measurements. Consistent with previous reports (Verger et al., 2016), the pipeline confirmed that *qua2-1* hypocotyls are shorter and additionally revealed that they are wider and exhibit greater tortuosity, reflecting increased overall waviness. Quantitative analysis across three biological replicates revealed clear and consistent observations, reflecting the known severity of these phenotypes. These results align with qualitative inspection of the images, while providing quantitative data for objective phenotype comparison.

RRQuant provides a new tool to quantify and compare epidermal integrity defects in seedlings. This approach is accessible, as based on freely available software and plugins, and adaptable, with the trainable segmentation model to fit specific experimental conditions and image acquisition systems. Future work will aim to increase both the speed and flexibility of the RRQuant pipeline. As more users adopt the tool, they will generate additional paired raw images and manually corrected masks that can be deposited in public repositories. These new datasets will be used to periodically retrain the base segmentation model, yielding successive versions that progressively require fewer manual corrections. At the same time, specialized segmentation models could be created for other plant structures such as light-grown hypocotyls, roots, cotyledons, and the apical hook. Because RRQuant can quantify any colour-based signal, it can also be adapted to a wide range of stains, pigments and reporter assays. Thus, although originally built for measuring epidermal integrity, the pipeline's modular design makes it a versatile platform for *in situ* quantification of plant tissue coloration, supporting both fundamental and applied plant-science research.

5. Conclusion and perspectives

Initially, the aim of this thesis was to develop tools to study cell-cell adhesion at the single cell scale. The plan was to review methods existing for animal cells and test them with plant cells (**Paper I**). When starting this project, we were not expecting that the most difficult part would be to obtain single plant cells, protoplasts with a regenerated CW, in suspension. Indeed, during more than half the time of my PhD, I could not get enough CW recovered protoplasts to test adhesion strength quantification methods. Moreover, the machine was not very cooperative and once the FACS protocol was tested and ready to be used the laser we relied on became defective. To palliate to this issue, we tried and optimized the protocol using other CW dyes. Yet, the FACS encountered new technical difficulties and became totally unusable for an extended period. This was probably the most challenging shift during my PhD. However, it was for the best as we then developed the Q-Warg pipeline (**Paper II**).

In parallel with the CW recovery protocol optimization, I worked on testing different methods to quantify cell adhesion strength, starting with the plate and wash assay, dual aspiration pipettes (DAP), AFM and learned how to conduct microfluidics experiments at all steps, from design to experiment and clean room manipulations. Using the Q-Warg pipeline, I optimized the CW recovery protocol, but we slightly changed focus and started to get interested on adhesion between the PM and the CW. Indeed, to work on the SPCs would have required to first characterize the composition and dynamics of CW recovery, this being an entire new project. From the preliminary tests, the method that we selected for PM-CW adhesion quantification in plant cells was microfluidic adhesion assays. Associated with the newly accessible optical tweezer (C-Trap LUMICKS) system at UPSC, we designed an experimental plan to investigate and quantify PM to CW interactions (**Paper III**) using those two systems.

In addition, we collectively (Verger group) developed the RRQuant workflow (**Paper IV**). I participated notably in the development of the

data analysis pipeline (R scripts), in writing the user guide and the protocol that served as basis for the manuscript.

5.1 Protoplasts and CW regeneration

Starting with protoplast extraction and culture, it quickly appeared that even though protoplasts are used by many research groups, working with them was not as trivial as it first seemed (paper II). Indeed, it came up that maintaining protoplast alive and promoting CW recovery required specific knowledge and handling. Often, in protocols, the "working" recipe is detailed but not the things that did not give the expected result. Additionally, how the experimenter is manipulating is difficult to describe on paper and sometimes, repeated actions are easy to forget to include in the protocol.

Many protocols use embedding to increase protoplast CW recovery (Damm and Willmitzer, 1988; Jeong *et al.*, 2021; Sakamoto *et al.*, 2022). We hypothesized that CW components are secreted in the extracellular space but without any net to retain them, they can float away from the protoplast PM. When I started CW recovery protocols, I always placed the protoplast culture under agitation, like the cell culture, assuming that it would avoid hypoxia of the cells, and it was not always a described parameter in literature. Yet, after discussions with other teams struggling with CW recovery, it appeared that that was more damaging for the cells than helpful. Indeed, when the protoplasts were grown quietly, I could observe an increase in viability and in CW recovery. To link this to the hypothesis, under agitation secreted CW components are moved away from the PM, while in a still environment, they may stay close and overtime form a polysaccharide network.

However, the lack of efficient CW recovery in suspension could also be linked to the absence of a mechanical signal around the protoplast. Our selected medium for protoplast culture (CRRUM, paper II) has a very high sugar concentration (1M Glucose). This high osmotic pressure might suffice to promote CW synthesis. To confirm this, additional experiments are needed with osmolytes that cannot be used by the cells such as mannitol.

Since more than 60 years (Cocking, 1960), protoplasts are used in a wide variety of fundamental and applied research projects. By developing the Q-Warg pipeline, we aimed at facilitating CW recovery protocol optimization. We also proposed to keep all data relative to protoplast extraction and culture in freely accessible repositories to be reviewed by others. Old data could also be reanalysed using the pipeline to quantify CW recovery or protoplast viability in a standardized manner. From this amount of data, certain patterns may be drawn leading to an increased efficiency of protocol establishment freeing time for the biological question of interest but also benefit the biotechnology sector.

5.2 Image analysis workflows

During my thesis I largely focused my efforts in developing image analysis workflows using primarily, ImageJ and R scripts. First, the quantitative cell wall regeneration (Q-Warg) pipeline enables the quantification of fluorescent intensity and morphological features of single cells or protoplasts. Similarly, the RRQuant workflow allows the quantification of coloured penetration-dyes and morphological characteristic of seedling hypocotyls. Both workflows have been developed with a specific aim in mind. However, they provide a working basis that could be extended to other aims. For example, Q-Warg can be used to quantify any fluorescent dye or reporter in protoplasts or single cell suspension increasing the number of possible outcomes. In the same way, we used RRQuant to quantify RR staining, but any other colour-based signal can be quantified. Such changes do not require modifications of the pipelines, and those workflows could also serve as basis to perform other kinds of image analysis. For example, RRQuant segmentation model could be trained to recognized other tissues. With open-source scripts, any willing user can adapt different parts of the pipelines to their specific needs.

The main advantages of such tools are the reproducibility and high throughput, because of the standardized and batched image processing and analysis. It also increases the efficiency of data analysis and limit experimenter bias. Because data are processed in a standardized way,

both repository organization and accessibility are improved. Such database could also be reused for new research questions and to predict and pinpoint the most important parameters for a specific experiment by experimental design.

5.3 DIY

In addition to programming with the development of image analysis workflows, the use of 3D printing and electronics was fully integrated in my PhD studies. One of the first things I did when starting my thesis, was to build the kit FDM 3D printer for the UPSC. Having this possibility of building my own or customizing machines, has proved useful more than once during my thesis, especially for the development of adhesion quantification methods. Among others, I designed and printed several microscopy stage adaptors for microfluidic experiments, built the OpenFlexure microscope (Collins *et al.*, 2020), that I used for long term observation of protoplast culture (paper II), and the syringe pump (Baas and Saggiomo, 2021), used for various microfluidic experiments (paper II, paper III).

As research subjects become more and more specialized, the equipment also need to be more specific. Although companies cover most of the needs of experimenters, it can be very expensive to buy customized solutions. Through 3D printing and other DIY approaches, this cost can be dramatically reduced (Del Rosario *et al.*, 2022). Also building equipment allows a very high degree of customization and adaptability to the specific needs as it is possible to modify them unlike a company product under guarantee. Associated with open-source design and potentially code, DIY approaches increase the transparency and reproducibility of specific methods. It is also a great tool to democratize science to the public and allow the use of advanced equipment for pedagogical purposes. Overall, DIY approaches in research do not only benefit the one customizing its equipment but the research community and beyond.

5.4 Single cell adhesion quantification methods

Paper III represents the end goal of my thesis. After testing various techniques with protoplasts or SPCs, we focused on two that appeared to be the most promising: microfluidic adhesion assays and optical tweezers. Those complementary techniques gave insights about adhesion mechanisms that, in our knowledge, have not been described before. Although, more experiments are required to draw any conclusions, we observed unexpected and interesting processes. First, the adhesion between the PM and the CW is strengthening over time and this has been observed with both methods. This indicates that adhesion is an active mechanism, maybe by the recruitment of additional cell surface receptors at the contact site with the substrate or by secretion of CW polysaccharides reinforcing the link between the substrate and the PM.

Surprisingly, during microfluidic assays, we observed a rolling behaviour of the cells onto the substrate. We first expected to observe a clear detachment of the protoplast because of their spherical shape. The surface of contact of a ball on a plane is not large, therefore, not many adhesion sites are available for attachment. However, protoplasts present structures at their surface resembling to animal cells filopods (Figure 2) that may also interact with the substrate. It has been shown that the protoplast filopods can form an adhesion foot for the protoplast to anchor itself, as would do an Hechtian strand (Dickmann *et al.*, 2024). The rolling of the protoplast on the substrate could thus be linked to cycles of detachment/attachment of the PM and/or several filopods or extended stretching of one filopod.

Using optical tweezers, we could pull tethers from protoplast's PM. Interestingly, for some sample, the force curve showed a sawtooth pattern indicating several events of detachment while pulling the tether. This might be due once more to the involvement of filopods attaching the coated bead. We also observed between the pectin-coated beads and the PM an interaction strong enough that the bead stayed attached to the PM and followed the retracting tether after releasing the bead from the optical trap. With those experiments, a great variation of the detachment forces was observed. This might be due to the non-homogeneous PM surface. As the PM is organised into

nanodomains, the force of interaction between the bead and the PM may be different depending on the number of cell surface receptors. Our observations remain rather preliminary at this stage. To homogenize the results and perform statistics, higher number of measurements is required in the future.

Overall, this thesis work brings new tools to study cell adhesion from the single cell to the tissue scale. These methods are promising tools to investigate the molecular players and mechanisms involved both in PM-CW and, with SPCs cell-cell adhesion, and have already revealed previously undescribed PM-CW adhesion behaviours.

References

Alam, F., Kumar, S. and Varadarajan, K.M. (2019) "Quantification of Adhesion Force of Bacteria on the Surface of Biomaterials: Techniques and Assays," *ACS Biomaterials Science & Engineering*, 5(5), pp. 2093–2110. Available at: https://doi.org/10.1021/acsbiomaterials.9b00213.

Anderson, C.T. (2019) "Pectic Polysaccharides in Plants: Structure, Biosynthesis, Functions, and Applications," in E. Cohen and H. Merzendorfer (eds.) *Extracellular Sugar-Based Biopolymers Matrices*. Cham: Springer International Publishing, pp. 487–514. Available at: https://doi.org/10.1007/978-3-030-12919-4_12.

Anderson, C.T. and Kieber, J.J. (2020) "Dynamic Construction, Perception, and Remodeling of Plant Cell Walls," *Annual Review of Plant Biology*, 71(Volume 71, 2020), pp. 39–69. Available at: https://doi.org/10.1146/annurev-arplant-081519-035846.

Arico, D.S. *et al.* (2023) "The plasma membrane – cell wall nexus in plant cells: focus on the Hechtian structure," *The Cell Surface*, 10, p. 100115. Available at: https://doi.org/10.1016/j.tcsw.2023.100115.

Arico, D.S. *et al.* (2025) "A molecular glue: LecRK-I.9 creates stiff plasma membrane – cell wall connections." bioRxiv, p. 2025.08.14.670329. Available at: https://doi.org/10.1101/2025.08.14.670329.

Arroyo, M. and Trepat, X. (2017) "Hydraulic fracturing in cells and tissues: fracking meets cell biology," *Current Opinion in Cell Biology*, 44, pp. 1–6. Available at: https://doi.org/10.1016/j.ceb.2016.11.001.

Asaoka, M. *et al.* (2021) "Stem integrity in Arabidopsis thaliana requires a load-bearing epidermis," *Development*, 148(4), p. dev198028. Available at: https://doi.org/10.1242/dev.198028.

Ashkin, A. *et al.* (1986) "Observation of a single-beam gradient force optical trap for dielectric particles," *Optics Letters*, 11(5), pp. 288–290. Available at: https://doi.org/10.1364/OL.11.000288.

Ashkin, A. and Dziedzic, J.M. (1987) "Optical Trapping and Manipulation of Viruses and Bacteria," *Science*, 235(4795), pp. 1517–1520. Available at: https://doi.org/10.1126/science.3547653.

Ashkin, A., Dziedzic, J.M. and Yamane, T. (1987) "Optical trapping and manipulation of single cells using infrared laser beams," *Nature*, 330(6150), pp. 769–771. Available at: https://doi.org/10.1038/330769a0.

Atakhani, A., Bogdziewiez, L. and Verger, S. (2022) "Characterising the mechanics of cell–cell adhesion in plants," *Quantitative Plant Biology*, 3, p. e2. Available at: https://doi.org/10.1017/qpb.2021.16.

Attree, S.M. and Sheffield, E. (1985) “Plasmolysis of Pteridium protoplasts: A study using light and scanning-electron microscopy,” *Planta*, 165(2), pp. 151–157. Available at: https://doi.org/10.1007/BF00395037.

Baas, S. and Saggiomo, V. (2021) “Ender3 3D printer kit transformed into open, programmable syringe pump set,” *HardwareX*, 10, p. e00219. Available at: https://doi.org/10.1016/j.ohx.2021.e00219.

Baba, A.I. *et al.* (2024) “Rhamnogalacturonan-II dimerization deficiency impairs the coordination between growth and adhesion maintenance in plants.” bioRxiv, p. 2024.11.26.625362. Available at: https://doi.org/10.1101/2024.11.26.625362.

Baba, A.I. and Verger, S. (2024) “Cell adhesion maintenance and controlled separation in plants,” *Frontiers in Plant Physiology*, 2. Available at: https://doi.org/10.3389/fphgy.2024.1369575.

Bachewich, C.L. and Heath, I.B. (1997) “Differential cytoplasm-plasma membrane-cell wall adhesion patterns and their relationships to hyphal tip growth and organelle motility,” *Protoplasma*, 200(1–2), pp. 71–86. Available at: https://doi.org/10.1007/BF01280736.

Baluska, F. *et al.* (2003) “Cytoskeleton-plasma membrane-cell wall continuum in plants. Emerging links revisited,” *Plant Physiology*, 133(2), pp. 482–491. Available at: https://doi.org/10.1104/pp.103.027250.

Basu, D. *et al.* (2005) “DISTORTED3/SCAR2 is a putative arabidopsis WAVE complex subunit that activates the Arp2/3 complex and is required for epidermal morphogenesis,” *The Plant Cell*, 17(2), pp. 502–524. Available at: https://doi.org/10.1105/tpc.104.027987.

Begum, R.A. and Fry, S.C. (2022) “Boron bridging of rhamnogalacturonan-II in Rosa and arabidopsis cell cultures occurs mainly in the endo-membrane system and continues at a reduced rate after secretion,” *Annals of Botany*, 130(5), pp. 703–715. Available at: https://doi.org/10.1093/aob/mcac119.

Benoit, M. *et al.* (2000) “Discrete interactions in cell adhesion measured by single-molecule force spectroscopy,” *Nature Cell Biology*, 2(6), pp. 313–317. Available at: https://doi.org/10.1038/35014000.

Besten, M. *et al.* (2024) “CarboTag: a modular approach for live and functional imaging of plant cell walls.” bioRxiv, p. 2024.07.05.597952. Available at: https://doi.org/10.1101/2024.07.05.597952.

Bidhendi, A.J. *et al.* (2023) “Cell geometry regulates tissue fracture,” *Nature Communications*, 14(1), p. 8275. Available at: https://doi.org/10.1038/s41467-023-44075-4.

Binnig, G. *et al.* (1982) “Surface Studies by Scanning Tunneling Microscopy,” *Physical Review Letters*, 49(1), pp. 57–61. Available at: https://doi.org/10.1103/PhysRevLett.49.57.

Bonin, C.P. *et al.* (1997) “The MUR1 gene of Arabidopsis thaliana encodes an isoform of GDP-d-mannose-4,6-dehydratase, catalyzing the first step in the

de novo synthesis of GDP-l-fucose," *Proceedings of the National Academy of Sciences*, 94(5), pp. 2085–2090. Available at: https://doi.org/10.1073/pnas.94.5.2085.

Bouwmeester, K. *et al.* (2014) "The Arabidopsis lectin receptor kinase LecRK-I.9 enhances resistance to Phytophthora infestans in Solanaceous plants," *Plant Biotechnology Journal*, 12(1), pp. 10–16. Available at: https://doi.org/10.1111/pbi.12111.

Buda, G.J. *et al.* (2009) "Three-dimensional imaging of plant cuticle architecture using confocal scanning laser microscopy," *The Plant Journal*, 60(2), pp. 378–385. Available at: https://doi.org/10.1111/j.1365-313X.2009.03960.x.

Canut, H. *et al.* (1998) "High affinity RGD-binding sites at the plasma membrane of Arabidopsis thaliana links the cell wall," *The Plant Journal: For Cell and Molecular Biology*, 16(1), pp. 63–71. Available at: https://doi.org/10.1046/j.1365-313x.1998.00276.x.

Chang, P.-F.L. *et al.* (1996) "Alterations in cell membrane structure and expression of a membrane-associated protein after adaptation to osmotic stress," *Physiologia Plantarum*, 98(3), pp. 505–516. Available at: https://doi.org/10.1111/j.1399-3054.1996.tb05705.x.

Chang, W. *et al.* (2024) "shiny: Web Application Framework for R." Available at: https://cran.r-project.org/web/packages/shiny/ (Accessed: February 19, 2025).

Chen, K. *et al.* (2023) "Isolation, Purification, and Application of Protoplasts and Transient Expression Systems in Plants," *International Journal of Molecular Sciences*, 24(23), p. 16892. Available at: https://doi.org/10.3390/ijms242316892.

Chen, L. *et al.* (2020) "An impedance-coupled microfluidic device for single-cell analysis of primary cell wall regeneration," *Biosensors and Bioelectronics*, 165, p. 112374. Available at: https://doi.org/10.1016/j.bios.2020.112374.

Cheng, X. *et al.* (2017) "Plasmolysis-deplasmolysis causes changes in endoplasmic reticulum form, movement, flow, and cytoskeletal association," *Journal of Experimental Botany*, 68(15), pp. 4075–4087. Available at: https://doi.org/10.1093/jxb/erx243.

Cheung, A.Y. and Wu, H.-M. (2025) "FERONIA: A Malectin-Domain Receptor Kinase with Intricate Signaling Mechanisms and Profound Importance to Plant Wellness," *The Yale Journal of Biology and Medicine*, 98(1), p. 53. Available at: https://doi.org/10.59249/PWYT9677.

Choong, F.X. *et al.* (2019) "Stereochemical identification of glucans by a donor–acceptor–donor conjugated pentamer enables multi-carbohydrate anatomical mapping in plant tissues," *Cellulose*, 26(7), pp. 4253–4264. Available at: https://doi.org/10.1007/s10570-019-02381-5.

Christ, K.V. *et al.* (2010) “Measurement of single-cell adhesion strength using a microfluidic assay,” *Biomedical Microdevices*, 12(3), pp. 443–455. Available at: https://doi.org/10.1007/s10544-010-9401-x.

Chupeau, M.-C. *et al.* (2013) “Characterization of the Early Events Leading to Totipotency in an Arabidopsis Protoplast Liquid Culture by Temporal Transcript Profiling,” *The Plant Cell*, 25(7), pp. 2444–2463. Available at: https://doi.org/10.1105/tpc.113.109538.

Cocking, E.C. (1960) “A Method for the Isolation of Plant Protoplasts and Vacuoles,” *Nature*, 187(4741), pp. 962–963. Available at: https://doi.org/10.1038/187962a0.

Coletta, A. *et al.* (2010) “Low-complexity regions within protein sequences have position-dependent roles,” *BMC Systems Biology*, 4(1), p. 43. Available at: https://doi.org/10.1186/1752-0509-4-43.

Colin, L. *et al.* (2020) “Cortical tension overrides geometrical cues to orient microtubules in confined protoplasts,” *Proceedings of the National Academy of Sciences*, 117(51), pp. 32731–32738. Available at: https://doi.org/10.1073/pnas.2008895117.

Collins, J.T. *et al.* (2020) “Robotic microscopy for everyone: the OpenFlexure microscope,” *Biomedical Optics Express*, 11(5), pp. 2447–2460. Available at: https://doi.org/10.1364/BOE.385729.

Coppinger, P. *et al.* (2004) “Overexpression of the plasma membrane-localized NDR1 protein results in enhanced bacterial disease resistance in Arabidopsis thaliana,” *The Plant Journal*, 40(2), pp. 225–237. Available at: https://doi.org/10.1111/j.1365-313X.2004.02203.x.

Cosgrove, D.J. (2024) “Structure and growth of plant cell walls,” *Nature Reviews Molecular Cell Biology*, 25(5), pp. 340–358. Available at: https://doi.org/10.1038/s41580-023-00691-y.

Cram, L.S. and Arndt-Jovin, D. (2005) “Mack Jett Fulwyler, pioneer of flow cytometry and flow sorting (1936–2001),” *Cytometry Part A*, 67A(2), pp. 53–60. Available at: https://doi.org/10.1002/cyto.a.20176.

Damm, B. and Willmitzer, L. (1988) “Regeneration of fertile plants from protoplasts of different Arabidopsis thaliana genotypes,” *Molecular and General Genetics MGG*, 213(1), pp. 15–20. Available at: https://doi.org/10.1007/BF00333392.

Dangl, J.L. and Lanier, L.L. (2013) “Founding father of FACS: Professor Leonard A. Herzenberg (1931–2013),” *Proceedings of the National Academy of Sciences*, 110(52), pp. 20848–20849. Available at: https://doi.org/10.1073/pnas.1321731111.

Del Rosario, M. *et al.* (2022) “The Field Guide to 3D Printing in Optical Microscopy for Life Sciences,” *Advanced Biology*, 6(4), p. 2100994. Available at: https://doi.org/10.1002/adbi.202100994.

Delaquilla, A. (2021) “History of Microfluidics,” *Elveflow* [Preprint]. Available at: https://www.elveflow.com/microfluidic-reviews/general-microfluidics/history-of-microfluidics/ (Accessed: August 1, 2025).

Dickmann, J.E.M. *et al.* (2024) “Dynamic cortical behavior of plant protoplasts reveals unexpected similarities between plant and animal cells.” bioRxiv, p. 2024.11.13.623369. Available at: https://doi.org/10.1101/2024.11.13.623369.

Diederich, B. *et al.* (2020) “A versatile and customizable low-cost 3D-printed open standard for microscopic imaging,” *Nature Communications*, 11(1), p. 5979. Available at: https://doi.org/10.1038/s41467-020-19447-9.

Dievart, A. *et al.* (2020) “Origin and Diversity of Plant Receptor-Like Kinases,” *Annual Review of Plant Biology*, 71(Volume 71, 2020), pp. 131–156. Available at: https://doi.org/10.1146/annurev-arplant-073019-025927.

Domozych, D.S. *et al.* (2003) “Plasmolysis, hechtian strand formation, and localized membrane-wall adhesions in the desmid, Closterium acerosum (Chlorophyta),” *Journal of Phycology*, 39(6), pp. 1194–1206. Available at: https://doi.org/10.1111/j.0022-3646.2003.03-033.x.

DRAKE, G.A., CARR, D.J. and ANDERSON, W.P. (1978) “Plasmolysis, Plasmodesmata, and the Electrical Coupling of Oat Coleoptile Cells,” *Journal of Experimental Botany*, 29(5), pp. 1205–1214. Available at: https://doi.org/10.1093/jxb/29.5.1205.

Duffy, D.C. *et al.* (1998) “Rapid Prototyping of Microfluidic Systems in Poly(dimethylsiloxane),” *Analytical Chemistry*, 70(23), pp. 4974–4984. Available at: https://doi.org/10.1021/ac980656z.

Dünser, K. *et al.* (2019) “Extracellular matrix sensing by FERONIA and Leucine-Rich Repeat Extensins controls vacuolar expansion during cellular elongation in Arabidopsis thaliana,” *The EMBO Journal*, 38(7), p. e100353. Available at: https://doi.org/10.15252/embj.2018100353.

Eine Methode zur Isolierung lebender Protoplasten / von John Af Klercker (1892). Available at: http://sammlungen.ub.uni-frankfurt.de/botanik/4449859 (Accessed: February 6, 2025).

Ellinger, D. and Voigt, C.A. (2014) “Callose biosynthesis in arabidopsis with a focus on pathogen response: What we have learned within the last decade,” *Annals of Botany*, 114(6), pp. 1349–1358. Available at: https://doi.org/10.1093/aob/mcu120.

Engelsdorf, T. *et al.* (2018) “The plant cell wall integrity maintenance and immune signaling systems cooperate to control stress responses in Arabidopsis thaliana,” *Science Signaling*, 11(536), p. eaao3070. Available at: https://doi.org/10.1126/scisignal.aao3070.

Erguvan, Ö. *et al.* (2025) “Outer epidermal edges mediate cell-cell adhesion for tissue integrity in plants.” bioRxiv, p. 2025.04.03.646819. Available at: https://doi.org/10.1101/2025.04.03.646819.

Favre-Bulle, I.A. and Scott, E.K. (2022) “Optical tweezers across scales in cell biology,” *Trends in Cell Biology*, 32(11), pp. 932–946. Available at: https://doi.org/10.1016/j.tcb.2022.05.001.

Ferrara, V. *et al.* (2024) “Phasor-FLIM analysis of cellulose paper ageing mechanism with carbotrace 680 dye,” *International Journal of Biological Macromolecules*, 260, p. 129452. Available at: https://doi.org/10.1016/j.ijbiomac.2024.129452.

Folch, A. *et al.* (1999) “Molding of Deep Polydimethylsiloxane Microstructures for Microfluidics and Biological Applications,” *Journal of Biomechanical Engineering*, 121(1), pp. 28–34. Available at: https://doi.org/10.1115/1.2798038.

Fruleux, A., Verger, S. and Boudaoud, A. (2019) “Feeling Stressed or Strained? A Biophysical Model for Cell Wall Mechanosensing in Plants,” *Frontiers in Plant Science*, 10. Available at: https://doi.org/10.3389/fpls.2019.00757.

Fuertes-Rabanal, M. *et al.* (2025) “Cell walls: a comparative view of the composition of cell surfaces of plants, algae, and microorganisms,” *Journal of Experimental Botany*, 76(10), pp. 2614–2645. Available at: https://doi.org/10.1093/jxb/erae512.

Galletti, R. *et al.* (2016) “Developing a ‘thick skin’: a paradoxical role for mechanical tension in maintaining epidermal integrity?,” *Development*, 143(18), pp. 3249–3258. Available at: https://doi.org/10.1242/dev.132837.

García, A.J., Ducheyne, P. and Boettiger, D. (1997) “Quantification of cell adhesion using a spinning disc device and application to surface-reactive materials,” *Biomaterials*, 18(16), pp. 1091–1098. Available at: https://doi.org/10.1016/S0142-9612(97)00042-2.

García-Gómez, B.I. *et al.* (2000) “Two bean cell wall proteins more abundant during water deficit are high in proline and interact with a plasma membrane protein,” *The Plant Journal: For Cell and Molecular Biology*, 22(4), pp. 277–288. Available at: https://doi.org/10.1046/j.1365-313x.2000.00739.x.

Gauthier, N.C., Masters, T.A. and Sheetz, M.P. (2012) “Mechanical feedback between membrane tension and dynamics,” *Trends in Cell Biology*, 22(10), pp. 527–535. Available at: https://doi.org/10.1016/j.tcb.2012.07.005.

Gonneau, M. *et al.* (2018) “Receptor Kinase THESEUS1 Is a Rapid Alkalinization Factor 34 Receptor in *Arabidopsis*,” *Current Biology*, 28(15), pp. 2452-2458.e4. Available at: https://doi.org/10.1016/j.cub.2018.05.075.

Gorshkova, T. *et al.* (2012) “Plant Fiber Formation: State of the Art, Recent and Expected Progress, and Open Questions,” *Critical Reviews in Plant Sciences*, 31(3), pp. 201–228. Available at: https://doi.org/10.1080/07352689.2011.616096.

Gouget, A. *et al.* (2006) “Lectin Receptor Kinases Participate in Protein-Protein Interactions to Mediate Plasma Membrane-Cell Wall Adhesions in

Arabidopsis," *Plant Physiology*, 140(1), pp. 81–90. Available at: https://doi.org/10.1104/pp.105.066464.

Gouguet, P. *et al.* (2021) "Connecting the dots: from nanodomains to physiological functions of REMORINs," *Plant Physiology*, 185(3), pp. 632–649. Available at: https://doi.org/10.1093/plphys/kiaa063.

Gronnier, J. *et al.* (2017) "Structural basis for plant plasma membrane protein dynamics and organization into functional nanodomains," *eLife*, 6, p. e26404. Available at: https://doi.org/10.7554/eLife.26404.

Habibullah, H. (2020) "30 Years of atomic force microscopy: Creep, hysteresis, cross-coupling, and vibration problems of piezoelectric tube scanners," *Measurement*, 159, p. 107776. Available at: https://doi.org/10.1016/j.measurement.2020.107776.

Hanstein, D.J. von (1879) *Botanische Abhandlungen aus dem Gebiet der Morphologie und Physiologie*. Adolph Marcus.

Harant, D. and Lang, I. (2020) "Stay in Touch—The Cortical ER of Moss Protonemata in Osmotic Stress Situations," *Plants*, 9(4), p. 421. Available at: https://doi.org/10.3390/plants9040421.

Haruta, M. *et al.* (2014) "A Peptide Hormone and Its Receptor Protein Kinase Regulate Plant Cell Expansion," *Science*, 343(6169), pp. 408–411. Available at: https://doi.org/10.1126/science.1244454.

Hdedeh, O. *et al.* (2025) "Membrane nanodomains to shape plant cellular functions and signaling," *New Phytologist*, 245(4), pp. 1369–1385. Available at: https://doi.org/10.1111/nph.20367.

He, Q., E, Y. and Li, R. (2025) "Protoplast Cell-Wall Regeneration: Unlocking New Potential for Genetic Improvement and Tree Breeding," *Plant, Cell & Environment*, 48(8), pp. 5786–5788. Available at: https://doi.org/10.1111/pce.15537.

HECHT, K. (1912) "Studien uber den Vorgang der Plasmolyse," *Beitrage zur Biologie der Pflanzen*, 11, pp. 133–192.

Hématy, K. *et al.* (2007) "A Receptor-like Kinase Mediates the Response of *Arabidopsis* Cells to the Inhibition of Cellulose Synthesis," *Current Biology*, 17(11), pp. 922–931. Available at: https://doi.org/10.1016/j.cub.2007.05.018.

Herger, A. *et al.* (2019) "Leucine-Rich Repeat Extensin Proteins and Their Role in Cell Wall Sensing," *Current biology: CB*, 29(17), pp. R851–R858. Available at: https://doi.org/10.1016/j.cub.2019.07.039.

Herzenberg, Leonard A. and Herzenberg, Leonore A. (2004) "Genetics, FACS, Immunology, and Redox: A Tale of Two Lives Intertwined," *Annual Review of Immunology*, 22(1), pp. 1–31. Available at: https://doi.org/10.1146/annurev.immunol.22.012703.104727.

Hocq, L., Pelloux, J. and Lefebvre, V. (2017) “Connecting Homogalacturonan-Type Pectin Remodeling to Acid Growth,” *Trends in Plant Science*, 22(1), pp. 20–29. Available at: https://doi.org/10.1016/j.tplants.2016.10.009.

Huh, H. *et al.* (2025) “Time-resolved tracking of cellulose biosynthesis and assembly during cell wall regeneration in live Arabidopsis protoplasts,” *Science Advances*, 11(12), p. eads6312. Available at: https://doi.org/10.1126/sciadv.ads6312.

Huxham, I.M. *et al.* (1999) “Electron-energy-loss spectroscopic imaging of calcium and nitrogen in the cell walls of apple fruits,” *Planta*, 208(3), pp. 438–443. Available at: https://doi.org/10.1007/s004250050580.

Hynes, R.O. (2002) “Integrins: bidirectional, allosteric signaling machines,” *Cell*, 110(6), pp. 673–687. Available at: https://doi.org/10.1016/s0092-8674(02)00971-6.

Ingram, G. and Nawrath, C. (2017) “The roles of the cuticle in plant development: organ adhesions and beyond,” *Journal of Experimental Botany*, 68(19), pp. 5307–5321. Available at: https://doi.org/10.1093/jxb/erx313.

Jarvis, M.C. and Apperley, D.C. (1995) “Chain conformation in concentrated pectic gels: evidence from 13C NMR,” *Carbohydrate Research*, 275(1), pp. 131–145. Available at: https://doi.org/10.1016/0008-6215(95)00033-P.

Javelle, M. *et al.* (2011) “Epidermis: the formation and functions of a fundamental plant tissue,” *New Phytologist*, 189(1), pp. 17–39. Available at: https://doi.org/10.1111/j.1469-8137.2010.03514.x.

Jayachandran, D. *et al.* (2023) “Engineering and characterization of carbohydrate-binding modules for imaging cellulose fibrils biosynthesis in plant protoplasts,” *Biotechnology and Bioengineering*, 120(8), pp. 2253–2268. Available at: https://doi.org/10.1002/bit.28484.

Jeong, Y.Y. *et al.* (2021) “Optimization of protoplast regeneration in the model plant Arabidopsis thaliana,” *Plant Methods*, 17(1), p. 21. Available at: https://doi.org/10.1186/s13007-021-00720-x.

Jiang, F., Zhu, J. and Liu, H.-L. (2013) “Protoplasts: a useful research system for plant cell biology, especially dedifferentiation,” *Protoplasma*, 250(6), pp. 1231–1238. Available at: https://doi.org/10.1007/s00709-013-0513-z.

Jones, E.B.G. (1994) “Fungal adhesion,” *Mycological Research*, 98(9), pp. 961–981. Available at: https://doi.org/10.1016/S0953-7562(09)80421-8.

Juliano, R.L. (2002) “Signal Transduction by Cell Adhesion Receptors and the Cytoskeleton: Functions of Integrins, Cadherins, Selectins, and Immunoglobulin-Superfamily Members,” *Annual Review of Pharmacology and Toxicology*, 42(Volume 42, 2002), pp. 283–323. Available at: https://doi.org/10.1146/annurev.pharmtox.42.090401.151133.

Kanchanawong, P. and Calderwood, D.A. (2023) “Organisation, dynamics and mechanoregulation of integrin-mediated cell–ECM adhesions,” *Nature*

reviews. Molecular cell biology, 24(2), pp. 142–161. Available at: https://doi.org/10.1038/s41580-022-00531-5.

Kang, H.H., Naing, A.H. and Kim, C.K. (2020) "Protoplast Isolation and Shoot Regeneration from Protoplast-Derived Callus of Petunia hybrida Cv. Mirage Rose," *Biology*, 9(8), p. 228. Available at: https://doi.org/10.3390/biology9080228.

Katsumi, A. *et al.* (2004) "Integrins in Mechanotransduction*," *Journal of Biological Chemistry*, 279(13), pp. 12001–12004. Available at: https://doi.org/10.1074/jbc.R300038200.

Kawakatsu, Y. *et al.* (2020) "An in vitro grafting method to quantify mechanical forces of adhering tissues," *Plant Biotechnology*, 37(4), pp. 451–458. Available at: https://doi.org/10.5511/plantbiotechnology.20.0925a.

Kemperman, J.A. and Barnes, B.V. (1976) "Clone size in American aspens," *Canadian Journal of Botany*, 54(22), pp. 2603–2607. Available at: https://doi.org/10.1139/b76-280.

Kesawat, M.S. *et al.* (2023) "Genome-wide analysis of proline-rich extensin-like receptor kinases (PERKs) gene family reveals their roles in plant development and stress conditions in *Oryza sativa* L.," *Plant Science*, 334, p. 111749. Available at: https://doi.org/10.1016/j.plantsci.2023.111749.

Klebe, R.J. (1974) "Isolation of a collagen-dependent cell attachment factor," *Nature*, 250(5463), pp. 248–251. Available at: https://doi.org/10.1038/250248a0.

Knepper, C., Savory, E.A. and Day, B. (2011a) "Arabidopsis NDR1 Is an Integrin-Like Protein with a Role in Fluid Loss and Plasma Membrane-Cell Wall Adhesion," *Plant Physiology*, 156(1), pp. 286–300. Available at: https://doi.org/10.1104/pp.110.169656.

Knepper, C., Savory, E.A. and Day, B. (2011b) "The role of NDR1 in pathogen perception and plant defense signaling," *Plant Signaling & Behavior*, 6(8), pp. 1114–1116. Available at: https://doi.org/10.4161/psb.6.8.15843.

Koch, M.D. and Shaevitz, J.W. (2017) "Introduction to Optical Tweezers," *Methods in Molecular Biology (Clifton, N.J.)*, 1486, pp. 3–24. Available at: https://doi.org/10.1007/978-1-4939-6421-5_1.

Kohorn, B.D. (2001) "WAKs; cell wall associated kinases," *Current Opinion in Cell Biology*, 13(5), pp. 529–533. Available at: https://doi.org/10.1016/s0955-0674(00)00247-7.

Kohorn, B.D. (2016) "Cell wall-associated kinases and pectin perception," *Journal of Experimental Botany*, 67(2), pp. 489–494. Available at: https://doi.org/10.1093/jxb/erv467.

Kohorn, B.D. *et al.* (2021) "Mutation of an Arabidopsis Golgi membrane protein ELMO1 reduces cell adhesion," *Development*, 148(10), p. dev199420. Available at: https://doi.org/10.1242/dev.199420.

van Kooten, T.G. *et al.* (1992) "Development and use of a parallel-plate flow chamber for studying cellular adhesion to solid surfaces," *Journal of Biomedical Materials Research*, 26(6), pp. 725–738. Available at: https://doi.org/10.1002/jbm.820260604.

Kuki, H. *et al.* (2017) "Quantitative confocal imaging method for analyzing cellulose dynamics during cell wall regeneration in Arabidopsis mesophyll protoplasts," *Plant Direct*, 1(6), p. e00021. Available at: https://doi.org/10.1002/pld3.21.

Kuki, H. *et al.* (2020) "Xyloglucan Is Not Essential for the Formation and Integrity of the Cellulose Network in the Primary Cell Wall Regenerated from Arabidopsis Protoplasts," *Plants*, 9(5), p. 629. Available at: https://doi.org/10.3390/plants9050629.

Kutschera, U. and Niklas, K.J. (2007) "The epidermal-growth-control theory of stem elongation: An old and a new perspective," *Journal of Plant Physiology*, 164(11), pp. 1395–1409. Available at: https://doi.org/10.1016/j.jplph.2007.08.002.

Langhans, M. *et al.* (2017) "The right motifs for plant cell adhesion: what makes an adhesive site?," *Protoplasma*, 254(1), pp. 95–108. Available at: https://doi.org/10.1007/s00709-016-0970-2.

Lang-Pauluzzi, I. and Gunning, B.E.S. (2000) "A plasmolytic cycle: The fate of cytoskeletal elements," *Protoplasma*, 212(3–4), pp. 174–185. Available at: https://doi.org/10.1007/BF01282918.

Leboeuf, E., Thoiron, S. and Lahaye, M. (2004) "Physico-chemical characteristics of cell walls from Arabidopsis thaliana microcalli showing different adhesion strengths," *Journal of Experimental Botany*, 55(405), pp. 2087–2097. Available at: https://doi.org/10.1093/jxb/erh225.

Lebret, K., Thabard, M. and Hellio, C. (2009) "4 - Algae as marine fouling organisms: adhesion damage and prevention," in Claire Hellio and D. Yebra (eds.) *Advances in Marine Antifouling Coatings and Technologies*. Woodhead Publishing (Woodhead Publishing Series in Metals and Surface Engineering), pp. 80–112. Available at: https://doi.org/10.1533/9781845696313.1.80.

Legland, D., Arganda-Carreras, I. and Andrey, P. (2016) "MorphoLibJ: integrated library and plugins for mathematical morphology with ImageJ," *Bioinformatics*, 32(22), pp. 3532–3534. Available at: https://doi.org/10.1093/bioinformatics/btw413.

Levengood, H., Zhou, Y. and Zhang, C. (2024) "Advancements in plant transformation: from traditional methods to cutting-edge techniques and emerging model species," *Plant Cell Reports*, 43(11), p. 273. Available at: https://doi.org/10.1007/s00299-024-03359-9.

Li, S. *et al.* (2003) “The putative Arabidopsis arp2/3 complex controls leaf cell morphogenesis,” *Plant Physiology*, 132(4), pp. 2034–2044. Available at: https://doi.org/10.1104/pp.103.028563.

LINDSAY, D.W., YEOMAN, M.M. and BROWN, R. (1974) “An Analysis of the Development of the Graft Union in Lycopersicon esculentum,” *Annals of Botany*, 38(3), pp. 639–646. Available at: https://doi.org/10.1093/oxfordjournals.aob.a084849.

Liners, F. *et al.* (1989) “Monoclonal Antibodies against Pectin: Recognition of a Conformation Induced by Calcium,” *Plant Physiology*, 91(4), pp. 1419–1424. Available at: https://doi.org/10.1104/pp.91.4.1419.

Lü, B. *et al.* (2012) “AT14A mediates the cell wall–plasma membrane–cytoskeleton continuum in Arabidopsis thaliana cells,” *Journal of Experimental Botany*, 63(11), pp. 4061–4069. Available at: https://doi.org/10.1093/jxb/ers063.

Lu, H. *et al.* (2004) “Microfluidic Shear Devices for Quantitative Analysis of Cell Adhesion,” *Analytical Chemistry*, 76(18), pp. 5257–5264. Available at: https://doi.org/10.1021/ac049837t.

Ma, Y. and Johnson, K. (2023) “Arabinogalactan proteins – Multifunctional glycoproteins of the plant cell wall,” *The Cell Surface*, 9, p. 100102. Available at: https://doi.org/10.1016/j.tcsw.2023.100102.

Maître, J.-L. and Heisenberg, C.-P. (2011) “The role of adhesion energy in controlling cell-cell contacts,” *Current Opinion in Cell Biology*, 23(5), pp. 508–514. Available at: https://doi.org/10.1016/j.ceb.2011.07.004.

Malivert, A. *et al.* (2021) “FERONIA and microtubules independently contribute to mechanical integrity in the Arabidopsis shoot,” *PLoS biology*, 19(11), p. e3001454. Available at: https://doi.org/10.1371/journal.pbio.3001454.

Marsollier, A.-C. and Ingram, G. (2018) “Getting physical: invasive growth events during plant development,” *Current Opinion in Plant Biology*, 46, pp. 8–17. Available at: https://doi.org/10.1016/j.pbi.2018.06.002.

Martinière, A. *et al.* (2011) “Building bridges: formin1 of Arabidopsis forms a connection between the cell wall and the actin cytoskeleton,” *The Plant Journal*, 66(2), pp. 354–365. Available at: https://doi.org/10.1111/j.1365-313X.2011.04497.x.

Martinière, A. *et al.* (2012) “Cell wall constrains lateral diffusion of plant plasma-membrane proteins,” *Proceedings of the National Academy of Sciences*, 109(31), pp. 12805–12810. Available at: https://doi.org/10.1073/pnas.1202040109.

Masson, J. and Paszkowski, J. (1992) “The culture response of Arabidopsis thaliana protoplasts is determined by the growth conditions of donor plants,” *The Plant Journal*, 2(5), pp. 829–833. Available at: https://doi.org/10.1111/j.1365-313X.1992.tb00153.x.

Mathur, J. *et al.* (2003) “Mutations in actin-related proteins 2 and 3 affect cell shape development in Arabidopsis,” *The Plant Cell*, 15(7), pp. 1632–1645. Available at: https://doi.org/10.1105/tpc.011676.

Mathur, J., Koncz, C. and Szabados, L. (1995) “A simple method for isolation, liquid culture, transformation and regeneration of Arabidopsis thaliana protoplasts,” *Plant Cell Reports*, 14(4), pp. 221–226. Available at: https://doi.org/10.1007/BF00233637.

McKenna, J.F. *et al.* (2019) “The cell wall regulates dynamics and size of plasma-membrane nanodomains in Arabidopsis,” *Proceedings of the National Academy of Sciences*, 116(26), pp. 12857–12862. Available at: https://doi.org/10.1073/pnas.1819077116.

Meier, M., Lucchetta, E.M. and Ismagilov, R.F. (2010) “Chemical stimulation of the Arabidopsis thaliana root using multi-laminar flow on a microfluidic chip,” *Lab on a Chip*, 10(16), pp. 2147–2153. Available at: https://doi.org/10.1039/C004629A.

Mellersh, D.G. *et al.* (2002) “H2O2 plays different roles in determining penetration failure in three diverse plant-fungal interactions,” *Plant Journal*, 29(3), pp. 257–268. Available at: https://doi.org/10.1046/j.0960-7412.2001.01215.x.

Melnyk, C.W. (2017) “Plant grafting: insights into tissue regeneration,” *Regeneration (Oxford, England)*, 4(1), pp. 3–14. Available at: https://doi.org/10.1002/reg2.71.

Moore, R. (1984) “Graft formation in Solanum pennellii (Solanaceae),” *Plant Cell Reports*, 3(5), pp. 172–175. Available at: https://doi.org/10.1007/BF00270192.

Mouille, G. *et al.* (2007) “Homogalacturonan synthesis in Arabidopsis thaliana requires a Golgi-localized protein with a putative methyltransferase domain,” *The Plant Journal*, 50(4), pp. 605–614. Available at: https://doi.org/10.1111/j.1365-313X.2007.03086.x.

Mukundan, N.S., Satyamoorthy, K. and Babu, V.S. (2025) “Advancing plant protoplasts: innovative techniques and future prospects,” *Plant Biotechnology Reports* [Preprint]. Available at: https://doi.org/10.1007/s11816-025-00957-1.

Murphy, E. and De Smet, I. (2014) “Understanding the RALF family: a tale of many species,” *Trends in Plant Science*, 19(10), pp. 664–671. Available at: https://doi.org/10.1016/j.tplants.2014.06.005.

Nakhamchik, A. *et al.* (2004) “A Comprehensive Expression Analysis of the Arabidopsis Proline-rich Extensin-like Receptor Kinase Gene Family using Bioinformatic and Experimental Approaches,” *Plant and Cell Physiology*, 45(12), pp. 1875–1881. Available at: https://doi.org/10.1093/pcp/pch206.

Nolan [aut, R. *et al.* (2023) “autothresholdr: An R Port of the ‘ImageJ’ Plugin ‘Auto Threshold.’” Available at: https://cran.r-

project.org/web/packages/autothresholdr/index.html (Accessed: February 19, 2025).

Notaguchi, M. *et al.* (2020) "Cell-cell adhesion in plant grafting is facilitated by β-1,4-glucanases," *Science*, 369(6504), pp. 698–702. Available at: https://doi.org/10.1126/science.abc3710.

Ohlsson, J.A. *et al.* (2024) "SPIRO – the automated Petri plate imaging platform designed by biologists, for biologists," *The Plant Journal*, 118(2), pp. 584–600. Available at: https://doi.org/10.1111/tpj.16587.

O'Neill, M.A. *et al.* (1996) "Rhamnogalacturonan-II, a pectic polysaccharide in the walls of growing plant cell, forms a dimer that is covalently cross-linked by a borate ester. In vitro conditions for the formation and hydrolysis of the dimer," *The Journal of Biological Chemistry*, 271(37), pp. 22923–22930. Available at: https://doi.org/10.1074/jbc.271.37.22923.

O'Neill, M.A. *et al.* (2001) "Requirement of Borate Cross-Linking of Cell Wall Rhamnogalacturonan II for Arabidopsis Growth," *Science*, 294(5543), pp. 846–849. Available at: https://doi.org/10.1126/science.1062319.

Ooms [aut, J. and cre (2024) "magick: Advanced Graphics and Image-Processing in R." Available at: https://cran.r-project.org/web/packages/magick/index.html (Accessed: February 19, 2025).

Oparka, K.J. (1994) "Plasmolysis: new insights into an old process," *New Phytologist*, 126(4), pp. 571–591. Available at: https://doi.org/10.1111/j.1469-8137.1994.tb02952.x.

Pabst, M. *et al.* (2013) "Rhamnogalacturonan II structure shows variation in the side chains monosaccharide composition and methylation status within and across different plant species," *The Plant Journal: For Cell and Molecular Biology*, 76(1), pp. 61–72. Available at: https://doi.org/10.1111/tpj.12271.

Parker, M.L. and Waldron, K.W. (1995) "Texture of Chinese water chestnut: Involvement of cell wall phenolics," *Journal of the Science of Food and Agriculture*, 68(3), pp. 337–346. Available at: https://doi.org/10.1002/jsfa.2740680313.

Pasternak, T., Paponov, I.A. and Kondratenko, S. (2021) "Optimizing Protocols for Arabidopsis Shoot and Root Protoplast Cultivation," *Plants*, 10(2), p. 375. Available at: https://doi.org/10.3390/plants10020375.

Pesquet, E. *et al.* (2010) "The Microtubule-Associated Protein AtMAP70-5 Regulates Secondary Wall Patterning in *Arabidopsis* Wood Cells," *Current Biology*, 20(8), pp. 744–749. Available at: https://doi.org/10.1016/j.cub.2010.02.057.

Piccinini, L., Nirina Ramamonjy, F. and Ursache, R. (2024) "Imaging plant cell walls using fluorescent stains: The beauty is in the details," *Journal of Microscopy*, 295(2), pp. 102–120. Available at: https://doi.org/10.1111/jmi.13289.

Planchais, S., Camborde, L. and Jupin, I. (2023) “Protocols for Studying Protein Stability in an Arabidopsis Protoplast Transient Expression System,” *Methods in Molecular Biology (Clifton, N.J.)*, 2581, pp. 179–199. Available at: https://doi.org/10.1007/978-1-0716-2784-6_13.

Pont-Lezica, R.F., McNALLY, J.G. and Pickard, B.G. (1993) “Wall-to-membrane linkers in onion epidermis: some hypotheses,” *Plant, Cell & Environment*, 16(2), pp. 111–123. Available at: https://doi.org/10.1111/j.1365-3040.1993.tb00853.x.

Pratyusha, D.S. and Sarada, D.V.L. (2025) “Rapid Alkalinization Factor – A cryptide regulating developmental and stress responses,” *Plant Science*, 359, p. 112600. Available at: https://doi.org/10.1016/j.plantsci.2025.112600.

Raggi, S. *et al.* (2015) “The Arabidopsis Class III Peroxidase AtPRX71 Negatively Regulates Growth under Physiological Conditions and in Response to Cell Wall Damage,” *Plant Physiology*, 169(4), pp. 2513–2525. Available at: https://doi.org/10.1104/pp.15.01464.

Razatos, A. *et al.* (1998) “Molecular determinants of bacterial adhesion monitored by atomic force microscopy,” *Proceedings of the National Academy of Sciences of the United States of America*, 95(19), pp. 11059–11064. Available at: https://doi.org/10.1073/pnas.95.19.11059.

Reed, K.M. and Bargmann, B.O.R. (2021) “Protoplast Regeneration and Its Use in New Plant Breeding Technologies,” *Frontiers in Genome Editing*, 3. Available at: https://doi.org/10.3389/fgeed.2021.734951.

Rotman, B., Zderic, J.A. and Edelstein, M. (1963) “FLUOROGENIC SUBSTRATES FOR β-D-GALACTOSIDASES AND PHOSPHATASES DERIVED FROM FLUORESCEIN (3, 6-DIHYDROXYFLUORAN) AND ITS MONOMETHYL ETHER*,” *Proceedings of the National Academy of Sciences*, 50(1), pp. 1–6. Available at: https://doi.org/10.1073/pnas.50.1.1.

Rui, Y. *et al.* (2025) “Cellulose Synthase Complex and Remorin Nanodomains Mediate Stress Resilience Through Cell Wall-Plasma Membrane Attachments.” bioRxiv, p. 2025.08.01.664786. Available at: https://doi.org/10.1101/2025.08.01.664786.

Sackmann, E. and Smith, A.-S. (2014) “Physics of cell adhesion: some lessons from cell-mimetic systems,” *Soft Matter*, 10(11), pp. 1644–1659. Available at: https://doi.org/10.1039/c3sm51910d.

Sakamoto, Y. *et al.* (2022) “Transcriptional activation of auxin biosynthesis drives developmental reprogramming of differentiated cells,” *The Plant Cell*, 34(11), pp. 4348–4365. Available at: https://doi.org/10.1093/plcell/koac218.

Samuels, L., Kunst, L. and Jetter, R. (2008) “Sealing Plant Surfaces: Cuticular Wax Formation by Epidermal Cells,” *Annual Review of Plant Biology*,

59(Volume 59, 2008), pp. 683–707. Available at: https://doi.org/10.1146/annurev.arplant.59.103006.093219.

Schindelin, J. *et al.* (2012) "Fiji: an open-source platform for biological-image analysis," *Nature Methods*, 9(7), pp. 676–682. Available at: https://doi.org/10.1038/nmeth.2019.

Schindler, M., Meiners, S. and Cheresh, D.A. (1989) "RGD-dependent linkage between plant cell wall and plasma membrane: consequences for growth.," *The Journal of cell biology*, 108(5), pp. 1955–1965. Available at: https://doi.org/10.1083/jcb.108.5.1955.

Schirawski, J., Planchais, S. and Haenni, A.L. (2000) "An improved protocol for the preparation of protoplasts from an established Arabidopsis thaliana cell suspension culture and infection with RNA of turnip yellow mosaic tymovirus: a simple and reliable method," *Journal of Virological Methods*, 86(1), pp. 85–94. Available at: https://doi.org/10.1016/s0166-0934(99)00173-1.

Senchou, V. *et al.* (2004) "High affinity recognition of a Phytophthora protein by Arabidopsis via an RGD motif," *Cellular and Molecular Life Sciences (CMLS)*, 61(4), pp. 502–509. Available at: https://doi.org/10.1007/s00018-003-3394-z.

Shafi, A. *et al.* (2019) "Ectopic expression of SOD and APX genes in Arabidopsis alters metabolic pools and genes related to secondary cell wall cellulose biosynthesis and improve salt tolerance," *Molecular Biology Reports*, 46(2), pp. 1985–2002. Available at: https://doi.org/10.1007/s11033-019-04648-3.

Sharkey, J.P. *et al.* (2016) "A one-piece 3D printed flexure translation stage for open-source microscopy," *Review of Scientific Instruments*, 87(2), p. 025104. Available at: https://doi.org/10.1063/1.4941068.

Showalter, A.M. (2001) "Arabinogalactan-proteins: structure, expression and function," *Cellular and molecular life sciences: CMLS*, 58(10), pp. 1399–1417. Available at: https://doi.org/10.1007/PL00000784.

Showalter, A.M. and Basu, D. (2016) "Extensin and Arabinogalactan-Protein Biosynthesis: Glycosyltransferases, Research Challenges, and Biosensors," *Frontiers in Plant Science*, 7. Available at: https://doi.org/10.3389/fpls.2016.00814.

Silva, N.F. and Goring, D.R. (2002) "The proline-rich, extensin-like receptor kinase-1 (PERK1) gene is rapidly induced by wounding," *Plant Molecular Biology*, 50(4–5), pp. 667–685. Available at: https://doi.org/10.1023/a:1019951120788.

Smith, A.G. *et al.* (2022) "RootPainter: deep learning segmentation of biological images with corrective annotation," *New Phytologist*, 236(2), pp. 774–791. Available at: https://doi.org/10.1111/nph.18387.

Somerville, C. (2006) “Cellulose synthesis in higher plants,” *Annual Review of Cell and Developmental Biology*, 22, pp. 53–78. Available at: https://doi.org/10.1146/annurev.cellbio.22.022206.160206.

Stajič, E. (2023) “Improvements in Protoplast Isolation Protocol and Regeneration of Different Cabbage (Brassica oleracea var. capitata L.) Cultivars,” *Plants*, 12(17), p. 3074. Available at: https://doi.org/10.3390/plants12173074.

Stringer, C. *et al.* (2021) “Cellpose: a generalist algorithm for cellular segmentation,” *Nature Methods*, 18(1), pp. 100–106. Available at: https://doi.org/10.1038/s41592-020-01018-x.

Stringer, C. and Pachitariu, M. (2024) “Cellpose3: one-click image restoration for improved cellular segmentation.” bioRxiv, p. 2024.02.10.579780. Available at: https://doi.org/10.1101/2024.02.10.579780.

Svagan, A.J. *et al.* (2014) “Photon Energy Upconverting Nanopaper: A Bioinspired Oxygen Protection Strategy,” *ACS Nano*, 8(8), pp. 8198–8207. Available at: https://doi.org/10.1021/nn502496a.

Tan, L. *et al.* (2013) “An Arabidopsis Cell Wall Proteoglycan Consists of Pectin and Arabinoxylan Covalently Linked to an Arabinogalactan Protein[W],” *The Plant Cell*, 25(1), pp. 270–287. Available at: https://doi.org/10.1105/tpc.112.107334.

Tanaka, T. *et al.* (2004) “A new method for rapid visualization of defects in leaf cuticle reveals five intrinsic patterns of surface defects in Arabidopsis,” *The Plant Journal*, 37(1), pp. 139–146. Available at: https://doi.org/10.1046/j.1365-313X.2003.01946.x.

Terry, S.C., Jerman, J.H. and Angell, J.B. (1979) “A gas chromatographic air analyzer fabricated on a silicon wafer,” *IEEE Transactions on Electron Devices*, 26(12), pp. 1880–1886. Available at: https://doi.org/10.1109/T-ED.1979.19791.

Tolmie, F. *et al.* (2017) “The cell wall of Arabidopsis thaliana influences actin network dynamics,” *Journal of Experimental Botany*, 68(16), pp. 4517–4527. Available at: https://doi.org/10.1093/jxb/erx269.

Ungai-Salánki, R. *et al.* (2019) “A practical review on the measurement tools for cellular adhesion force,” *Advances in Colloid and Interface Science*, 269, pp. 309–333. Available at: https://doi.org/10.1016/j.cis.2019.05.005.

Verger, S. *et al.* (2018) “A tension-adhesion feedback loop in plant epidermis,” *eLife*. Edited by C.S. Hardtke and D.C. Bergmann, 7, p. e34460. Available at: https://doi.org/10.7554/eLife.34460.

Verger, S., Cerutti, G. and Hamant, O. (2018) “An Image Analysis Pipeline to Quantify Emerging Cracks in Materials or Adhesion Defects in Living Tissues,” *Bio-protocol*, 8(19). Available at: https://doi.org/10.21769/BioProtoc.3036.

Verger, S., Liu, M. and Hamant, O. (2019) “Mechanical conflicts in twisting growth revealed by cell-cell adhesion defects,” *Frontiers in plant science*, 10, p. 173.

Voxeur, A. and Fry, S.C. (2014) “Glycosylinositol phosphorylceramides from Rosa cell cultures are boron-bridged in the plasma membrane and form complexes with rhamnogalacturonan II,” *The Plant Journal*, 79(1), pp. 139–149. Available at: https://doi.org/10.1111/tpj.12547.

Wang, Lin *et al.* (2015) “Overexpression of AT14A confers tolerance to drought stress-induced oxidative damage in suspension cultured cells of Arabidopsis thaliana,” *Protoplasma*, 252(4), pp. 1111–1120. Available at: https://doi.org/10.1007/s00709-014-0744-7.

Weber, G.F., Bjerke, M.A. and DeSimone, D.W. (2011) “Integrins and cadherins join forces to form adhesive networks,” *Journal of Cell Science*, 124(8), pp. 1183–1193. Available at: https://doi.org/10.1242/jcs.064618.

Whitewoods, C.D. (2021) “Riddled with holes: Understanding air space formation in plant leaves,” *PLoS Biology*, 19(12), p. e3001475. Available at: https://doi.org/10.1371/journal.pbio.3001475.

Wickham, H. *et al.* (2019) “Welcome to the Tidyverse,” *Journal of Open Source Software*, 4(43), p. 1686. Available at: https://doi.org/10.21105/joss.01686.

Willats, W.G.T. *et al.* (2001) “Modulation of the Degree and Pattern of Methyl-esterification of Pectic Homogalacturonan in Plant Cell Walls: IMPLICATIONS FOR PECTIN METHYL ESTERASE ACTION, MATRIX PROPERTIES, AND CELL ADHESION*,” *Journal of Biological Chemistry*, 276(22), pp. 19404–19413. Available at: https://doi.org/10.1074/jbc.M011242200.

Winklbauer, R. (2015) “Cell adhesion strength from cortical tension - an integration of concepts,” *Journal of Cell Science*, 128(20), pp. 3687–3693. Available at: https://doi.org/10.1242/jcs.174623.

Wolf, S. (2017) “Plant cell wall signalling and receptor-like kinases,” *Biochemical Journal*, 474(4), pp. 471–492. Available at: https://doi.org/10.1042/BCJ20160238.

Wu, F.-H. *et al.* (2009) “Tape-Arabidopsis Sandwich - a simpler Arabidopsis protoplast isolation method,” *Plant Methods*, 5(1), p. 16. Available at: https://doi.org/10.1186/1746-4811-5-16.

Xia, Y. and Whitesides, G.M. (1998) “Soft Lithography,” *Angewandte Chemie (International Ed. in English)*, 37(5), pp. 550–575. Available at: https://doi.org/10.1002/(SICI)1521-3773(19980316)37:5%253C550::AID-ANIE550%253E3.0.CO;2-G.

Xu, Y. *et al.* (2022) “Protoplasts: small cells with big roles in plant biology,” *Trends in Plant Science*, 27(8), pp. 828–829. Available at: https://doi.org/10.1016/j.tplants.2022.03.010.

Yanagisawa, N. *et al.* (2021) “Microfluidics-Based Bioassays and Imaging of Plant Cells,” *Plant and Cell Physiology*, 62(8), pp. 1239–1250. Available at: https://doi.org/10.1093/pcp/pcab067.

Yetisen, A.K. *et al.* (2011) “A microsystem-based assay for studying pollen tube guidance in plant reproduction,” *Journal of Micromechanics and Microengineering*, 21(5), p. 054018. Available at: https://doi.org/10.1088/0960-1317/21/5/054018.

Yoneda, A. *et al.* (2020) “Hechtian Strands Transmit Cell Wall Integrity Signals in Plant Cells,” *Plants*, 9(5), p. 604. Available at: https://doi.org/10.3390/plants9050604.

Yoo, S.-D., Cho, Y.-H. and Sheen, J. (2007) “Arabidopsis mesophyll protoplasts: a versatile cell system for transient gene expression analysis,” *Nature Protocols*, 2(7), pp. 1565–1572. Available at: https://doi.org/10.1038/nprot.2007.199.

Zamil, M.S. and Geitmann, A. (2017) “The middle lamella-more than a glue,” *Physical Biology*, 14(1), p. 015004. Available at: https://doi.org/10.1088/1478-3975/aa5ba5.

Zamil, M.S., Yi, H. and Puri, V.M. (2014) “Mechanical characterization of outer epidermal middle lamella of onion under tensile loading,” *American Journal of Botany*, 101(5), pp. 778–787. Available at: https://doi.org/10.3732/ajb.1300416.

Zehrer, A.C. *et al.* (2023) “An open-source, high resolution, automated fluorescence microscope.” bioRxiv, p. 2023.05.31.542706. Available at: https://doi.org/10.1101/2023.05.31.542706.

Zhang, G. *et al.* (2025) “Cell wall remodeling during plant regeneration,” *Journal of Integrative Plant Biology*, 67(4), pp. 1060–1076. Available at: https://doi.org/10.1111/jipb.13911.

Zhang, X., Zhao, J. and LeCun, Y. (2016) “Character-level Convolutional Networks for Text Classification.” arXiv. Available at: https://doi.org/10.48550/arXiv.1509.01626.

Zheng, Y. *et al.* (2021) “Microfluidic droplet-based functional materials for cell manipulation,” *Lab on a Chip*, 21(22), pp. 4311–4329. Available at: https://doi.org/10.1039/d1lc00618e.

Popular science summary

In plants, each cell is enclosed by a structure called cell wall, which surrounds the inner living part known as the protoplast. The cell wall functions much like the mortar between bricks: it holds cells together, provides structural support, and shields them from environmental challenges such as drought, pathogens, or mechanical forces like wind. Unlike mortar, however, the cell wall is not fixed. It is constantly remodelled, allowing plants to grow, adjust to internal pressures, and respond to external stresses.

While the importance of adhesion in plants is well established, the actual strength of these adhesive forces remains largely unknown. This knowledge gap is due to the absence of reliable methods for directly measuring such forces in plants.

This thesis seeks to overcome that limitation by adapting techniques originally developed for animal cells and applying them to plant systems. These newly developed methods make it possible, for the first time, to quantify the forces that both bind plant cells together and link the protoplast to its wall. In doing so, they lay the foundation for a deeper understanding of the mechanisms underlying adhesion and mechanical resistance in plant tissues.

Populärvetenskaplig sammanfattning

I växter är varje cell omgiven av en struktur som kallas cellvägg, som omger den inre levande delen som kallas protoplast. Cellväggen fungerar ungefär som murbruk mellan tegelstenar: den håller ihop cellerna, ger strukturellt stöd och skyddar dem från miljöfaktorer som torka, patogener eller mekaniska krafter som vind. Till skillnad från murbruk är cellväggen dock inte fast. Den omformas ständigt, vilket gör att växterna kan växa, anpassa sig till inre tryck och reagera på yttre påfrestningar.

Även om vidhäftningens betydelse i växter är väl etablerad, är den faktiska styrkan hos dessa vidhäftningskrafter fortfarande i stort sett okänd. Denna kunskapslucka beror på avsaknaden av tillförlitliga metoder för att direkt mäta sådana krafter i växter.

Denna avhandling syftar till att övervinna denna begränsning genom att anpassa tekniker som ursprungligen utvecklats för djurceller och tillämpa dem på växtsystem. Dessa nyutvecklade metoder gör det för första gången möjligt att kvantifiera de krafter som både binder samman växtceller och kopplar protoplasten till dess vägg. På så sätt lägger de grunden för en djupare förståelse av de mekanismer som ligger till grund för vidhäftning och mekanisk resistens i växtvävnader.

Synthèse de vulgarisation

Chez les plantes, chaque cellule est constituée d'un protoplaste entouré de sa paroi cellulaire. A l'image du mortier entre des briques, cette paroi permet de maintenir les cellules ensembles pour former des organismes multicellulaires. La paroi a aussi pour rôle de rigidifier la structure et de protéger les cellules contre divers stresses biotiques (pathogènes) ou abiotiques (sècheresse, …). Cependant, contrairement au ciment, la paroi est dynamique et en constant renouvellement pour permettre à la plante de faire face aux nombreuses contraintes mécaniques. Ces contraintes proviennent tant de facteurs externes, comme le vent, ou qu'à des tensions internes liées à la croissance et la multiplication des cellules.

Bien que l'importance de l'adhésion cellulaire soit établie, peu d'informations sont disponibles quant à la force d'adhésion entre deux cellules ou entre une cellule et sa paroi. Ce manque de connaissance est lié à l'absence de méthodes existant pour quantifier ces forces chez les plantes.

En prenant appui sur des techniques développées pour l'étude des cellules animales, cette thèse présente de nouveaux outils pour mesurer les forces impliquées à la fois pour maintenir les cellules ensemble mais aussi le lien entre le protoplaste et sa paroi. Ces approches ouvrent la voie à une compréhension plus précise des mécanismes d'adhésion et de résistance mécanique dans les tissus végétaux.

Acknowledgements

First, I would like to thank my supervisor **Stéphane Verger**. You allowed me to come here in Sweden and work on plants even though that was not my educational background. But also, I learned as much in plant biology than in microscopy, 3D printing, electronics and programming, which are now at least hobbies and hopefully will also be part of my future job. You also supported me when the machines were letting me down and pushed me to learn anything I wanted to. So, merci for the freedom and open-mindedness!

Thank you to the **Verger team** present and past members for your help and discussions about cell-cell adhesion. Special thanks to **Giannis**, who did not leave me alone with handling the cell culture and shared the trip to Vienna and the loneliness with all the animal cell people.

Many thanks to my interns, **Ambroise** and **Jeanne**, you both worked hard and helped me a lot. It was fun to show you everything as much as learn from you as well.

I would like to thank my PhD committee: **Ewa Mellerowicz**, **Totte Niittylä** and **Magnus Andersson** for your enthusiasm about the project progress, and a special thanks to Magnus who helped me more than once with physical concepts.

I also would like to thank **Åsa Strand** and **Xu Jin** for providing us the cell culture and showing me how to keep it healthy as well as the authorization to use the C-Trap.

Special thanks to **Jan Karlsson** and **Marta Derba-Maceluch** who both helped me to set up new experiments.

Many thanks to **Rubén Casanova-Sáez** who worked hard on the C-Trap experiments when I was not in the best PhD mood.

Thanks to **Ioanna Antoniadi** and **Vladimír Skalický** for all your help and support with the FACS and feedback.

I would like to thank the **microscopy platform**, the **greenhouse**, the **administration** and **other UPSC staff** to create a nice work environment where we can do experiments as smoothly as possible.

I would like to thank the **FATE consortium**. I really appreciated to be part of such a big project with such cool novel techniques and approaches!

Madeleine Ramstedt, thank you for the ZetaSizer training but also for your enthusiasm and willingness to help.

Thank you to **Dmitry Malyshev** and **Daniel Nilsson** for your comments and help on the C-Trap analysis and sometimes on microfluidics.

I would like to thank **Roushdey Sahl** for the cleanroom training and keeping the access open for my experiments.

I am grateful to **Anna Svagan**, who welcomed me to her lab to teach me layer-by-layer coating.

Many thanks to **Joris Sprakel**, **Patricia Schöppl** and **Rik Froeling** for showing interest and collaborating on the Q-Warg paper.

Merci **Jacques Fattaccioli** for all your help on microfluidics.

To the **conspiracy table**, even though I was not present that often, it was always a good break to have lunch with all of you. Special mention to the adventurers, I hope we will manage to continue our quest.

Tack så mycket to the **Rundvik families** and **Nordmaling associates** to make me feel welcome and appreciated. I hope to spend many more afternoons with all our loud kids around or maybe evenings without them...

Candice, merci pour toutes les histoires, si j'avais la moitié de ton énergie, j'en serai probablement à ma 2e thèse.

Eli, Sandy, merci pour les encouragements et les soirées jeux ! Vivement qu'on puisse se refaire une soirée punch et potins IRL (= in real life, Eli)!

Mireille, **José**, merci de m'avoir acceptée dans la famille en tant que presque bru.

And now to those without who I would for sure not be the same…

Père, Mère vous m'avez toujours poussé à faire ce que je voulais en étude ou en dehors. Si j'en suis là c'est définitivement parce que vous m'avez aidée et laissée faire ! Merci de tout votre soutien, je vous aime fort mes parents hélicoptères.

Mes sœurs, Axoul, Rox, merci d'être là et de faire au moins semblant de vous intéresser à mon travail et de me dire que ça va aller. Même si c'est parfois de loin, je vous aime pour toujours.

Martin, **Méloé** et **Laelio**, vous avez tous les 3 une place spéciale. Nièce et neveu, j'ai hâte de vous emmener en vadrouille (sans vos parents) et de vous apprendre moult bêtises.

Last but for sure not least… **Mon aimé**, merci d'avoir toujours confiance en moi et de me pousser à me faire confiance. Merci de me m'encourager et de me suivre pour tout et n'importe quel projet. On est la meilleure équipe. (Et aussi merci d'avoir enduré la lecture complète et les quelques meltdowns…) Jag älskar dig så jättemycket. **Ma Mistouille**, grâce à toi, je sais que le travail n'est vraiment pas tout. Merci de m'avoir « forcée » à prendre des vraies pauses et à remplir ma tête avec des moments bien plus importants. Je t'aime jusqu'au soleil, jusqu'aux étoiles et jusqu'à la lune.

I

Quantitative Plant Biology

cambridge.org/qpb

Characterising the mechanics of cell–cell adhesion in plants

Asal Atakhani, Léa Bogdziewiez and Stéphane Verger

Department of Forest Genetics and Plant Physiology, Umeå Plant Science Centre, Swedish University of Agricultural Sciences, Umeå, Sweden

Review

Cite this article: A. Atakhani et al. Characterising the mechanics of cell–cell adhesion in plants. *Quantitative Plant Biology*, **3**:e2, 1–13
https://dx.doi.org/10.1017/qpb.2021.16

Received: 8 September 2021
Revised: 7 December 2021
Accepted: 9 December 2021

Keywords:
adhesion strength; cell–cell adhesion; multicellularity; plant; single cell; tissue.

Author for correspondence:
S. Verger,
E-mail: stephane.verger@slu.se
Atakhani and Bogdziewiez contributed equally to this work.

Abstract

Cell–cell adhesion is a fundamental feature of multicellular organisms. To ensure multicellular integrity, adhesion needs to be tightly controlled and maintained. In plants, cell–cell adhesion remains poorly understood. Here, we argue that to be able to understand how cell–cell adhesion works in plants, we need to understand and quantitatively measure the mechanics behind it. We first introduce cell–cell adhesion in the context of multicellularity, briefly explain the notions of adhesion strength, work and energy and present the current knowledge concerning the mechanisms of cell–cell adhesion in plants. Because still relatively little is known in plants, we then turn to animals, but also algae, bacteria, yeast and fungi, and examine how adhesion works and how it can be quantitatively measured in these systems. From this, we explore how the mechanics of cell adhesion could be quantitatively characterised in plants, opening future perspectives for understanding plant multicellularity.

1. Multicellularity and cell-adhesion mechanics

All living organisms are exposed to physical stresses such as tension and compression, that are experienced during growth and development, or imposed by external stimuli. At the supracellular level, tension has been found to pull adjacent cells apart in mutant organisms in which the proper control of cell–cell adhesion is defective (Thomas et al., 2013; Verger et al., 2018). However, living organisms have evolved mechanisms to continuously respond and adapt to these mechanical forces to ensure the maintenance of their cellular and supracellular integrity (Hamant & Saunders, 2020; Hannezo & Heisenberg, 2019; Trinh et al., 2021). In turn, cell–cell adhesion not only enables adjacent cells to stick to each other in a passive manner, but it is also dynamically controlled and maintained over time during growth and development (Baum & Georgiou, 2011; Leckband & de Rooij, 2014; Yap et al., 2018). The precise fine-tuning of adhesion tightening and loosening ensures tissue cohesion and integrity while allowing cell migration (in animals) or, for example, intrusive cell growth (e.g., fibre cell elongation in wood formation; Gorshkova et al., 2012; Marsollier & Ingram, 2018), developmentally controlled organ abscission (e.g., leaf or petal shedding in plants; Olsson & Butenko, 2018) and cell separation (e.g., lateral root emergence, root cap shedding or intercellular space formation; Stoeckle et al., 2018) in plants. Understanding the mechanics of cell adhesion and how adhesion resists and adapts to separating forces is thus crucial to understand how multicellularity is successfully achieved through cell adhesion.

2. Cell-adhesion mechanics: strength, work and energy

The physics of adhesion is highly studied for a number of industrial applications, and some of this well-established knowledge can also be applied to the question of cell adhesion in living organisms (Creton & Ciccotti, 2016; Packham, 2017). When characterising adhesion mechanics, it is common to refer to the term adhesion 'strength', but adhesion 'work' and 'energy' are two other parameters describing the adhesion mechanics that should also be considered. A first estimation of adhesion mechanics (strength and work) can be obtained by simply pulling apart the adhesive cells and measuring the force required to separate them. Strictly speaking, it is

John Innes Centre
Unlocking Nature's Diversity
CAMBRIDGE UNIVERSITY PRESS

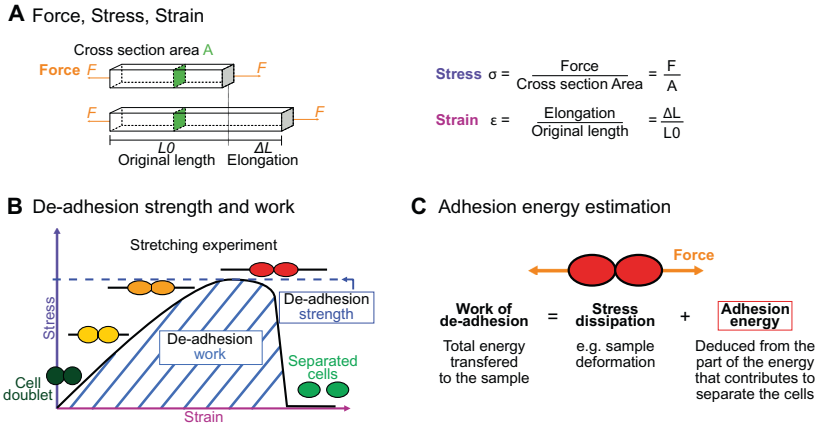

Fig. 1. Mechanics of cell adhesion. (a) Force, stress and strain. When a force (orange arrow) is applied on an object, it generates a mechanical stress and a strain (deformation). The stress corresponds to the ratio of the force *F* applied to the cross-sectional area *A* of the object on which the force is applied. The strain is the ratio of the elongation ΔL of the object to the original length L_0 of the object. (b) De-adhesion strength and work. When a doublet of cells is stretched apart, the cells are deformed (strain) and the stress in the sample increases until the stress is high enough to break the links between the cells. The maximal amount of stress applied before the cells detached from each other corresponds to the de-adhesion strength (blue dashed line). The area under the stress–strain curve is measured as the de-adhesion work (blue hatched area). After separation, the cell shape can be changed due to their plasticity. (c) Adhesion energy can in principle be deduced from the work of de-adhesion by considering stress dissipation.

in fact not directly a measure of the adhesion; instead, adhesion mechanics is inferred from measuring the de-adhesion. When performing a de-adhesion experiment, both the amount of force applied and the deformation of the cells can be measured, extracting the relation of the exerted force due to the applied displacement. Using the geometry of the sample and the values of force and displacement, a stress–strain curve can be generated (Figure 1a,b). From this curve, both adhesion strength and work can be calculated. The de-adhesion strength is determined by the maximal (ultimate) stress that was applied before the cells separated (Figure 1b). De-adhesion work corresponds to the energy that is transferred to the sample during the stretching. It is a function of both the amount of force and displacement (pulling) and is thus calculated as the area under the stress–strain curve of the de-adhesion experiment (Figure 1b). By contrast, the adhesion energy, which corresponds to the force generated by the molecular bonds formed between the cells, is not directly measurable with these approaches (Maître & Heisenberg, 2011; Sackmann & Smith, 2014; Winklbauer, 2015). Although it is in principle possible to infer the de-adhesion energy from a pulling experiment (Figure 1c), when energy is transferred to the sample by stretching, much of this energy can be dissipated in elastic and plastic deformation (extension) of the sample. The energy is either temporarily stored in the elastic deformation, or consumed in breaking molecular bonds within the sample, creating irreversible extension rather than separation at the cell–cell interface (Arroyo & Trepat, 2017). Other factors such as cell geometry and pre-existing stress can further contribute positively or negatively in dissipating the stress (da Silva et al., 2018; Lenne et al., 2021). It is thus complex to separate the effect of stress dissipation and infer the underlying de-adhesion energy and further the adhesion energy. Models from soft matter physics of adhesion have been proposed to predict adhesion energy in living cells, where cells are approximated to solid homogeneous spheres (Brochard-Wyart & de Gennes, 2009; Chu et al., 2005).

Because we know very little about the mechanics of cell–cell adhesion in plants, in this review, our aim is to explore our knowledge of cell adhesion in general and hypothesise on how the mechanics of adhesion could be quantitatively characterised in plants.

3. Cell–cell adhesion in plants

Adhesion between plant cells is mediated by their cell walls (Figure 2; Bou Daher & Braybrook, 2015; Jarvis et al., 2003; Knox, 1992). While adhesion is first established during cell division, each cell then synthesises its own cell wall through the secretion of polysaccharides (cellulose, hemicelluloses and pectins) and structural glycoproteins (Anderson & Kieber, 2020), creating a layered structure with a pectin-rich middle lamella between the walls of adjacent cells (Zamil & Geitmann, 2017). Beyond the middle lamella, tricellular junction and the edges of partially separated cells may represent mechanical hotspots in which mechanical stress is focused and adhesion is specifically reinforced (Jarvis, 1998; Roland, 1978; Willats et al., 2001). On the other hand, while strategically located, the contribution of plasmodesmata (intercellular channels) for cell–cell adhesion strength remains to be characterised. Overall, the cross-linking of the cell wall polysaccharides creates a continuous polysaccharide network that ensures cell–cell adhesion (Figure 2; Anderson & Kieber, 2020). Nevertheless, pectins, which are the main constituents of the middle lamella, are generally considered to be the main determinant of cell adhesion in the early stage of tissue growth and development (Bou Daher & Braybrook, 2015). Pectins are, in fact, a complex set of polysaccharides mainly composed of homogalacturonans (HGs), rhamnogalacturonans I, and rhamnogalacturonans II (RGIIs; Anderson, 2019). The HG is a linear chain of galacturonic acids (GalAs) that is

https://doi.org/10.1017/qpb.2021.16 Published online by Cambridge University Press

synthesised in a highly methyl esterified form, and that can be de-esterified after secretion to the cell wall by proteins called pectin methylesterases (Hocq et al., 2017). The de-esterification process leaves negatively charged residues on the GalAs, and if more than 9 consecutive de-esterified GalAs are present, they can form calcium-mediated bridges with another de-esterified HG under the so-called egg-box conformation, effectively cross-linking independent HG chains potentially coming from adjacent cells (Huxham et al., 1999; Jarvis & Apperley, 1995; Liners et al., 1989; Willats et al., 2001). Similarly, RGII, a very complex polysaccharide (Bar-Peled et al., 2012), also allows cross-linking of polymers through dimerisation mediated by the presence of Boron (O'Neill et al., 2001). The importance of these types of cross-linking for cell adhesion has been supported by the characterisation of cell-adhesion defective mutants. For instance, in Arabidopsis, several mutations in genes involved in HG synthesis (Bouton et al., 2002; Du et al., 2020; Lathe et al., 2021; Mouille et al., 2007; Temple et al., 2021), remodelling (Francis et al., 2006; Lionetti et al., 2015) or degradation (Ogawa et al., 2009; Rhee et al., 2003; Rui et al., 2019) harbour cell-adhesion phenotypes (loss of cell adhesion or incapacity of cell separation). Furthermore, selectively digesting the cell wall with pectin degrading enzymes, such as polygalacturonases, and even chelating the cell wall calcium with chelators, such as EDTA, can also lead to cell separation (Letham, 1960; McCartney & Knox, 2002; Ng et al., 2000; Zhang et al., 2000). However, not all cell types can be separated with these approaches (McCartney & Knox, 2002). Different tissues, cell types and even cell faces have significantly different cell wall compositions, and adhesion in those different contexts may rely on a different combination of polysaccharides and cross-links. Other work suggests that these are not the only molecular links that are responsible for cell adhesion and ferulic acids (Ng et al., 1997) as well as xyloglucan-like polysaccharide may, for instance, be involved (Ikegaya et al., 2008; Ordaz-Ortiz et al., 2009). Furthermore, during abscission events, many cell wall remodelling enzymes, other than pectin degrading enzymes, get expressed and likely act in concert with the pectin degrading enzymes to promote cell separation (Cai & Lashbrook, 2008; Lashbrook & Cai, 2008; Meir et al., 2010). The recent isolation and characterisation of the suppressor of an Arabidopsis mutant deficient in HG and showing cell-adhesion defect also revealed that adhesion could be restored without directly compensating for the HG deficiency in the cell wall (Verger et al., 2016). The loss of cell adhesion in these HG-deficient mutants may instead be largely due to secondary responses to cell wall integrity defects and further cell wall degradation (Du et al., 2020). Thus, other components and cross-links in the primary cell wall likely also play an important role in cell–cell adhesion. Although much less described, when transitioning to secondary cell wall formation, the pectins appear to be largely replaced by lignins which in turn take up the role of keeping the cells attached (Ciesielski et al., 2014; Li & Chapple, 2010; Yang et al., 2020). Similarly, other plant species, like most grass, have cell walls that contain very small amounts of pectins, such that adhesion should rely on different types of cross-links in these plants. Overall, a number of studies have started to investigate the chemical basis of cell adhesion. Furthermore, many of the cell wall properties and modifications identified as playing a role in adhesion have been correlated in other studies with specific mechanical properties (Grones et al., 2019; Zhang et al., 2019). For instance, de-esterification of the HG can lead to a stiffening of the cell wall due to increased calcium mediated cross-linking and could thus correlate with a stronger adhesion (Willats et al., 2001). On the other hand, pectin de-esterification has also been associated with cell wall softening (Peaucelle et al., 2011; Wang et al., 2020). This could be a consequence of a higher susceptibility of de-esterified HG to pectin degrading enzymes [e.g., polygalacturonases (PGs)] or result from electrostatic repulsion of the carboxyl groups (Cosgrove & Anderson, 2020; Haas et al., 2020; 2021; Wang et al., 2020). Thus, while pectin digestion by PGs would lead to cell separation, cell wall softening without HG degradation could instead make the cell–cell connection more elastic and resilient to external stress and strain (da Silva et al., 2018). Similarly, while increased calcium-mediated cross-linking is intuitively expected to make adhesion stronger, the matrix stiffening could instead make the cell–cell interface more brittle and increase the risk of cell wall fracture and cell separation. However, at this point, it remains very difficult to predict how chemical modifications of the cell wall affect the mechanical properties of the cell wall (Zhang et al., 2016) and furthermore how the mechanical properties of the cell wall affect adhesion strength, work and energy.

Beyond direct cell wall regulators, a number of molecular players are known to be involved in the regulation of cell-adhesion maintenance and developmentally regulated cell separation. So far, most interest has been given to the signalling events leading to cell separation (Olsson & Butenko, 2018). Briefly, patterning transcription factors define abscission and dehiscence zones (Mao et al., 2000), and auxin and ethylene act, respectively, as inhibitors and activators of the abscission process (Meir et al., 2010), which is then regulated by small peptides and receptor-like kinase signalling (Stenvik et al., 2008). This triggers a mitogen-activated protein (MAP) kinase signalling cascade which ultimately activates transcription factors that promote the expression of cell wall remodelling enzymes leading to cell wall digestion and cell separation (Shi et al., 2011). On the other hand, much less is known about the molecular mechanisms that contribute to maintaining cell adhesion during growth and development, but the isolation of various cell-adhesion defective mutants brings some clues. For instance, in Arabidopsis, mutants defective in actin filament nucleation (Le et al., 2003; Mathur et al., 2003a; 2003b; Qiu et al., 2002; Saedler et al., 2004), a putative mechanosensitive calcium channel (Galletti et al., 2015; Tran et al., 2017) and epidermal identity transcription factors (Abe et al., 2003), show cell-adhesion defects. Interestingly, these mutants hint at a complex regulation of cell-adhesion maintenance through mechanical feedback as well as developmental control. Much remains to be clarified about the actual mechanochemical basis of cell–cell adhesion in plants. On the other hand, our understanding of cell adhesion in animals is much more advanced in part due to the existence of quantitative micromechanical methods to measure cell-adhesion mechanics.

4. Cell adhesion in animals, fungi, bacteria and algae

In animals, cell–cell and cell–substrate adhesion is primarily mediated by a group of proteins called cell-adhesion molecules (CAMs), that includes the cadherins (Halbleib & Nelson, 2006; Leckband & de Rooij, 2014) and integrins (Iwamoto & Calderwood, 2015; Lodish et al., 2008; Roberts et al., 2002). The CAMs are transmembrane proteins that harbour an extracellular domain at the surface of the cell, that can either bind to another CAM, the extracellular matrix or a substrate (Figure 2). They organise in patches called cell junctions that are responsible for cell–cell and cell–substrate adhesion, and mediate the dynamics of motile cells. During cell–cell adhesion, the cadherins also interact with the actin network

https://doi.org/10.1017/qpb.2021.16 Published online by Cambridge University Press

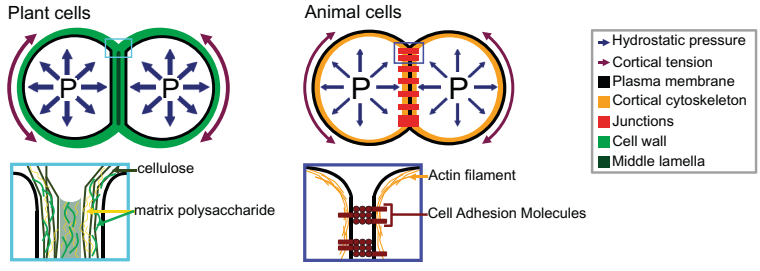

Fig. 2. Adhesion in plant and animal cells. The top drawings represent cell doublets, and the bottom drawings are close-up representations of the edge of the cell–cell interface. In both plant (left) and animal (right) cells, the cell shape is governed by an equilibrium between the internal hydrostatic pressure and the cortical tension. The plant cell adhesion is mediated by a cell wall mostly composed of cellulose and matrix polysaccharides. At the interface, the middle lamella is enriched in pectins and believed to play an important role in adhesion. The animal cell adhesion is mediated via proteins located at the plasma membrane. Cell-adhesion molecules are linked to the actin cytoskeleton which contributes to the cortical tension.

through the catenins and vinculin (Halbleib & Nelson, 2006; Harris & Tepass, 2010; Hartsock & Nelson, 2008). Together they form a mechanosensing complex sensitive to intrinsic (actin/myosin contractility) and extrinsic mechanical signals (Yap et al., 2018). Any force in the range of 5 pN, such as the force generated by the movement of myosin II motor in the cytoskeleton, can cause a conformational change of the α-catenin and increase the affinity to vinculin. The recruited vinculin promotes actin nucleation and the recruitment of additional cadherins, which changes the cell's mechanical properties and cell-adhesion strength (Pinheiro & Bellaïche, 2018; Yap et al., 2018). But comparing the cadherin binding energy (5×10^{-20} J per cadherin) to the cell–cell binding energy (0.02–4.1 mJ/m^2) reveals the need for essential factors to justify the adhesion strength as the role of cadherin–cadherin junctions are less than 30%. The cadherin–cadherin adhesion tension is just enough to create contacts between the cells. Studying the cell junctions showed that the adhesion strength is either due to an increased overall cortical tension or the increase in cadherin density in the cortex (Winklbauer, 2015). In parallel to cell–cell adhesion, during cell–substrate adhesion, integrins interact with the substrate as well as with actin network through the talin and vinculin (Zamir & Geiger, 2013). As for cell–cell adhesion, tension induces adhesion strengthening leading to the formation of focal adhesions sites at the end of so-called actin stress fibres (Haase et al. 2014; Harris et al., 2012; Kuo, 2014; Rosen & Dube, 2006). For more detailed information on the molecular mechanism of adhesion in animals, see Garcia and Gallant (2003), Harris and Tepass (2010), Leckband and de Rooij (2014) and Pinheiro and Bellaïche (2018).

Further away from the animal cells are fungi, bacteria and algae. Because of their cell wall, cell adhesion in these organisms may be more similar to plant cells. These organisms are found in the form of unicellular biofilms and multicellular organisms depending on the environmental conditions and species (Carpentier, 2014; de Groot et al., 2013; Hall-Stoodley et al., 2004; Nagy et al., 2018; Raven & Giordano, 2014; Sheng et al., 2007). In many of these organisms, cell–substrate adhesion has been intensively studied. In general, it is a two-stage process, starting with a passive adhesion followed by an active adhesion. The passive adhesion is the first stage of the attachment, and it is reversible (Jones, 1994; Lebret et al., 2009; Razatos et al., 1998). This is mediated by the pre-existing cell wall or extracellular matrix and happens due to the existence of Van der Waals Forces, short-range hydrophobic interactions, electrostatic interactions and hydrogen bonding between the cell wall and the substrate. In the active adhesion stage, the organisms further generate a glue-like substance in aqueous environments to enhance the adherence to the substrate or the host cell. There is a large diversity of components in the cell wall and the extracellular matrix of living organisms that can bind to and alter the substrate. This creates strong anchorage between an organism and its substrate or host cells (Epstein & Nicholson, 2016; Kostakioti et al., 2013). For further information on the molecular mechanism of adhesion in fungi, bacteria and algae, see Nagy et al. (2018), Raven and Giordano (2014) and Tuson and Weibel (2013).

Overall, research on the characterisation of cell–cell adhesion mechanics is already quite advanced concerning animal cells. Similarly, much research on mechanical characterisation of cell–substrate adhesion have been done in animals, bacteria, yeast, algae and fungi. On the other hand, mechanical and quantitative characterisation of cell adhesion in plants is largely lacking to date. The mechanics of adhesion is also different in principle from that of animal cells, since in plants and other walled organisms, adhesion is mediated by their large cell wall, whereas in animals, it is mediated by clusters of adhesion proteins located at the cell surface. During the de-adhesion process, walled cells may separate from crack initiation in the cell wall and propagation in a manner similar to a crack in a hydrogel (Arroyo & Trepat, 2017; Creton & Ciccotti, 2016) rather than by the dissociation of CAMs (proteins, e.g., cadherins). In plants, a distinct cell wall layer, the middle lamella (Zamil & Geitmann, 2017), plays the role of interface between adjacent cells, and when cells separate, such cracks may preferentially propagate along the middle lamella when it is weakened. Furthermore, compared to animals, adhesion in plants appears as a less dynamics process because it is mediated by their rigid cell wall. But adhesion in plants is not static as cells can detach, reattach and grow intrusively. Interestingly, the active stage of cell–substrate adhesion described for yeast, algae and fungi could share functional similarities with the mechanisms of cell–cell adhesion maintenance in plant or the mechanisms allowing plant grafting. In turn, unicellular green algae with cell wall composition similar to that of embryophytes (true plants) have been proposed as models to understand plant cell–cell adhesion (Domozych et al., 2007, 2014). As such, the methods applied to study cell–

https://doi.org/10.1017/qpb.2021.16 Published online by Cambridge University Press

substrate adhesion in these 'walled' organisms could also be useful to understand cell–cell adhesion in plants.

5. Methods to quantify cell adhesion

5.1. Quantifying large-scale cell–substrate adhesion

Most of the early adhesion measurement methods that have been developed focused on measuring cell–substrate adhesion. They are based on applying shear stress on cells thanks to fluid flow or centrifugation and study a large number of cells at once to obtain a relative value for adhesion strength (i.e., percentage of cells detached by a given force). The plate-and-wash assay was the first quantitative method developed to measure cell-adhesion strength. In this method, the cells are placed in contact with a substrate for a certain time in order to let them adhere to the substrate (Klebe, 1974). Then a washing step is executed by removing the growth medium and replacing it with a new one. The flow created by the removal and addition of the medium creates shear stress that leads to the detachment of the least adhesive cells (Figure 3a). The number of cells attached is thus counted before and after this washing step. This technique gives a first idea of the adhesion between a cell type and a substrate; however, it lacks sensitivity, and the applied forces are weak and very difficult to control (Alam et al., 2019). To contravene these limitations, more advanced fluidic-based assays have been developed (Figure 3). In the centrifugation assay, the sample and the substrate are placed in 96-well plates allowing multiple measurements at the same time. A controlled detachment force, perpendicular to the cell–substrate contact area, is applied directly on the cells removing the nonadherent cells from the substrate surface (Figure 3b). Again, the number of cells is counted before and after the application of a force which in this case can be calculated more precisely based on the properties of the centrifuge. In another type of approach based on hydrodynamic flow, a fluid flow passing in a channel over a large population of adherent cells creates a detachment shear force (Figure 3c; Garcia & Gallant, 2003). In this case, the shear stress can also be determined precisely, and depends on the cross-sectional area of the channel containing the cells and through which the fluid is passing, the viscosity of the fluid and the flow rate (Ungai-Salánki et al., 2019). Several shapes of flow chambers exist like the radial flow chamber, the spinning disc or the parallel plate assay (Figure 3c; García et al., 1997; Kooten et al., 1992; Ungai-Salánki et al., 2019). More recently, microfluidic devices have replaced these flow chambers. Micrometer range channels ensure a laminar flow, and the microfabrication allows complex designs with multiple channels of increasing sizes which allows for a large range of fluid velocities, including high shear stress (Figure 3d; Christ et al., 2010; Lu et al., 2004). This is a major improvement for this approach since many cell-adhesion measurement techniques are limited by the amount of force that can be applied to the cells. Overall, these methods have been proved very useful to understand cell–substrate adhesion and have been largely improved in terms of accuracy, but they are designed and often limited to the study of cell–substrate adhesion rather than cell–cell adhesion.

5.2. Cell shape-based adhesion energy estimation

Computational imaging techniques can be used to study the cell–cell or cell–substrate adhesion mechanics in a noninvasive manner (Veldhuis et al., 2017). They are based on studying the mechanical equilibrium between the cell's cortical tension and adhesion (Figure 3e). More precisely, the cell's hydrostatic pressure creates a cortical tension at the surface of the cell, such that a single cell tends to minimise its surface tension and therefore becomes spherical (Winklbauer, 2015). However, when two cells are attached to each other or a cell adheres to a substrate, a flat contact interface is formed where the adhesion takes place, which goes against minimising the cell's surface tension. In this case, the adhesion energy is high enough to counteract the surface tension that would make the cell round. In turn, knowing the cortical tension and cell geometry, it is possible to deduce the adhesion energy when assuming the cells generally behave as fluids. This approach can be extended to a tissue where the cells still minimise their surface tension but are adherent to other cells and similarly the shape of the cells will then depend on an equilibrium of the adhesion and the cortical tension (Manning et al., 2010; Veldhuis et al., 2017; Winklbauer, 2015). Interestingly, with this approach and contrary to the other approaches that measure de-adhesion, it is directly the cell-adhesion energy that is predicted. However current methods depend on the assumption that cells behave like fluids.

5.3. Micromanipulation assays

Another range of techniques employs direct and precise cell micromanipulation, to grab, put cells in contact and pull them apart or from a substrate and measure the force necessary to do so. These uses either microaspiration of the cells with micropipettes or attachment of a cell to a cantilever. The dual pipette aspiration method uses a pair of micropipettes that can each grab a single cell by microaspiration. The two cells can then be placed in contact with each other for a given time to establish adhesion and then pulled apart to measure the adhesion that has developed (Sung et al., 1986), while the manipulation takes place under a microscope to monitor the detachment of the cells. In recent implementations, the microaspiration is precisely controlled by microfluidic pumps providing negative pressure (suction) and the pipettes are held by motorised micromanipulators (Biro & Maître, 2015). Adhesion strength is then measured using the step-pressure assay (Figure 3h). Once the cells adhere to each other, one micropipette is moved backwards to pull the cells apart. At low suction in the measuring pipette, the cell held by the measuring pipette will detach from it rather than from the other cell. In the next step, the measuring pipette is brought back to the cell, the suction inside the measuring micropipette is increased and the cells are pulled again. These cycles continue until the suction is strong enough to separate the cells. The minimal suction needed to detach the cells is then used to calculate a value for the de-adhesion strength. Another approach called single-cell force spectroscopy uses an atomic force microscope (AFM) to quantify cell de-adhesion strength and work. In single-cell force spectroscopy (SCFS), a cell is attached to an AFM cantilever (without tip) and then placed in contact with a substrate (tissue, cell or functionalised surface; Benoit et al., 2000; Figure 3f). When attempting to detach the cell, the cantilever is first bent as the pulling force increases until the force is high enough to detach the cell and the cantilever then regains its original shape. The AFM measures this bending by quantifying the deflection of a laser pointed at the cantilever. In turn, knowing the spring constant of the cantilever, it is possible to calculate the force applied throughout the pulling experiment and derive a stress–strain curve from which the de-adhesion strength and work can be precisely calculated. The main difficulty of the SCFS is the necessity to coat the cantilever to attach the cell on it since the cell-cantilever adhesion must be higher than the cell–cell or cell–substrate adhesion and the

https://doi.org/10.1017/qpb.2021.16 Published online by Cambridge University Press

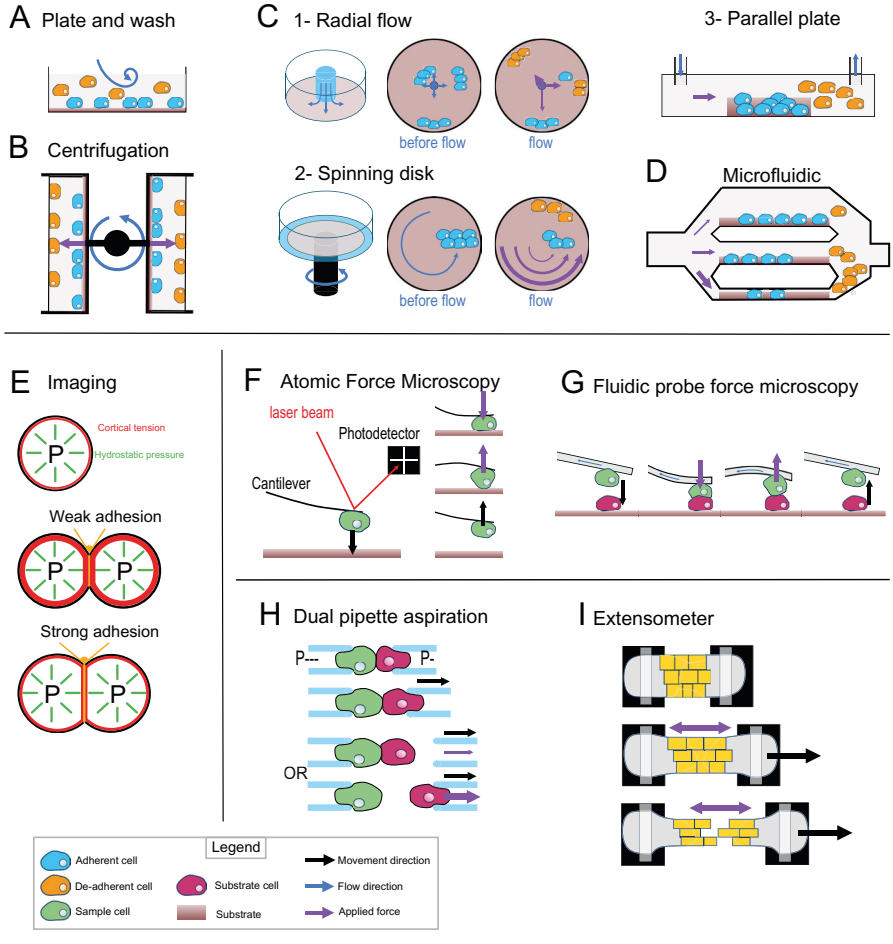

Fig. 3. Cell-adhesion quantification methods. (a) Plate and wash assay. After placing the cells in contact with the substrate for a period, the medium is replaced, removing the nonadherent cells. (b) Centrifugal assay. A 96-well plate is coated with a substrate. A cell suspension is added and allowed to adhere to the substrate. Then the wells are sealed, and the plate is spun at a specific speed and duration. (c) Hydrodynamic flow assays. (c1) The radial flow chamber. An outward radial flow. Different intensities of shear stress are applied on the cells depending on their position in the chamber according to a gradient inversely proportional to the radial position. (c2) The spinning disc assay uses a rotating flow to apply a hydrodynamic shear force on the sample. The cells are in contact with a substrate on a plate, which is rotating in a chamber containing liquid. The applied forces vary linearly with radial distance. (c3) The parallel plate. The cells are in a rectangular chamber, and a constant flow is maintained during one experiment. (d) Microfluidic chamber. The cells are in micrometre-range channels where a laminar flow is running. The smaller the channel is, the higher is the shear stress applied on the sample. (e) Cell shape-based imaging technique. The cell shape depends on an equilibrium between the internal hydrostatic pressure and the cortical tension. The strength of cell–cell adhesion can be deduced from the area of contact and the angle at the junction of cells. (f) Single-cell force spectroscopy. A cell is attached to the cantilever of an atomic force microscope then put in contact with a substrate. The cantilever first approaches and pushes the cell on the substrate. Then the cell is pulled from the surface. The adhesion force between the cell and the substrate will bend the cantilever until the cell detaches. A laser is reflected by the cantilever to a photodetector. This will draw a force curve giving information on the force of adhesion between the cell and the substrate. (g) Fluidic probe force microscopy. The same principle as the single-cell force spectroscopy, but the cantilever contains a microchannel that can suck the cell like a micropipette. (h) Step pressure assay. Two motorised micropipettes are connected to a microfluidic pump. First, the two cells are in contact to allow the adhesion. One micropipette keeps the cell in position with a high constant suction, whereas the other one pulls its cell away with a lower suction. If the adhesion is stronger than the measuring pipette suction, the cell will slip out the micropipette. The suction in this pipette is then increased until it is strong enough to separate the cells. (i) Extensometer used for tensile test. The tissue sample is held at each end and stretched with a specific force. The stretching and the tearing are monitored with microscopic observation. For additional information on the methods presented, including the quantitative/mathematical framework used to derive adhesion mechanics values, see Alam et al. (2019), Garcia and Gallant (2003) and Ungai-Salánki et al. (2019).

coating can chemically disrupt the state of the cell and therefore modify its adhesion properties (Cohen et al., 2017; Guillaume-Gentil et al., 2014). This issue can be avoided by using fluidic probe force microscopy (Meister et al., 2009). In this case, the cantilever contains a microchannel and can thus act as a micropipette, which sucks the cell so that no coating of the cantilever is needed to hold

https://doi.org/10.1017/qpb.2021.16 Published online by Cambridge University Press

the cell (Figure 3g). Overall, these micromanipulation techniques bring a much higher precision in the measurement of adhesion compared to the other methods described above but have a much lower throughput and are limited to the study of single cell–cell or cell–substrate adhesion.

5.4. Tissue-level measurements

Most of the methods existing to investigate the mechanics of cell adhesion are single-cell techniques. Measuring mechanical properties at the tissue level can be difficult because of the heterogeneity of the cells or extracellular material that compose a tissue, but a few methods exist. The 90° peel test method has been used on cell layers cultured on a substrate to measure the adhesion force of this cell layer to its substrate (Uesugi et al., 2013). Tensile tests have also been developed to explore the mechanical properties of a tissue and have been applied to measure cell adhesion in the tissue context. For such methods, the sample is placed in an extensometer, a device that allows the stretching of the samples and a measurement of the load applied during stretching (Figure 3i). The sample is attached at its extremities and is then stretched while the deformations and cell detachments are monitored with a microscope (Harris et al., 2012). Similarly, to the single-cell approaches, the tissue is stretched until the cells separate, and the de-adhesion strength is calculated locally from the observed strain and predicted stress during the stretching. While more complex to analyse, such a tissue-level approach brings more physiologically relevant information concerning cell–cell adhesion in the tissue context compared to single-cell approaches.

5.5. Cell-adhesion quantification methods in plants

While still very limited compared to other organisms, quantification of cell-adhesion mechanics has already been approached in plants. Following a method first established by Parker and Waldron (1995), Leboeuf et al. (2004) used 'vortex-induced cell separation' to study the differences in adhesion between *Arabidopsis thaliana* microcalli suspension cultures at several time points during growth. The method consists of measuring with a particle size analyser the size of cell clusters from in vitro cell cultures before and after vortexing at 40 Hz. However, this method remains rather imprecise, the force applied to detach the cells is not measured and it is not entirely clear whether cell clusters get fragmented because of cell detachments or cell ruptures. Tensile tests have also been used on plant samples to explore cell-adhesion establishment after grafting (Kawakatsu et al., 2020; Lindsay et al., 1974; Moore, 1984; Notaguchi et al., 2020), but again it remains difficult to determine if cells are being separated or if tissues rupture. Melnyk et al. (2018) used an automated confocal micro-extensometer (ACME; Robinson et al., 2017) in such experiments to determine grafting adhesion. Since this device is coupled with a confocal microscope which allows live 3D imaging during the stretching, it revealed that indeed most cells at the grafting interface appear to break rather than separate when the sample is stretch until rupture, suggesting that cell adhesion of previously separated cells becomes stronger than the cohesive strength of the cell cortex (cell wall). Tensile tests have also been used at the level of the cell wall, in strips of microdissected onion outer epidermal cell wall containing cell–cell junctions (Zamil et al., 2014). Interestingly, it also revealed that the cell walls did not separate at the cell–cell junction but rather broke within the cell cortex. Another model of study of adhesion in plants is the pollen grain and its adhesion to a substrate or to the stigma. Jauh et al. (1997) developed a method similar to the plate and wash assay to measure pollen adhesion on an artificial matrix. They blotted exudates from Lily (*Lilium sp.*) styles on nitrocellulose membranes and tested the adhesion of pollen grains after gently washing with a liquid buffer. Similarly, Zinkl et al. (1999) used a plate and wash-like liquid assay. They directly used unpollinated pistils, pollinated them and washed away the nonadherent pollen with a liquid buffer. While this method still lacks precision in terms of the force applied, they also developed a high-precision approach that resembles single-cell force spectroscopy to study pollen adhesion strength of a single pollen grain to the stigma. This system has similarities with the force measurement principle of an AFM but directly uses pistils to bind the pollen grain from each side. One pistil is maintained on a translation stage and serves as a substrate. Another pistil is glued to a glass fibre cantilever. A pollen grain is then placed in between the two stigmas, and the translation stage is moved away from the cantilever, while the bending of the cantilever is measured via a reflecting laser beam. When the force is too high for one of the pollen adhesion sites, the cantilever retracts and the adhesion strength can be determined. Finally, other researchers have approached the study of plant cell-adhesion mechanics form the modelling side by developing analytical models (Jarvis, 1998) and finite element simulations of the middle lamella (Shafayet Zamil et al., 2017) as well as de-adhesion mechanics (Diels et al., 2019; Liedekerke et al., 2011) that were then compared with experimental data (Diels et al., 2019). Overall, while these approaches have initiated the investigation of cell-adhesion mechanics measurements in plants, they are still either limited to a specific case (pollen, grafting), remain very imprecise in terms of the actual forces applied (vortex) or are theoretical (modelling). In the remainder of this review, we thus want to explore and hypothesise on the methods that could be implemented to precisely quantify cell–cell adhesion mechanics in plants.

6. Implementing cell-adhesion measurement methods in plants

Studying cell adhesion in plants brings additional challenges. Plants have large and relatively rigid cell walls which are under high tensions due to the high turgor pressure of the cells. Plants cells (with the exception of specific cases like pollen grains) do not seem to adhere specifically to substrates contrary to most animals, bacteria, algae and fungi. Furthermore, here our focus is to understand cell–cell adhesion in the context of multicellularity rather than to study how a plant cell would attach to a substrate. Nevertheless, many of the approaches presented above could in principle be adapted to study plant cell adhesion, including the cell–substrate adhesion quantification methods. As explained above, some versions of the plate and wash assay have already been applied to the study of pollen grain adhesion, but they will likely not be as straightforward to apply to other plant cell types. Similarly, important adaptations may be needed for hydrodynamic flow approaches. Indeed, in order to isolate single plant cells, it is necessary to first remove them from their tissue by digesting their cell wall. The protoplasts obtained are very fragile and lack the cell wall that is the structure that mediates cell adhesion in a physiological context. It is thus necessary to first wait for the cell wall to regenerate (Pasternak et al., 2021). The adhesion of most plant cell types is actually cell–cell rather than cell–substrate, so another major adaptation will be the substrate to be used. A first possibility would be to use a live sample or a cell

https://doi.org/10.1017/qpb.2021.16 Published online by Cambridge University Press

layer such as the inner side of an epidermal peel as a substrate for an approach similar to a plate and wash assay. However, this still brings the limitation of not being able to measure the actual force imposed on the cells during the washing step and may not be applicable to flow and microfluidic chamber approaches. Yet, it could still be a very useful approach to quantitatively compare adhesion of wild type and mutant cells or in response to treatments. An alternative would be to mimic an adjacent cell wall using purified cell wall components such as pectins, celluloses and hemicelluloses, cell wall extracts blotted on a nitrocellulose membrane or coated in flow or microfluidic chambers or even other artificial scaffolds as recently developed (Calcutt et al., 2021). While it remains to be determined whether such study of plant cell adhesion to a substrate would provide physiologically relevant information, using different substrates with different composition could be very informative to further understand the chemical determinants of cell adhesion and similarly to compare wild type, mutants and treatments in a context in which the force applied on a large number of cells can be precisely quantified.

The computational imaging-based techniques would be at first glance the easiest to apply to plant cells. Starting from isolated cells, it is possible to let the single cells divide and spontaneously form cell doublets. One important limitation, however, is that it is unlikely that we can consider plant cells with a regenerated cell wall to behave as liquid. In turn, the calculation of adhesion energy based on the shape and cortical tension of the cell doublet may not directly apply here. However, the observation of cell contact shape in wild type, mutants and treated samples could still be very informative (Calcutt et al., 2021). The cell doublets could be trapped in microfluidics chambers allowing time-lapse live observation while changing the osmolarity of the medium and thus the turgor pressure and cell wall tensions. Increases in cortical cell wall tension could in principle force the cells into more spherical shapes and induce partial separations. Using finite element simulation of the system and considering measurable physical properties, such as cell wall elasticity, plasticity, thickness, turgor pressure, cell shapes and strain, following the changes of pressure, could generate an informative prediction of the local stresses in the cell wall and at the cell–cell interface. This would bring the possibility to deduce the cell–cell adhesion strength of cells that would partially detach as a consequence of changes in tension (Diels et al., 2019; Jarvis, 1998). While still far from a physiological context, such approach would allow the study of actual cell–cell adhesion of the cell doublet and in a minimally invasive system. One limitation, however, may be that in many cases, including untreated wild-type cells, the tensions induced by the changes in pressure may not be sufficient to separate the cells, or that they would only induce cell wall extension rather than separation of the interface. Conversely, micromanipulation techniques could be used to directly apply separating forces to cell doublets until the cells would separate. The step pressure assay with motorised dual micropipette could be used to attempt to separate spontaneously generated cell doublets or be used to put in contact single plant cells and measure the cell–cell adhesion strength developing over time. Similarly, the fluidic probe-based single-cell force spectroscopy approaches could in principle be used to measure the adhesion of a plant cell to a synthetic cell wall-like substrate. While the suction developed by the currently available micropipette-based setups may not be sufficient to separate the potentially very strong plant cell–cell adhesion (e.g., in the case of wild-type untreated spontaneously generated cell doublet), new implementations using micropipettes with larger diameters adapted to the size of plant cells and high negative pressure fluidic pump could be developed to attempt to solve this issue. It remains that, as previously shown (Melnyk et al., 2018; Zamil et al., 2014), the cell cortex strength may often be weaker than the cell–cell adhesion. In this context, such a setup would ideally be able to develop pulling forces high enough to bring the cell to rupture and allow to assess the maximal measurable adhesion strength. On the other hand, at the tissue scales, stretching until rupture is already achievable in plants with a micro-extensometer. Similarly, to the case of grafting, a tissue sample can be firmly attached to opposite arms of an extensometer and stretched until it ruptures while measuring the force applied. The ACME setup allows the 3D live imaging of cell detachment in mutant samples (Robinson & Durand-Smet, 2020) and could be particularly useful to compare different cell-adhesion-defective mutants or the effect of different treatments. Here, the main limitation rather lies in the complexity of the sample. Most tissues are composed of multiple-cell layers, including the epidermis, cortex and the vasculature. While previous work has shown that the epidermis is put under tension by the extensometer stretching (Robinson & Kuhlemeier, 2018), it is not clear what is the load-bearing contribution of the different cell layers. In particular, the epidermis appears to be the first to yield and may at first be under the most tension, whereas the vasculature seems to be the last to yield. As such, quantifying the ultimate force and thus the strength of the samples will likely not really provide information regarding the properties of cell–cell adhesion in the samples, but rather on the toughness of the vasculature. In turn, a more complex analysis of the stress–strain curve in parallel with the microscopic observation with confocal microscopy (ACME) and coupled with computational mechanical simulation of the system (Diels et al., 2019) would be required to determine adhesion strength in the epidermis or cortex and compare different mutants or treatments. Finally, an alternative to this problem would be to study epidermal peels. While these may be particularly difficult to obtain from adhesion-defective mutants since the epidermal cells would easily detach from each other, this may be a very useful tool to study the effect of treatments or even study adhesion in transgenic lines in which cell-adhesion defect could be induced by the controlled expression of cell-separating enzymes or the controlled knockdown of genes involved in cell adhesion.

To summarise, from these ideas and hypotheses, much remains to be done and tested to determine if or which of these approaches will be the most useful and applicable for the mechanical quantification of cell adhesion in plants. We can hope that this will be the case for many of them, offering a range of techniques from relative measurement of the adhesion of large populations of cells to the very precise measurements in single-cell adhesion or adhesion in the tissue context. A successful approach could also be a combination of some of the approaches proposed (e.g., combining micromanipulation with finite element methods), or require the design and development of completely new approaches.

7. Conclusion

When it comes to multicellular organisms, we know adhesion is responsible for their integrity. We also have some knowledge on how this adhesion is mediated and kept through the organism's life span. In some organisms, like in animals, adhesion has been intensively studied at the single-cell level and molecular scale. Collaborations among biologists, physicists and engineers have led to the development of different devices and methods to determine

https://doi.org/10.1017/qpb.2021.16 Published online by Cambridge University Press

or measure the adhesion strength from the molecular to the tissue scale. But the focus of previous studies and methods developed has been rather on the single cell–substrate adhesion than multicellular cell–cell adhesion. The lack of methods for measuring cell–cell adhesion in plants is currently the main bottleneck for the field, and largely hampers our current understanding of the mechanisms controlling cell–cell adhesion in plants. As shown for the animal cells, methods to quantify cell adhesion have had a major impact to understand the molecular basis of cell adhesion but also the complex biophysical implications such as the fact that beyond cell–cell adhesion strength, the regulation of cortical tension, as well as mechanical feedbacks, plays a major role in controlling and maintaining adhesion (Lenne et al., 2021). Future development of precise quantitative methods for measuring cell adhesion in plants should thus open the door for major breakthroughs in the field and have a broad impact on our understanding of plant biomechanics.

Acknowledgement

We are grateful to Rawen Ben-Malek and Grégory Mouille (IJPB, INRAE) for their helpful comments on the manuscript.

Conflicts of interest. The authors declare that no competing interests exist.

Financial support. This work was supported by grants from the Kempe Foundation (A.A.; grant number JCK-1912.2), Åforsk (L.B.; grant number 20.502) and the support of Bio4Energy (S.V.) and the UPSC Centre for Forest Biotechnology (L.B.).

Authorship contributions. All the authors wrote the manuscript. L.B. made the figures.

Data availability statement. No data or code was generated as part of this manuscript.

References

Abe, M., **Katsumata, H.**, **Komeda, Y.**, & **Takahashi, T.** (2003). Regulation of shoot epidermal cell differentiation by a pair of homeodomain proteins in Arabidopsis. *Development*, **130**, 635–643. https://doi.org/10.1242/dev.00292

Alam, F., **Kumar, S.**, & **Varadarajan, K. M.** (2019). Quantification of adhesion force of bacteria on the surface of biomaterials: Techniques and assays. *ACS Biomaterials Science & Engineering*, **5**, 2093–2110. https://doi.org/10.1021/acsbiomaterials.9b00213

Anderson, C. T. (2019). Pectic polysaccharides in plants: Structure, biosynthesis, functions, and applications. In E. Cohen & H. Merzendorfer (Eds.), *Extracellular sugar-based biopolymers matrices* (pp. 487–514). Springer. https://doi.org/10.1007/978-3-030-12919-4_12

Anderson, C. T., & **Kieber, J. J.** (2020). Dynamic construction, perception, and remodeling of plant cell walls. *Annual Review of Plant Biology*, **71**, 39–69. https://doi.org/10.1146/annurev-arplant-081519-035846

Arroyo, M., & **Trepat, X.** (2017). Hydraulic fracturing in cells and tissues: Fracking meets cell biology. *Current Opinion in Cell Biology*, **44**, 1–6. https://doi.org/10.1016/j.ceb.2016.11.001

Bar-Peled, M., **Urbanowicz, B. R.**, & **O'Neill, M. A.** (2012). The synthesis and origin of the pectic polysaccharide rhamnogalacturonan II—Insights from nucleotide sugar formation and diversity. *Frontiers in Plant Science*, **3**. https://doi.org/10.3389/fpls.2012.00092

Baum, B., & **Georgiou, M.** (2011). Dynamics of adherens junctions in epithelial establishment, maintenance, and remodeling. *The Journal of Cell Biology*, **192**, 907–917. https://doi.org/10.1083/jcb.201009141

Benoit, M., **Gabriel, D.**, **Gerisch, G.**, & **Gaub, H. E.** (2000). Discrete interactions in cell adhesion measured by single-molecule force spectroscopy. *Nature Cell Biology*, **2**, 313–317. https://doi.org/10.1038/35014000

Biro, M., & **Maître, J.-L.** (2015). Chapter 14—Dual pipette aspiration: A unique tool for studying intercellular adhesion. In E. K. Paluch (Ed.), *Methods in cell biology* (Vol. 125, pp. 255–267). Academic Press. https://doi.org/10.1016/bs.mcb.2014.10.007

Bou Daher, F., & **Braybrook, S. A.** (2015). How to let go: Pectin and plant cell adhesion. *Frontiers in Plant Science*, **6**. https://doi.org/10.3389/fpls.2015.00523

Bouton, S., **Leboeuf, E.**, **Mouille, G.**, **Leydecker, M.-T.**, **Talbotec, J.**, **Granier, F.**, **Lahaye, M.**, **Höfte, H.**, & **Truong, H.-N.** (2002). *QUASIMODO1* encodes a putative membrane-bound glycosyltransferase required for normal pectin synthesis and cell adhesion in Arabidopsis. *The Plant Cell*, **14**, 2577–2590. https://doi.org/10.1105/tpc.004259

Brochard-Wyart, F., & **de Gennes, P.-G.** (2009). Unbinding of adhesive vesicles. In *P.G. De Gennes' impact on science?* (Vol. II, pp. 139–145). World Scientific. https://doi.org/10.1142/9789814280648_0015

Cai, S., & **Lashbrook, C. C.** (2008). Stamen abscission zone transcriptome profiling reveals new candidates for abscission control: Enhanced retention of floral organs in transgenic plants overexpressing Arabidopsis *ZINC FINGER PROTEIN2*. *Plant Physiology*, **146**, 1305–1321. https://doi.org/10.1104/pp.107.110908

Calcutt, R., **Vincent, R.**, **Dean, D.**, **Arinzeh, T. L.**, & **Dixit, R.** (2021). Plant cell adhesion and growth on artificial fibrous scaffolds as an in vitro model for plant development. *Science Advances*, **7**, eabj1469. https://doi.org/10.1126/sciadv.abj1469

Carpentier, B. (2014). Biofilms. In C. A. Batt & M. L. Tortorello (Eds.), *Encyclopedia of food microbiology* (2nd ed., pp. 259–265). Academic Press. https://doi.org/10.1016/B978-0-12-384730-0.00039-2

Christ, K. V., **Williamson, K. B.**, **Masters, K. S.**, & **Turner, K. T.** (2010). Measurement of single-cell adhesion strength using a microfluidic assay. *Biomedical Microdevices*, **12**, 443–455. https://doi.org/10.1007/s10544-010-9401-x

Chu, Y.-S., **Dufour, S.**, **Thiery, J. P.**, **Perez, E.**, & **Pincet, F.** (2005). Johnson–Kendall–Roberts theory applied to living cells. *Physical Review Letters*, **94**, 028102. https://doi.org/10.1103/PhysRevLett.94.028102

Ciesielski, P. N., **Resch, M. G.**, **Hewetson, B.**, **Killgore, J. P.**, **Curtin, A.**, **Anderson, N.**, **Chiaramonti, A. N.**, **Hurley, D. C.**, **Sanders, A.**, **Himmel, M. E.**, **Chapple, C.**, **Mosier, N.**, & **Donohoe, B. S.** (2014). Engineering plant cell walls: Tuning lignin monomer composition for deconstructable biofuel feedstocks or resilient biomaterials. *Green Chemistry*, **16**, 2627–2635. https://doi.org/10.1039/C3GC42422G

Cohen, N., **Sarkar, S.**, **Hondroulis, E.**, **Sabhachandani, P.**, & **Konry, T.** (2017). Quantification of intercellular adhesion forces measured by fluid force microscopy. *Talanta*, **174**, 409–413. https://doi.org/10.1016/j.talanta.2017.06.038

Cosgrove, D. J., & **Anderson, C. T.** (2020). Plant cell growth: Do pectins drive lobe formation in Arabidopsis pavement cells? *Current Biology*, **30**, R660–R662. https://doi.org/10.1016/j.cub.2020.04.007

Creton, C., & **Ciccotti, M.** (2016). Fracture and adhesion of soft materials: A review. *Reports on Progress in Physics*, **79**, 046601. https://doi.org/10.1088/0034-4885/79/4/046601

da Silva L. F. M., **Öchsner, A.**, & **AdamsR. D.** (2018). *Handbook of adhesion technology*. Springer.

de Groot, P. W. J., **Bader, O.**, **de Boer, A. D.**, **Weig, M.**, & **Chauhan, N.** (2013). Adhesins in human fungal pathogens: Glue with plenty of stick. *Eukaryotic Cell*, **12**, 470–481. https://doi.org/10.1128/EC.00364-12

Diels, E., **Wang, Z.**, **Nicolai, B.**, **Ramon, H.**, & **Smeets, B.** (2019). Discrete element modelling of tomato tissue deformation and failure at the cellular scale. *Soft Matter*, **15**, 3362–3378. https://doi.org/10.1039/C9SM00149B

Domozych, D. S., **Elliott, L.**, **Kiemle, S. N.**, & **Gretz, M. R.** (2007). Pleurotaenium trabecula, a desmid of wetland biofilms: The extracellular matrix and adhesion mechanisms. *Journal of Phycology*, **43**, 1022–1038. https://doi.org/10.1111/j.1529-8817.2007.00389.x

Domozych, D. S., **Srensen, I.**, **Popper, Z. A.**, **Ochs, J.**, **Andreas, A.**, **Fangel, J. U.**, **Pielach, A.**, **Sacks, C.**, **Brechka, H.**, **Ruisi-Besares, P.**, **Willats, W. G. T.**, & **Rose, J. K. C.** (2014). Pectin metabolism and assembly in the cell wall of the charophyte green alga *Penium margaritaceum*. *Plant Physiology*, **165**, 105–118. https://doi.org/10.1104/pp.114.236257

Du, J., Kirui, A., Huang, S., Wang, L., Barnes, W. J., Kiemle, S. N., Zheng, Y., Rui, Y., Ruan, M., Qi, S., Kim, S. H., Wang, T., Cosgrove, D. J., Anderson, C. T., & Xiao, C. (2020). Mutations in the pectin methyltransferase *QUASIMODO2* influence cellulose biosynthesis and wall integrity in Arabidopsis. *The Plant Cell*, **32**, 3576–3597. https://doi.org/10.1105/tpc.20.00252

Epstein, L., & Nicholson, R. (2016). Adhesion and adhesives of fungi and oomycetes. In A. M. Smith (Ed.), *Biological adhesives* (pp. 25–55). Springer. https://doi.org/10.1007/978-3-319-46082-6_2

Francis, K. E., Lam, S. Y., & Copenhaver, G. P. (2006). Separation of Arabidopsis pollen tetrads is regulated by *QUARTET1*, a pectin methylesterase gene. *Plant Physiology*, **142**, 1004–1013. https://doi.org/10.1104/pp.106.085274

Galletti, R., Johnson, K. L., Scofield, S., San-Bento, R., Watt, A. M., Murray, J. A. H., & Ingram, G. C. (2015). DEFECTIVE KERNEL 1 promotes and maintains plant epidermal differentiation. *Development*, **142**, 1978–1983. https://doi.org/10.1242/dev.122325

García, A. J., Ducheyne, P., & Boettiger, D. (1997). Quantification of cell adhesion using a spinning disc device and application to surface-reactive materials. *Biomaterials*, **18**, 1091–1098. https://doi.org/10.1016/S0142-9612(97)00042-2

Garcia, A. J., & Gallant, N. D. (2003). Stick and grip. *Cell Biochemistry and Biophysics*, **39**, 61–73. https://doi.org/10.1385/CBB:39:1:61

Gorshkova, T., Brutch, N., Chabbert, B., Deyholos, M., Hayashi, T., Lev-Yadun, S., Mellerowicz, E. J., Morvan, C., Neutelings, G., & Pilate, G. (2012). Plant fiber formation: State of the art, recent and expected progress, and open questions. *Critical Reviews in Plant Sciences*, **31**, 201–228. https://doi.org/10.1080/07352689.2011.616096

Grones, P., Raggi, S., & Robert, S. (2019). FORCE-ing the shape. *Current Opinion in Plant Biology*, **52**, 1–6. https://doi.org/10.1016/j.pbi.2019.05.008

Guillaume-Gentil, O., Potthoff, E., Ossola, D., Franz, C. M., Zambelli, T., & Vorholt, J. A. (2014). Force-controlled manipulation of single cells: From AFM to FluidFM. *Trends in Biotechnology*, **32**, 381–388. https://doi.org/10.1016/j.tibtech.2014.04.008

Haas, K. T., Wightman, R., Meyerowitz, E. M., & Peaucelle, A. (2020). Pectin homogalacturonan nanofilament expansion drives morphogenesis in plant epidermal cells. *Science*, **367**, 1003–1007. https://doi.org/10.1126/science.aaz5103

Haas, K. T., Wightman, R., Peaucelle, A., & Höfte, H. (2021). The role of pectin phase separation in plant cell wall assembly and growth. *The Cell Surface*, **7**, 100054. https://doi.org/10.1016/j.tcsw.2021.100054

Haase, K., Al-Rekabi, Z., & Pelling, A. E. (2014). Chapter 5—Mechanical cues direct focal adhesion dynamics. In A. J. Engler & S. Kumar (Eds.), *Progress in molecular biology and translational science* (Vol. **126**, pp. 103–134). Academic Press. https://doi.org/10.1016/B978-0-12-394624-9.00005-1

Halbleib, J. M., & Nelson, W. J. (2006). Cadherins in development: Cell adhesion, sorting, and tissue morphogenesis. *Genes & Development*, **20**, 3199–3214. https://doi.org/10.1101/gad.1486806

Hall-Stoodley, L., Costerton, J. W., & Stoodley, P. (2004). Bacterial biofilms: From the natural environment to infectious diseases. *Nature Reviews Microbiology*, **2**, 95–108. https://doi.org/10.1038/nrmicro821

Hamant, O., & Saunders, T. E. (2020). Shaping organs: Shared structural principles across kingdoms. *Annual Review of Cell and Developmental Biology*, **36**, 385–410. https://doi.org/10.1146/annurev-cellbio-012820-103850

Hannezo, E., & Heisenberg, C.-P. (2019). Mechanochemical feedback loops in development and disease. *Cell*, **178**, 12–25. https://doi.org/10.1016/j.cell.2019.05.052

Harris, A. R., Peter, L., Bellis, J., Baum, B., Kabla, A. J., & Charras, G. T. (2012). Characterizing the mechanics of cultured cell monolayers. *Proceedings of the National Academy of Sciences of the United States of America*, **109**, 16449–16454. https://doi.org/10.1073/pnas.1213301109

Harris, T. J. C., & Tepass, U. (2010). Adherens junctions: From molecules to morphogenesis. *Nature Reviews Molecular Cell Biology*, **11**, 502–514. https://doi.org/10.1038/nrm2927

Hartsock, A., & Nelson, W. J. (2008). Adherens and tight junctions: Structure, function and connections to the actin cytoskeleton. *Biochimica et Biophysica Acta (BBA)—Biomembranes*, **1778**, 660–669. https://doi.org/10.1016/j.bbamem.2007.07.012

Hocq, L., Pelloux, J., & Lefebvre, V. (2017). Connecting homogalacturonan-type pectin remodeling to acid growth. *Trends in Plant Science*, **22**, 20–29. https://doi.org/10.1016/j.tplants.2016.10.009

Huxham, I. M., Jarvis, M. C., Shakespeare, L., Dover, C. J., Johnson, D., Knox, J. P., & Seymour, G. B. (1999). Electron-energy-loss spectroscopic imaging of calcium and nitrogen in the cell walls of apple fruits. *Planta*, **208**, 438–443. https://doi.org/10.1007/s004250050580

Ikegaya, H., Hayashi, T., Kaku, T., Iwata, K., Sonobe, S., & Shimmen, T. (2008). Presence of xyloglucan-like polysaccharide in spirogyra and possible involvement in cell–cell attachment. *Phycological Research*, **56**, 216–222. https://doi.org/10.1111/j.1440-1835.2008.00503.x

Iwamoto, D. V., & Calderwood, D. A. (2015). Regulation of integrin-mediated adhesions. *Current Opinion in Cell Biology*, **36**, 41–47. https://doi.org/10.1016/j.ceb.2015.06.009

Jarvis, M. C. (1998). Intercellular separation forces generated by intracellular pressure. *Plant, Cell & Environment*, **21**, 1307–1310. https://doi.org/10.1046/j.1365-3040.1998.00363.x

Jarvis, M. C., & Apperley, D. C. (1995). Chain conformation in concentrated pectic gels: Evidence from 13C NMR. *Carbohydrate Research*, **275**, 131–145. https://doi.org/10.1016/0008-6215(95)00033-P

Jarvis, M. C., Briggs, S. P. H., & Knox, J. P. (2003). Intercellular adhesion and cell separation in plants. *Plant, Cell & Environment*, **26**, 977–989. https://doi.org/10.1046/j.1365-3040.2003.01034.x

Jauh, G. Y., Eckard, K. J., Nothnagel, E. A., & Lord, E. M. (1997). Adhesion of lily pollen tubes on an artificial matrix. *Sexual Plant Reproduction*, **10**, 173–180. https://doi.org/10.1007/s004970050085

Jones, E. B. G. (1994). Fungal adhesion. *Mycological Research*, **98**, 961–981. https://doi.org/10.1016/S0953-7562(09)80421-8

Kawakatsu, Y., Sawai, Y., Kurotani, K., Shiratake, K., & Notaguchi, M. (2020). An in vitro grafting method to quantify mechanical forces of adhering tissues. *Plant Biotechnology*, **37**, 451–458. https://doi.org/10.5511/plantbiotechnology.20.0925a

Klebe, R. J. (1974). Isolation of a collagen-dependent cell attachment factor. *Nature*, **250**, 248–251. https://doi.org/10.1038/250248a0

Knox, J. P. (1992). Cell adhesion, cell separation and plant morphogenesis. *The Plant Journal*, **2**, 137–141. https://doi.org/10.1111/j.1365-313X.1992.00137.x

Kooten, T. G. v., Schakenraad, J. M., Mei, H. C. V. d., & Busscher, H. J. (1992). Development and use of a parallel-plate flow chamber for studying cellular adhesion to solid surfaces. *Journal of Biomedical Materials Research*, **26**, 725–738. https://doi.org/10.1002/jbm.820260604

Kostakioti, M., Hadjifrangiskou, M., & Hultgren, S. J. (2013). Bacterial biofilms: Development, dispersal, and therapeutic strategies in the dawn of the postantibiotic era. *Cold Spring Harbor Perspectives in Medicine*, **3**, a010306. https://doi.org/10.1101/cshperspect.a010306

Kuo, J.-C. (2014). Focal adhesions function as a mechanosensor. *Progress in Molecular Biology and Translational Science*, **126**, 55–73. https://doi.org/10.1016/B978-0-12-394624-9.00003-8

Lashbrook, C. C., & Cai, S. (2008). Cell wall remodeling in Arabidopsis stamen abscission zones. *Plant Signaling & Behavior*, **3**, 733–736. https://doi.org/10.4161/psb.3.9.6489

Lathe, R. S., McFarlane, H. E., Khan, G. A., Ebert, B., Ramírez-Rodríguez, E. A., Noord, N., Bhalerao, R., & Persson, S. (2021). A DUF1068 protein acts as a pectin biosynthesis scaffold and maintains Golgi morphology and cell adhesion in Arabidopsis. *BioRxiv*: 2021.05.03.442108. https://doi.org/10.1101/2021.05.03.442108

Le, J., El-Assal, S. E.-D., Basu, D., Saad, M. E., & Szymanski, D. B. (2003). Requirements for Arabidopsis *ATARP2* and *ATARP3* during epidermal development. *Current Biology*, **13**, 1341–1347. https://doi.org/10.1016/s0960-9822(03)00493-7

Leboeuf, E., Thoiron, S., & Lahaye, M. (2004). Physico-chemical characteristics of cell walls from *Arabidopsis thaliana* microcalli showing different adhesion strengths. *Journal of Experimental Botany*, **55**, 2087–2097. https://doi.org/10.1093/jxb/erh225

Lebret, K., Thabard, M., & Hellio, C. (2009). Chapter 4—Algae as marine fouling organisms: Adhesion damage and prevention. In C. Hellio & D. Yebra

(Eds.), *Advances in marine antifouling coatings and technologies* (pp. 80–112). Woodhead. https://doi.org/10.1533/9781845696313.1.80

Leckband, D. E., & **de Rooij, J.** (2014). Cadherin adhesion and mechanotransduction. *Annual Review of Cell and Developmental Biology*, **30**, 291–315. https://doi.org/10.1146/annurev-cellbio-100913-013212

Lenne, P.-F., **Rupprecht, J.-F.**, & **Viasnoff, V.** (2021). Cell junction mechanics beyond the bounds of adhesion and tension. *Developmental Cell*, **56**, 202–212. https://doi.org/10.1016/j.devcel.2020.12.018

Letham, D. S. (1960). The separation of plant cells with ethylenediaminetetraacetic acid. *Experimental Cell Research*, **21**, 353–360. https://doi.org/10.1016/0014-4827(60)90267-6

Li, X., & **Chapple, C.** (2010). Understanding lignification: Challenges beyond monolignol biosynthesis. *Plant Physiology*, **154**, 449–452. https://doi.org/10.1104/pp.110.162842

Liedekerke, P. V., **Ghysels, P.**, **Tijskens, E.**, **Samaey, G.**, **Roose, D.**, & **Ramon, H.** (2011). Mechanisms of soft cellular tissue bruising. A particle based simulation approach. *Soft Matter*, **7**, 3580–3591. https://doi.org/10.1039/C0SM01261K

Lindsay, D. W., **Yeoman, M. M.**, & **Brown, R.** (1974). An analysis of the development of the graft union in *Lycopersicon esculentum*. *Annals of Botany*, **38**, 639–646. https://doi.org/10.1093/oxfordjournals.aob.a084849

Liners, F., **Letesson, J. J.**, **Didembourg, C.**, & **Van Cutsem, P.** (1989). Monoclonal antibodies against pectin: Recognition of a conformation induced by calcium. *Plant Physiology*, **91**, 1419–1424. https://doi.org/10.1104/pp.91.4.1419

Lionetti, V., **Cervone, F.**, & **De Lorenzo, G.** (2015). A lower content of demethylesterified homogalacturonan improves enzymatic cell separation and isolation of mesophyll protoplasts in Arabidopsis. *Phytochemistry*, **112**, 188–194. https://doi.org/10.1016/j.phytochem.2014.07.025

Lodish, H., **Berk, A.**, **Kaiser, C. A.**, **Kaiser, C.**, **Krieger, M.**, **Scott, M. P.**, **Bretscher, A.**, **Ploegh, H.**, & **Matsudaira, P.** (2008). *Molecular cell biology*. Macmillan.

Lu, H., **Koo, L. Y.**, **Wang, W. M.**, **Lauffenburger, D. A.**, **Griffith, L. G.**, & **Jensen, K. F.** (2004). Microfluidic shear devices for quantitative analysis of cell adhesion. *Analytical Chemistry*, **76**, 5257–5264. https://doi.org/10.1021/ac049837t

Maitre, J.-L., & **Heisenberg, C.-P.** (2011). The role of adhesion energy in controlling cell–cell contacts. *Current Opinion in Cell Biology*, **23**, 508–514. https://doi.org/10.1016/j.ceb.2011.07.004

Manning, M. L., **Foty, R. A.**, **Steinberg, M. S.**, & **Schoetz, E.-M.** (2010). Coaction of intercellular adhesion and cortical tension specifies tissue surface tension. *Proceedings of the National Academy of Sciences*, **107**, 12517–12522

Mao, L., **Begum, D.**, **Chuang, H. W.**, **Budiman, M. A.**, **Szymkowiak, E. J.**, **Irish, E. E.**, & **Wing, R. A.** (2000). JOINTLESS is a MADS-box gene controlling tomato flower abscission zone development. *Nature*, **406**, 910–913. https://doi.org/10.1038/35022611

Marsollier, A.-C., & **Ingram, G.** (2018). Getting physical: Invasive growth events during plant development. *Current Opinion in Plant Biology*, **46**, 8–17. https://doi.org/10.1016/j.pbi.2018.06.002

Mathur, J., **Mathur, N.**, **Kernebeck, B.**, & **Hülskamp, M.** (2003a). Mutations in actin-related proteins 2 and 3 affect cell shape development in Arabidopsis. *The Plant Cell*, **15**, 1632–1645. https://doi.org/10.1105/tpc.011676

Mathur, J., **Mathur, N.**, **Kirik, V.**, **Kernebeck, B.**, **Srinivas, B. P.**, & **Hülskamp, M.** (2003b). Arabidopsis CROOKED encodes for the smallest subunit of the ARP2/3 complex and controls cell shape by region specific fine F-actin formation. *Development*, **130**, 3137–3146. https://doi.org/10.1242/dev.00549

McCartney, L., & **Knox, J. P.** (2002). Regulation of pectic polysaccharide domains in relation to cell development and cell properties in the pea testa. *Journal of Experimental Botany*, **53**, 707–713. https://doi.org/10.1093/jexbot/53.369.707

Meir, S., **Philosoph-Hadas, S.**, **Sundaresan, S.**, **Selvaraj, K. S. V.**, **Burd, S.**, **Ophir, R.**, **Kochanek, B.**, **Reid, M. S.**, **Jiang, C.-Z.**, & **Lers, A.** (2010). Microarray analysis of the abscission-related transcriptome in the tomato flower abscission zone in response to auxin depletion. *Plant Physiology*, **154**, 1929–1956. https://doi.org/10.1104/pp.110.160697

Meister, A., **Gabi, M.**, **Behr, P.**, **Studer, P.**, **Vörös, J.**, **Niedermann, P.**, **Bitterli, J.**, **Polesel-Maris, J.**, **Liley, M.**, **Heinzelmann, H.**, & **Zambelli, T.** (2009). FluidFM: Combining atomic force microscopy and nanofluidics in a universal liquid delivery system for single cell applications and beyond. *Nano Letters*, **9**, 2501–2507. https://doi.org/10.1021/nl901384x

Melnyk, C. W., **Gabel, A.**, **Hardcastle, T. J.**, **Robinson, S.**, **Miyashima, S.**, **Grosse, I.**, & **Meyerowitz, E. M.** (2018). Transcriptome dynamics at Arabidopsis graft junctions reveal an intertissue recognition mechanism that activates vascular regeneration. *Proceedings of the National Academy of Sciences*, **115**, E2447–E2456

Moore, R. (1984). Graft formation in *Solanum pennellii* (Solanaceae). *Plant Cell Reports*, **3**, 172–175. https://doi.org/10.1007/BF00270192

Mouille, G., **Ralet, M.-C.**, **Cavelier, C.**, **Eland, C.**, **Effroy, D.**, **Hématy, K.**, **McCartney, L.**, **Truong, H. N.**, **Gaudon, V.**, **Thibault, J.-F.**, **Marchant, A.**, & **Höfte, H.** (2007). Homogalacturonan synthesis in *Arabidopsis thaliana* requires a Golgi-localized protein with a putative methyltransferase domain. *The Plant Journal*, **50**, 605–614. https://doi.org/10.1111/j.1365-313X.2007.03086.x

Nagy, L. G., **Kovács, G. M.**, & **Krizsán, K.** (2018). Complex multicellularity in fungi: Evolutionary convergence, single origin, or both? *Biological Reviews*, **93**, 1778–1794. https://doi.org/10.1111/brv.12418

Ng, A., **Greenshields, R. N.**, & **Waldron, K. W.** (1997). Oxidative cross-linking of corn bran hemicellulose: Formation of ferulic acid dehydrodimers. *Carbohydrate Research*, **303**, 459–462. https://doi.org/10.1016/S0008-6215(97)00193-6

Ng, A., **Parker, M. L.**, **Parr, A. J.**, **Saunders, P. K.**, **Smith, A. C.**, & **Waldron, K. W.** (2000). Physicochemical characteristics of onion (*Allium cepa* L.) tissues. *Journal of Agricultural and Food Chemistry*, **48**, 5612–5617. https://doi.org/10.1021/jf991206q

Notaguchi, M., **Kurotani, K.**, **Sato, Y.**, **Tabata, R.**, **Kawakatsu, Y.**, **Okayasu, K.**, **Sawai, Y.**, **Okada, R.**, **Asahina, M.**, **Ichihashi, Y.**, **Shirasu, K.**, **Suzuki, T.**, **Niwa, M.**, & **Higashiyama, T.** (2020). Cell–cell adhesion in plant grafting is facilitated by β-1,4-glucanases. *Science*, **369**, 698–702. https://doi.org/10.1126/science.abc3710

O'Neill, M. A., **Eberhard, S.**, **Albersheim, P.**, & **Darvill, A. G.** (2001). Requirement of borate cross-linking of cell wall rhamnogalacturonan II for Arabidopsis growth. *Science*, **294**, 846–849. https://doi.org/10.1126/science.1062319

Ogawa, M., **Kay, P.**, **Wilson, S.**, & **Swain, S. M.** (2009). ARABIDOPSIS DEHISCENCE ZONE POLYGALACTURONASE1 (ADPG1), ADPG2, and QUARTET2 are polygalacturonases required for cell separation during reproductive development in Arabidopsis. *The Plant Cell*, **21**, 216–233. https://doi.org/10.1105/tpc.108.063768

Olsson, V., & **Butenko, M. A.** (2018). Abscission in plants. *Current Biology*, **28**, R338–R339. https://doi.org/10.1016/j.cub.2018.02.069

Ordaz-Ortiz, J. J., **Marcus, S. E.**, & **Paul Knox, J.** (2009). Cell wall microstructure analysis implicates hemicellulose polysaccharides in cell adhesion in tomato fruit pericarp parenchyma. *Molecular Plant*, **2**, 910–921. https://doi.org/10.1093/mp/ssp049

Packham, D. E. (2017). Theories of fundamental adhesion. In L. F. M. da Silva, A. Öchsner, & R. D. Adams (Eds.), *Handbook of adhesion technology* (pp. 1–31). Springer. https://doi.org/10.1007/978-3-319-42087-5_2-2

Parker, M. L., & **Waldron, K. W.** (1995). Texture of Chinese water chestnut: Involvement of cell wall phenolics. *Journal of the Science of Food and Agriculture*, **68**, 337–346. https://doi.org/10.1002/jsfa.2740680313

Pasternak, T., **Paponov, I. A.**, & **Kondratenko, S.** (2021). Optimizing protocols for Arabidopsis shoot and root protoplast cultivation. *Plants*, **10**, 375. https://doi.org/10.3390/plants10020375

Peaucelle, A., **Braybrook, S. A.**, **Le Guillou, L.**, **Bron, E.**, **Kuhlemeier, C.**, & **Höfte, H.** (2011). Pectin-induced changes in cell wall mechanics underlie organ initiation in Arabidopsis. *Current Biology*, **21**, 1720–1726. https://doi.org/10.1016/j.cub.2011.08.057

Pinheiro, D., & **Bellaïche, Y.** (2018). Mechanical force-driven adherens junction remodeling and epithelial dynamics. *Developmental Cell*, **47**, 3–19. https://doi.org/10.1016/j.devcel.2018.09.014

Qiu, J.-L., **Jilk, R.**, **Marks, M. D.**, & **Szymanski, D. B.** (2002). The Arabidopsis *SPIKE1* gene is required for normal cell shape control and tissue development. *The Plant Cell*, **14**, 101–118. https://doi.org/10.1105/tpc.010346

https://doi.org/10.1017/qpb.2021.16 Published online by Cambridge University Press

Raven, J. A., & **Giordano, M.** (2014). Algae. *Current Biology*, **24**, R590–R595. https://doi.org/10.1016/j.cub.2014.05.039

Razatos, A., **Ong, Y.-L.**, **Sharma, M. M.**, & **Georgiou, G.** (1998). Molecular determinants of bacterial adhesion monitored by atomic force microscopy. *Proceedings of the National Academy of Sciences*, **95**, 11059–11064

Rhee, S. Y., **Osborne, E.**, **Poindexter, P. D.**, & **Somerville, C. R.** (2003). Microspore separation in the quartet 3 mutants of Arabidopsis is impaired by a defect in a developmentally regulated polygalacturonase required for pollen mother cell wall degradation. *Plant Physiology*, **133**, 1170–1180. https://doi.org/10.1104/pp.103.028266

Roberts, K., **Alberts, B.**, **Johnson, A.**, **Lewis, J.**, **Raff, M.**, & **Walter, P.** (2002). *Molecular biology of the cell*. Garland Science.

Robinson, S., & **Durand-Smet, P.** (2020). Combining tensile testing and microscopy to address a diverse range of questions. *Journal of Microscopy*, **278**, 145–153. https://doi.org/10.1111/jmi.12863

Robinson, S., **Huflejt, M.**, **de Reuille, P.**, **Braybrook, S. A.**, **Schorderet, M.**, **Reinhardt, D.**, & **Kuhlemeier, C.** (2017). An automated confocal micro-extensometer enables in vivo quantification of mechanical properties with cellular resolution. *The Plant Cell*, **29**, 2959–2973. https://doi.org/10.1105/tpc.17.00753

Robinson, S., & **Kuhlemeier, C.** (2018). Global compression reorients cortical microtubules in Arabidopsis hypocotyl epidermis and promotes growth. *Current Biology*, **28**, 1794–1802.e2. https://doi.org/10.1016/j.cub.2018.04.028

Roland, J. C. (1978). Cell wall differentiation and stages involved with intercellular gas space opening. *Journal of Cell Science*, **32**, 325–336. https://doi.org/10.1242/jcs.32.1.325

Rosen, G. D., & **Dube, D. S.** (2006). ADHESION, CELL–MATRIX | focal contacts and signaling. In G. J. Laurent & S. D. Shapiro (Eds.), *Encyclopedia of respiratory medicine* (pp. 41–47). Academic Press. https://doi.org/10.1016/B0-12-370879-6/00013-2

Rui, Y., **Chen, Y.**, **Yi, H.**, **Purzycki, T.**, **Puri, V. M.**, & **Anderson, C. T.** (2019). Synergistic pectin degradation and guard cell pressurization underlie stomatal pore formation. *Plant Physiology*, **180**, 66–77. https://doi.org/10.1104/pp.19.00135

Sackmann, E., & **Smith, A.-S.** (2014). Physics of cell adhesion: Some lessons from cell-mimetic systems. *Soft Matter*, **10**, 1644–1659. https://doi.org/10.1039/C3SM51910D

Saedler, R., **Zimmermann, I.**, **Mutondo, M.**, & **Hülskamp, M.** (2004). The Arabidopsis *KLUNKER* gene controls cell shape changes and encodes the AtSRA1 homolog. *Plant Molecular Biology*, **56**, 775–782. https://doi.org/10.1007/s11103-004-4951-z

Shafayet Zamil, M., **Yi, H.**, & **Puri, V. M.** (2017). A multiscale FEA framework for bridging cell-wall to tissue-scale mechanical properties: The contributions of middle lamella interface and cell shape. *Journal of Materials Science*, **52**, 7947–7968. https://doi.org/10.1007/s10853-017-0999-4

Sheng, X., **Ting, Y. P.**, & **Pehkonen, S. O.** (2007). Force measurements of bacterial adhesion on metals using a cell probe atomic force microscope. *Journal of Colloid and Interface Science*, **310**, 661–669. https://doi.org/10.1016/j.jcis.2007.01.084

Shi, C.-L., **Stenvik, G.-E.**, **Vie, A. K.**, **Bones, A. M.**, **Pautot, V.**, **Proveniers, M.**, **Aalen, R. B.**, & **Butenko, M. A.** (2011). Arabidopsis class I KNOTTED-like homeobox proteins act downstream in the IDA-HAE/HSL2 floral abscission signaling pathway. *The Plant Cell*, **23**, 2553–2567. https://doi.org/10.1105/tpc.111.084608

Stenvik, G.-E., **Tandstad, N. M.**, **Guo, Y.**, **Shi, C.-L.**, **Kristiansen, W.**, **Holmgren, A.**, **Clark, S. E.**, **Aalen, R. B.**, & **Butenko, M. A.** (2008). The EPIP peptide of INFLORESCENCE DEFICIENT IN ABSCISSION is sufficient to induce abscission in Arabidopsis through the receptor-like kinases HAESA and HAESA-LIKE2. *The Plant Cell*, **20**, 1805–1817. https://doi.org/10.1105/tpc.108.059139

Stoeckle, D., **Thellmann, M.**, & **Vermeer, J. E.** (2018). Breakout—Lateral root emergence in *Arabidopsis thaliana*. *Current Opinion in Plant Biology*, **41**, 67–72. https://doi.org/10.1016/j.pbi.2017.09.005

Sung, K. L., **Sung, L. A.**, **Crimmins, M.**, **Burakoff, S. J.**, & **Chien, S.** (1986). Determination of junction avidity of cytolytic T cell and target cell. *Science*, **234**, 1405–1408. https://doi.org/10.1126/science.3491426

Temple, H., **Phyo, P.**, **Yang, W.**, **Lyczakowski, J. J.**, **Echevarría-Poza, A.**, **Yakunin, I.**, **Parra-Rojas, J. P.**, **Terrett, O. M.**, **Saez-Aguayo, S.**, **Dupree, R.**, **Orellana, A.**, **Hong, M.**, & **Dupree, P.** (2021). Discovery of putative Golgi S-adenosyl methionine transporters reveals the importance of plant cell wall polysaccharide methylation. *BioRxiv*: 2021.07.06.451061. https://doi.org/10.1101/2021.07.06.451061

Thomas, W. A., **Boscher, C.**, **Chu, Y.-S.**, **Cuvelier, D.**, **Martinez-Rico, C.**, **Seddiki, R.**, **Heysch, J.**, **Ladoux, B.**, **Thiery, J. P.**, **Mege, R.-M.**, & **Dufour, S.** (2013). α-Catenin and vinculin cooperate to promote high E-cadherin-based adhesion strength. *Journal of Biological Chemistry*, **288**, 4957–4969. https://doi.org/10.1074/jbc.M112.403774

Tran, D., **Galletti, R.**, **Neumann, E. D.**, **Dubois, A.**, **Sharif-Naeini, R.**, **Geitmann, A.**, **Frachisse, J.-M.**, **Hamant, O.**, & **Ingram, G. C.** (2017). A mechanosensitive Ca^{2+} channel activity is dependent on the developmental regulator DEK1. *Nature Communications*, **8**, 1009. https://doi.org/10.1038/s41467-017-00878-w

Trinh, D.-C., **Alonso-Serra, J.**, **Asaoka, M.**, **Colin, L.**, **Cortes, M.**, **Malivert, A.**, **Takatani, S.**, **Zhao, F.**, **Traas, J.**, **Trehin, C.**, & **Hamant, O.** (2021). How mechanical forces shape plant organs. *Current Biology*, **31**, R143–R159. https://doi.org/10.1016/j.cub.2020.12.001

Tuson, H. H., & **Weibel, D. B.** (2013). Bacteria–surface interactions. *Soft Matter*, **9**, 4368–4380. https://doi.org/10.1039/C3SM27705D

Uesugi, K., **Akiyama, Y.**, **Hoshino, T.**, **Akiyama, Y.**, **Yamato, M.**, **Okano, T.**, & **Morishima, K.** (2013). Measuring adhesion force of a cell sheet by the ninety-degree peel test using a multi hook type fixture. *Journal of Biomechanical Science and Engineering*, **8**, 129–138. https://doi.org/10.1299/jbse.8.129

Ungai-Salánki, R., **Peter, B.**, **Gerecsei, T.**, **Orgovan, N.**, **Horvath, R.**, & **Szabó, B.** (2019). A practical review on the measurement tools for cellular adhesion force. *Advances in Colloid and Interface Science*, **269**, 309–333. https://doi.org/10.1016/j.cis.2019.05.005

Veldhuis, J. H., **Ehsandar, A.**, **Maître, J.-L.**, **Hiiragi, T.**, **Cox, S.**, & **Brodland, G. W.** (2017). Inferring cellular forces from image stacks. *Philosophical Transactions of the Royal Society B: Biological Sciences*, **372**, 20160261. https://doi.org/10.1098/rstb.2016.0261

Verger, S., **Chabout, S.**, **Gineau, E.**, & **Mouille, G.** (2016). Cell adhesion in plants is under the control of putative O-fucosyltransferases. *Development*, **143**, 2536–2540. https://doi.org/10.1242/dev.132308

Verger, S., **Long, Y.**, **Boudaoud, A.**, & **Hamant, O.** (2018). A tension-adhesion feedback loop in plant epidermis. *eLife*, **7**, e34460. https://doi.org/10.7554/eLife.34460

Wang, X., **Wilson, L.**, & **Cosgrove, D. J.** (2020). Pectin methylesterase selectively softens the onion epidermal wall yet reduces acid-induced creep. *Journal of Experimental Botany*, **71**, 2629–2640. https://doi.org/10.1093/jxb/eraa059

Willats, W. G., **Orfila, C.**, **Limberg, G.**, **Buchholt, H. C.**, **van Alebeek, G. J.**, **Voragen, A. G.**, **Marcus, S. E.**, **Christensen, T. M.**, **Mikkelsen, J. D.**, **Murray, B. S.**, & **Knox, J. P.** (2001). Modulation of the degree and pattern of methyl-esterification of pectic homogalacturonan in plant cell walls. Implications for pectin methyl esterase action, matrix properties, and cell adhesion. *Journal of Biological Chemistry*, **276**, 19404–19413. https://doi.org/10.1074/jbc.M011242200

Winklbauer, R. (2015). Cell adhesion strength from cortical tension—An integration of concepts. *Journal of Cell Science*, **128**, 3687–3693. https://doi.org/10.1242/jcs.174623

Yang, H., **Benatti, M. R.**, **Karve, R. A.**, **Fox, A.**, **Meilan, R.**, **Carpita, N. C.**, & **McCann, M. C.** (2020). Rhamnogalacturonan-I is a determinant of cell–cell adhesion in poplar wood. *Plant Biotechnology Journal*, **18**, 1027–1040. https://doi.org/10.1111/pbi.13271

Yap, A. S., **Duszyc, K.**, & **Viasnoff, V.** (2018). Mechanosensing and mechanotransduction at cell–cell junctions. *Cold Spring Harbor Perspectives in Biology*, **10**, a028761. https://doi.org/10.1101/cshperspect.a028761

Zamil, M. S., & **Geitmann, A.** (2017). The middle lamella—More than a glue. *Physical Biology*, **14**, 015004. https://doi.org/10.1088/1478-3975/aa5ba5

Zamil, M. S., **Yi, H.**, & **Puri, V. M.** (2014). Mechanical characterization of outer epidermal middle lamella of onion under tensile loading. *American Journal of Botany*, **101**, 778–787. https://doi.org/10.3732/ajb.1300416

https://doi.org/10.1017/qpb.2021.16 Published online by Cambridge University Press

Zamir, E., & **Geiger, B.** (2013). Focal adhesions and related integrin contacts. In W. J. Lennarz & M. D. Lane (Eds.), *Encyclopedia of biological chemistry* (2nd ed., pp. 318–323). Academic Press. https://doi.org/10.1016/B978-0-12-378630-2.00473-4

Zhang, J., **Henriksson, G.**, & **Johansson, G.** (2000). Polygalacturonase is the key component in enzymatic retting of flax. *Journal of Biotechnology*, **81**, 85–89. https://doi.org/10.1016/S0168-1656(00)00286-8

Zhang, T., **Tang, H.**, **Vavylonis, D.**, & **Cosgrove, D. J.** (2019). Disentangling loosening from softening: Insights into primary cell wall structure. *The Plant Journal*, **100**, 1101–1117. https://doi.org/10.1111/tpj.14519

Zhang, T., **Zheng, Y.**, & **Cosgrove, D. J.** (2016). Spatial organization of cellulose microfibrils and matrix polysaccharides in primary plant cell walls as imaged by multichannel atomic force microscopy. *The Plant Journal*, **85**, 179–192. https://doi.org/10.1111/tpj.13102

Zinkl, G. M., **Zwiebel, B. I.**, **Grier, D. G.**, & **Preuss, D.** (1999). Pollen-stigma adhesion in Arabidopsis: A species-specific interaction mediated by lipophilic molecules in the pollen exine. *Development*, **126**, 5431–5440. https://doi.org/10.1242/dev.126.23.5431

https://doi.org/10.1017/qpb.2021.16 Published online by Cambridge University Press

II

Plant Direct

WILEY | American Society of Plant Biologists | SEB SOCIETY FOR EXPERIMENTAL BIOLOGY

RESEARCH ARTICLE OPEN ACCESS

The Q-Warg Pipeline: A Robust and Versatile Workflow for Quantitative Analysis of Protoplast Culture Conditions

Léa Bogdziewiez[1] | Rik Froeling[2] | Patricia Schöppl[2] | Jeanne Juquel[3] | Ioanna Antoniadi[1] | Vladimìr Skalický[1] | Ambroise Mathey[1] | Jacques Fattaccioli[4,5] | Joris Sprakel[2] | Stéphane Verger[1,3]

[1]Umeå Plant Science Centre (UPSC), Department of Forest Genetics and Plant Physiology, Swedish University of Agricultural Sciences, Umeå, Sweden | [2]Laboratory of Biochemistry, Wageningen University and Research, Wageningen, the Netherlands | [3]Umeå Plant Science Centre (UPSC), Department of Plant Physiology, Umeå University, Umeå, Sweden | [4]Pasteur, Département de Chimie, Ecole Normale Supérieure, PSL Université, Sorbonne université, CNRS, Paris, France | [5]Institut Pierre-Gilles de Gennes Pour la Microfluidique, Paris, France

Correspondence: Stéphane Verger (stephane.verger@umu.se)

Received: 11 March 2025 | **Revised:** 13 June 2025 | **Accepted:** 19 June 2025

Funding: This work was supported by Vetenskapsrådet (VR) (2020-03974), Novo Nordisk Fonden (NNF) (NNF21OC0067282), Aforsk (20-502), Knut och Alice Wallenbergs Stiftelse (Knut and Alice Wallenberg Foundation) (2022.0029, 2016.0352, and 2020.0240), Vetenskapsrådet (VR) (2021-04938), TopSector TKI Horticulture and Starting Materials (TU202312), EC | European Research Council (ERC) (101000981),

Kempestiftelserna (Kempe Foundations) (SMK21-0041), VINNOVA (Swedish Governmental Agency for Innovation Systems) (2016-00504), and Bio4Energy.

Keywords: *Arabidopsis thaliana* | cell wall | fluorescence | protoplasts | quantification | recovery | regeneration | viability

ABSTRACT

Single cells offer a simplified model for investigating complex mechanisms such as cell–cell adhesion. Protoplasts, plant cells without cell walls (CWs), have been instrumental in plant research, industrial applications, and breeding. However, because of the absence of a CW, protoplasts are not considered "true" plant cells, making them less relevant for biophysical studies. Current protocols for CW recovery in protoplasts vary widely among laboratories and starting materials, requiring lab-specific optimizations that often depend on expert knowledge and qualitative assessments. To address this, we have developed a user-friendly streamlined workflow, the Q-Warg pipeline, which enables quantitative comparison of various conditions for CW recovery post-protoplasting. This pipeline employs fluorescence imaging and tailored processing to measure parameters such as morphometry, cell viability, and CW staining intensity. Using this approach, we optimized culture conditions to obtain single plant cells (SPCs) with recovered CWs. Additionally, we demonstrated the robustness and versatility of the workflow by quantifying different fluorescent signals in protoplast suspensions. Overall, the Q-Warg pipeline provides a widely accessible and user-friendly solution for robust and unbiased characterization of protoplasts culture. The quantitative data generated by the pipeline will be useful in the future to decipher the mechanisms regulating protoplast viability and regeneration.

1 | Introduction

Multicellular organisms are made of millions or trillions of cells coming together in complex tissues with heterogeneities at several scales. While these heterogeneities characterize the form and functions of those tissues, they often complicate our understanding of biological mechanisms occurring within them. For instance, studying the phenomenon of cell–cell adhesion in the tissue context is complex because tissue topology, cell geometry, and cell–cell interface heterogeneities can have major confounding effects on the apparent strength of cell adhesion (Bidhendi and Geitmann 2016). On the contrary, working with single cells provides a strongly simplified framework to study cell–cell interaction (Atakhani et al. 2022). Beyond

the example of adhesion, such consideration applies to a large spectrum of biological questions, which explains why cell cultures are such a widely used model system in animal sciences (Verma et al. 2020). However, when it comes to studying plants, "single plant cell cultures" do not really exist. It is possible to cultivate cells in vitro under the form of microcalli, which are small clusters of cells arising from division events and thus not real single cells (Pesquet, Wagner, et al. 2019; Krasteva et al. 2021). It is also possible to isolate and study protoplasts (see further details below; Mukundan et al. 2025), which are effectively single cells but lack the cell wall, a crucial component of plant cells that controls their shape, mechanics, adhesion, and growth and plays major roles in signaling, defense, and cell-to-cell communication (Yokoyama, Shinohara et al. 2014; Anderson and Kieber 2020; Cosgrove 2024; Anderson and Pelloux 2025). It would thus be particularly useful for the plant science community to establish an approach to generate single plant cell (SPC) populations to use them as a new model system. One possibility is to start by extracting protoplasts and letting them recover their cell wall. The challenge lies in identifying culture conditions that promote strong and homogeneous cell wall recovery while ensuring minimal cell division and high cell survival rate over several days.

A protoplast is a plant cell without its cell wall (CW, term introduced by Hanstein in 1880). In 1892, the first isolation of protoplasts was successfully conducted by Klercker (Eine Methode zur Isolierung lebender Protoplasten/von John Af Klercker 1892). In 1970, Nagata and Takebe regenerated a full plant from tobacco leaves protoplasts (Nagata and Takebe 1970). Protoplasts have proven their usefulness not only in plant research to study various cellular processes such as cell division, cell wall synthesis, or cell differentiation (Jiang et al. 2013; Yokoyama, Kuki, et al. 2016; Pasternak, Lystvan, et al. 2020; Gilliard et al. 2021) but also in industry for metabolites production (Xu et al. 2022). They are also employed as a breeding technology because a whole plant can be regenerated from genetically transformed protoplasts (Reed and Bargmann 2021; Reyna-Llorens et al. 2023; Mukundan et al. 2025). Furthermore, recent development of non-transgenic genome editing with CRISPR/Cas9 and ribonucleoproteins (Yue et al. 2021; Laforest and Nadakuduti 2022) has renewed the interest in protoplasts.

Despite more than a century of research, it is still challenging to work with protoplasts as exemplified by the large number of protocols for protoplast extraction and tissue/plant regeneration that exist (Table S2). The first step of extracting the protoplasts from a plant tissue is relatively straightforward and has been done from various plant species (Kumari 2019). Most protocols use enzymatic digestion of the CW to release protoplasts. As the CW composition can vary from one tissue to another, enzymes must be carefully selected (Mukundan et al. 2025). Once the protoplasts are isolated, the first challenge is to find the right conditions to keep them alive. Without their CW, protoplasts are fragile and cannot withstand physical/mechanical stress. They require high osmolarity and low to no agitation to avoid bursting before the cell wall is recovered. However, the subsequent steps leading to CW recovery and cell division, toward tissue regeneration, appear to be the most challenging to establish and optimize (Xu et al. 2022; He et al. 2025).

Plant cells are normally surrounded by their CW, which is mainly composed of cellulose and a matrix of other polysaccharides deposited outside of the plasma membrane (Cosgrove 2024). The first challenge for the protoplasts to rebuild their CW is to retain newly synthesized CW polysaccharides at their surface. Matrix polysaccharides are secreted from the Golgi and may at first simply end up in the liquid medium (Oda et al. 2020; Hoffmann et al. 2021). Similarly, cellulose is synthesized at the surface of the plasma membrane and may primarily be extruded outward rather than sticking to the membrane (Paredez et al. 2006; Purushotham et al. 2020). Yet, those cellulose microfibrils are tethered to the membrane via the cellulose synthase complex and may act as traps for secreted polysaccharides such as xyloglucans (Park and Cosgrove 2012). It is also possible that Golgi-synthesized polysaccharides already interact with membrane-bound protein before secretion and thus remain partially attached to the surface upon secretion (McKenna et al. 2014; Fruleux et al. 2019). Furthermore, glycosylphosphatidylinositol (GPI)-anchored arabinogalactan proteins, with their extensive glycosylation and anchorage at the membrane, may be one of the players contributing to retain polysaccharides at the membrane surface (Tan et al. 2013; Leszczuk et al. 2023). Over time, the cell wall polysaccharides may begin to accumulate in patches, while the cellulose could develop into a network that will then efficiently retain additional CW deposits on the cell surface (Tagawa et al. 2019). Ultimately, a rather uniform CW may be recovered around the protoplast (Tagawa et al. 2019). However, this scenario remains very speculative, as the mechanisms of CW recovery are still largely unknown.

Although it seems that CW recovery would be almost inevitable over time, in reality, depending on the growth conditions, many protoplasts are unable to recover their CWs and instead remain as seemingly wall-less protoplasts (Xu et al. 2022). Some protocols aiming to regenerate whole plants from protoplasts take the approach of embedding the protoplasts into a gel (alginate) to help the CW recovery and callus formation (Damm and Willmitzer 1988; Masson and Paszkowski 1992; Jeong et al. 2021; Sakamoto et al. 2022). This embedding likely allows the full retention of secreted polysaccharides at the protoplast surface and thus an efficient recovery of the CW, paving the way for the first cell division, microcalli formation, and later on tissue regeneration. While CW recovery is a crucial step, for applications aiming toward tissue regeneration, it is generally enough that small proportions of the protoplasts recover their CW (Jeong et al. 2021). These cells can then divide, proliferate, and ultimately constitute the majority of the cell culture over the protoplasts that did not recover their CW. It is likely for those reasons, along with protoplast embedding methods, that optimizing protoplast CW generation has not been a major research focus in the past. Yet, with the renewed interest in biomechanical studies in plants, our intention is to obtain large, homogeneous populations of SPCs with "native" CWs (e.g., to test their adhesion properties) that can be manipulated as individual cells. Hence, we aim for the majority of the protoplasts to recover their CWs. Embedding is not an

option as it either traps the cells, preventing manipulation, or may "contaminate" the CW surface with polymers from the gelling agent.

Several methods and protocols have been developed and claimed to yield high CW recovery (Table S2). Preliminary results in our hand did not yield CW recovery at levels comparable to the literature values. Indeed, the existence of protocols with substantial variations in medium composition and growth conditions suggests that CW recovery efficiency may be highly lab dependent. A protocol that works optimally in a given lab and its local conditions may not work efficiently in another lab. Parameters like temperature, local water parameters, air moisture level, local provider of chemicals, and medium components could have direct or indirect effects on the medium and growth environment of the cells and may be challenging to track down. Instead, ideal medium and growth conditions may need to be tested and optimized in each lab. Furthermore, medium optimization is generally required when it comes to different species, varieties, or even different tissues within the same species (Reed and Bargmann 2021). Surprisingly, from a non-expert point of view, the approaches to optimize in vitro culture conditions almost appear as an art, often based on qualitative observations and relying on the skills and expertise of exceptional researchers and research groups with decades of experience. Most studies that document their optimization procedure report qualitative observations or largely manual measurements because of the lack of widely available quantitative and high-throughput methods. From the literature gathered in Table S1, in most cases, optimization is based on microscopy observations without quantification or with manual scoring of the protoplast viability (e.g., Schirawski et al. 2000; Pasternak, Paponov, et al. 2021). This implies that the experimenter must already have a good experience of what a "good culture" looks like as stated in the largely cited protocol of Yoo et al. (2007). In theory, fluorescence-activated cell sorting (FACS) offers a high-throughput, quantitative, and unbiased approach to objectively characterize cells after protoplasting (Antoniadi et al. 2022), but it unfortunately remains rarely accessible in many research labs and usually also requires advanced skills and expertise.

Here, we present an accessible workflow, developed to quantify cell viability and CW recovery after protoplasting. Using widely available fluorescence imaging and a custom image processing workflow, the quantitative cell wall regeneration (Q-Warg) pipeline reports several parameters of a cell or protoplast suspension, such as morphometry (size, circularity, etc.), viability, and CW staining intensities (see additional files or https://github.com/VergerLab/Q-Warg for user guide, protocol, and scripts). This allows quick screening of numerous parameters to optimize and compare them with quantitative data. Thanks to this pipeline, we could optimize conditions to obtain SPCs derived from protoplasts. We also further investigated approaches to select a homogeneous population of SPCs. To test the robustness of our workflow, we used it to optimize high cell viability and fast CW recovery in media designed to accelerate subsequent cell division and tissue regeneration. Finally, we demonstrate the versatility of the workflow by using it to quantify the proportion of protoplasts containing chloroplasts after protoplast extraction from seedlings. Overall, we provide a new approach and set of tools to improve efficiency, accuracy, and reproducibility when working with protoplasts, their viability, and their CW recovery and demonstrate their usefulness in different scenarios.

2 | Results and Discussion

2.1 | Q-WARG: Quantitative Cell Wall Regeneration Pipeline

The Q-Warg pipeline (Quantitative cell WAll ReGeneration) was originally designed as a quantitative screening approach to optimize in vitro culture conditions for cell viability and CW recovery after protoplasting. Note that throughout the manuscript, we use the term recovery instead of regeneration to avoid confusion with the process of protoplast regeneration that implies the growth of a whole plant from one protoplast. The screening is based on brightfield and widefield fluorescence imaging, followed by quantitative image processing and data analysis (Figure 1). Such quantitative analysis helps screen optimal culture conditions in a more objective and trackable way. Semi-automated imaging along with batch image processing and quantitative analysis makes the process high throughput compared to classical manual quantification or qualitative observation. Compared to flow sorting methods, our approach uses tools widely available in research labs or core microscopy facilities (fluorescence light microscope), which makes it accessible to most research labs without specialized equipment. In this section, we describe the main principles of this workflow, key considerations we applied during its development, as well as considerations for its usage. All the computational components of the workflow are available as Supporting Information and on a GitHub repository (for the latest updates and potential bug fixes) along with a detailed protocol, user guide, and tutorial videos (https://github.com/VergerLab/Q-Warg, additional Files 1–5).

Sample preparation (Figure 1A–D): Depending on the aim of the experiment, this step might differ. Protoplasts may be extracted from various tissues, leading to differences in the extraction method (Method S1 and Tables S1 and S2). After extraction and/or cultivation (Figure 1A–C), the protoplasts or cells viability can be assessed by fluorescein-diacetate (FDA) staining and their CW recovery by Calcofluor staining (Figure 1D). Those dyes are widely used to image cell viability and CW and have the advantage of being very quick to stain. They can also be imaged with brightfield microscopy to estimate their size and sphericity. Thus, in this workflow, we use co-staining with Calcofluor and FDA and image the cells with brightfield and widefield fluorescence microscopy to acquire three-channel images: brightfield, FDA, and Calcofluor (Figure 1G). Note that alternative staining for cell viability or CW could also be used, for example, CarboTrace or CarboTag for CW (Besten et al. 2025) or intrinsic fluorescent markers for viability (Huh et al. 2025). In particular, it is important to consider that while Calcofluor is the most commonly used dye for this application, it shows a dual affinity to both cellulose and callose (Sasamoto et al. 2003; Matsuo et al. 2014; Tagawa et al. 2019). Cellulose staining with Calcofluor is generally homogeneous but weaker than the more patchy and bright staining of callose. A double staining with aniline blue and a cellulose dye (e.g., CarboTrace rather than Calcofluor

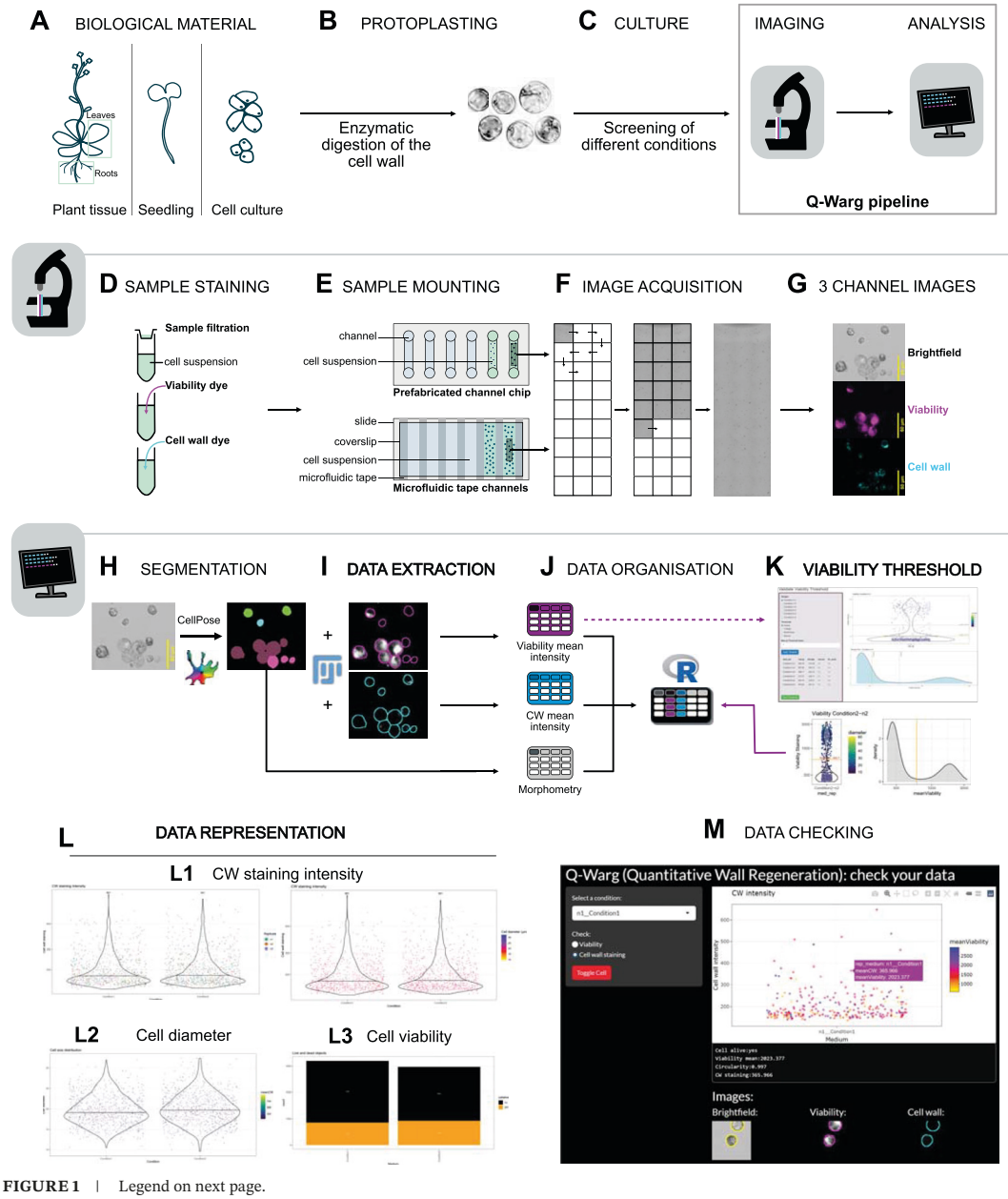

FIGURE 1 | Legend on next page.

to avoid fluorescence excitation and emission overlap) could help distinguish the callose from the cellulose (Tagawa and Kondo 2018). Depending on the aim of this study, staining might not be required (e.g., for morphometry measurements like size or circularity or intrinsic fluorescent markers).

High-throughput imaging (Figure 1E–G): For accurate quantitative analysis and high throughput of this workflow, it is useful to be able to image many cells at a time. Imaging plant cells in suspension as they are found after protoplasting and culture can be challenging for several reasons. Simply mounting the cells between slide and cover slip often leads to the cells being physically compressed and bursting. On the other hand, leaving the cells freely floating in a glass bottom dish leads to cells floating around at different focal planes, potentially overlapping and moving around during microscope

FIGURE 1 | Overview of the Q-Warg screening pipeline. Q-Warg pipeline to screen and optimize protoplast culture conditions for viability and CW recovery after protoplasting. Panels describe each step from the experimental stage to the analysis. (A–C) Description of the experimental procedure in the wet lab. (A) Starting biological material can be any plant tissue. (B) Cell wall from tissue is digested by enzymes to release protoplasts. Protoplasting protocols depend on the plant tissue. (C) Protoplasts are cultivated in different conditions to be compared. Following a period of culture, the cell suspension is imaged and analyzed. (D–G) Description of the imaging process proposed in the Q-WARG workflow. (D) Sample staining for viability (in this paper, FDA was used) and cell wall staining (Calcofluor). (E) Sample is mounted in prefabricated channel chips (loaded in the entry of the channel with a micropipette) or in microfluidic tape channels: Microfluidic channels maintain a distance between the slide and the coverslip to avoid crushing the cells. Cell suspension is loaded by capillarity. (F) Image acquisition using the microscope tiling system. Large imaging by stitching multiple low-magnification images to cover a large part of the sample. (G) Three-channel images are recorded: brightfield, viability, and cell wall. (H–M) Description of the analysis process proposed in the Q-WARG workflow. (H) Segmentation based on the brightfield image using CellPose (cyto3 model). (I) ImageJ macro using MorpholibJ plugin to extract data from fluorescent images based on the label image and morphometry information. (J) Data tables are combined and organized, thanks to an Rscript to be ready for analysis. (K) Viability threshold based on the viability staining is applied on the data to analyze only the living objects in the cell suspension. (L) Data plots: (L1) cell wall staining intensity for all conditions, the color gradient shows the cell size. (L2) cell diameter for all conditions, the color gradient shows the cell wall intensity. (L3) Cell viability proportion and living cells count. Orange shows the living cells, and black shows the dead objects. (M) Data checking in Shiny app to make the link between quantitative data in the plot and images.

stage movement. All those issues would lead to complications during cell segmentation and fluorescence intensity quantification. Thus, to limit such issues, we used either prefabricated microfluidic channel chips (μ-Slide VI 0.4; Ibidi) or microfluidic tape (S5005DC, Adhesive Applications) between microscopy glass slide and cover slip to re-create microfluidic chip-like channels (Figure 1E). Loading cells in such devices is practical because cells spread out evenly and remain on a similar focal plane without being compressed, and because of the low volume of liquid, no flux is created during stage movements, so cells stay in place during imaging. Thanks to this approach, it is then possible to semi-automatically acquire large tile images with the motorized stage of the microscope (Figure 1F). Here, we used 3×9 (27) image tiles acquired with a 10× objective to keep a good balance between resolution and field of view. This generally allows the imaging of 1000–5000 cell-like objects per scan (depending on the original sample density, usually 10^5 to 10^6cells/mL), but the workflow is not limited in this respect and can process smaller or larger tile scans or single images at different resolutions and magnifications. Image tiles can also be acquired manually and stitched computationally afterwards for microscopes without motorized stages.

Quantification (Figure 1H,I): Once images are acquired, they can be used to quantify cell morphology, viability, and CW recovery. The first step of the analysis is to segment the cells from the brightfield channel image. We used CellPose (cyto3 pretrained model; Stringer and Pachitariu 2025) to obtain the label images, containing individually labeled masks for each individually segmented cell or cell-like object (Figure 1H). Note that any other segmentation method may be used at this step as long as the output is (or is made) compatible with the rest of the workflow (Method S2). We then developed a Fiji macro to extract data from the label image and the corresponding fluorescence channels (Figure 1I). In this macro, we use the plugin MorpholibJ (Legland et al. 2016) to quantify several morphometric parameters (including cell size and circularity) from the segmented labels, as well as to measure the mean signal intensity for the viability and CW fluorescence channels. The macro generates three data tables containing information about the morphometry, viability signal intensity, and CW signal intensity.

Analysis (Figure 1J,K): We conceived an R-based pipeline (R notebook) for data processing and visualization (Figure 1J–L). From the three data tables generated by the Fiji macro, we first use the R script to combine the information in a single table (Figure 1J). Because many segmented cell-like objects may not be cells or be alive, we use the FDA staining value to screen the segmented dataset and keep only what can be considered as living cells based on FDA staining intensity. Because of the quantitative nature of the analysis, the value of the signal quantified for viability and CW is not binary. There may also be heterogeneities of background signal and noise acquired from one image to the next. Thus, even dead cells may appear to have a background level of fluorescence as quantified by the workflow. Nevertheless, we generally observe a clear bi-modal distribution of fluorescence signal for FDA staining, with one low fluorescence intensity peak corresponding to dead cells and a higher intensity peak for live cells (Figure 1K). For unbiased analysis, the workflow allows the use of automated thresholding techniques to differentiate between dead and living cell populations. On our samples, Huang and Triangle methods were the most accurate, but other thresholding algorithms can also be used, such as MaxEntropy. It is noteworthy that the algorithms consistently identify a threshold, even in scenarios where the entire cell population falls into a single category (typically all dead). Consequently, there is a potential for misclassification, where a subset of cells might be wrongly categorized as viable in a predominantly nonviable population. To address this limitation, we developed an R-based Shiny application (Figure 1K) that facilitates user intervention in the thresholding process. This tool allows for the selection of the most appropriate automated method or the application of a manual threshold. However, it is crucial to emphasize that any manual threshold adjustment must be applied judiciously to maintain data integrity and avoid introducing bias into the analysis. To further avoid having false positives, like debris that are close to a living cell and are illuminated by the FDA staining of this cell, the workflow also applies a cell circularity filter. Indeed, the isolated living cells are generally very spherical (circularity close to one) as they recover their CW without environmental pressure (in suspension) while debris have various shapes. Based on preliminary observations, we chose a high circularity index (0.9) to discriminate single cells from debris and cell aggregates.

Results representation (Figure 1L): The processed and filtered data are then plotted (Figure 1L). The first representation shows the CW intensity for each CW recovery condition tested, where the color gradient of the dots represents the size of the cells (Figure 1 L1). The number of living cells in each condition is noted at the top of the graph. The second plot shows the size of the cells, where the color gradient of the dots represents CW staining intensity (Figure 1 L2). Both plots are also saved with the color of the dots representing each experimental replicate. The last plot shows the proportion of living cells compared to dead cell-like objects (Figure 1 L3). While viability staining data usually show a clear bimodal distribution from which we can define a threshold for dead versus alive, CW intensity rarely shows such a clear distribution. Thus, contrary to what is usually described in publications reporting qualitative CW recovery from protoplasts, this pipeline does not output a binary yes/no answer for CW recovery. We believe that this is a more accurate output that better reflects the progressive nature of CW recovery as opposed to the more binary nature of cell viability.

Inspection (Figure 1M): Because this workflow segments and quantifies in batch thousands of cells at a time, there is always a risk of inaccurate segmentation or signal quantification leading to errors and biases in the final analysis. For instance, an incorrectly segmented cell could encompass a brightly stained CW debris, thus incorrectly assigning a high CW recovery value to that cell. With regular plots, it is nearly impossible to trace back a specific point in a plot to the corresponding cell in the raw image from which data were extracted to check the validity of the quantification. We thus aimed to develop a tool that would allow us to interactively check the dataset from the plotted data. We developed a Shiny app (R) making use of the plotly library (https://plotly.com/r/; Figure 1M) where we can choose which condition to observe and look at the cells individually by browsing through the plot. This allows us to check if the highest points are indeed real living cells or debris highly stained with Calcofluor. It is also possible to randomly check points to ensure that the value reported fits what a user can see in the microscopy image as well as if the segmentation has been done properly.

Advantages, limitations, and versatility: With the Q-Warg pipeline, many conditions to maintain a protoplast culture and recover CWs can be rapidly screened at once. It can be used after any protoplasting method and is not limited to the experimental conditions described here. Multiple parameters can be tested at once and compared quantitatively based on automatized measurements, eliminating the bias of phenotypical/qualitative observations. The workflow requires fluorescence images of the cell suspension as input. Those images can be acquired with any fluorescent microscope as long as the images can be converted to TIFF format, making this pipeline usable by most of the labs. The possible low sensitivity of widefield fluorescence microscopes can be one downfall compared to techniques that allow high detection of low signals such as FACS. Using a confocal microscope can improve the detection of such low signals but requires acquisition of Z-stacks instead of one-plane image to get signal from the entire surface of cells. Additional image processing scripts can be used to generate 2D Z-projections in batch and facilitate image formatting from the microscope format into TIFF (see https://github.com/VergerLab/Q-Warg for an example). All software (CellPose, Fiji, and RStudio) are free and do not require high computational power nor specific operating system (can be used on Windows, Linux, or MacOS). Despite our efforts to make the pipeline as user-friendly as possible, three different software packages are required to do the analysis, which can be overwhelming in the first place. Yet, once the user is familiar with the workflow, making modifications becomes straightforward, allowing for a high degree of adaptability within the pipeline. As a proof of concept, for this study, the Q-Warg pipeline was successfully used by two different teams, using different imaging systems (epifluorescence microscope Leica Dmi8 and confocal microscope Nikon ECLIPSE Ti2) and biological material (root cell culture, PSB-D, and seedlings). In this paper, special attention is paid to CW recovery after protoplasting. Viability alone is also a crucial parameter monitored after any type of protoplasting-based experiments. This can be quantified in an accurate and traceable way by our pipeline. As this pipeline is based on fluorescence images, other parameters could be quantified instead of the CW and viability (e.g., transformation efficiency, and gene expression). While the pipeline currently reports simple metrics (shape, size, and fluorescence intensity), the data acquired could be further refined using machine learning to classify and cluster cells or with deep-learning models to improve the accuracy of the analysis (i.e., by excluding signals coming from CW debris attached to a protoplast or predicting cell viability without the use of a binary threshold).

2.2 | Screening for Improved CW Recovery After Protoplasting Liquid-Grown Habituated Arabidopsis Cell Culture

We developed the Q-Warg workflow to solve the challenge we encountered when attempting to obtain "single plant cells" (SPC; isolated cells with recovered CW). Our aim was to obtain large populations of SPCs with relatively homogeneous size, recovered CWs, and no cell divisions, to establish them as a model system for plant CW and biophysical studies. Their largely spherical shape is ideal for physical and mechanical considerations and potential computational modeling approach. Such cells could then be used in studies of cell adhesion strength or CW mechanics. Our intention was to start with protoplasting and letting the cells recover their CW before using them. However, while many methods, publications, and protocols exist to promote CW recovery after protoplasting (Schirawski et al. 2000; Wu et al. 2009; Kuki, Higaki, et al. 2017; Pasternak, Paponov, et al. 2021; Jayachandran et al. 2023), none of the ones we tried yielded the expected results in our hands. Our preliminary observations led us to choose Arabidopsis-habituated root cell cultures (Pesquet, Korolev, et al. 2010; Ménard et al. 2017, 2024) as the starting material based on their apparent homogeneity. Similarly, our preliminary tests led us to use a modified protoplast extraction protocol (Yoo et al. 2007) and a modified regeneration medium (M; mannitol instead of trehalose (Kuki, Higaki, et al. 2017)) as the foundation for further optimization. Those preliminary protocol refinements, based on literature searches (Table S2), were assessed with qualitative observations of the protoplasts' shape and debris in the medium (issued from cell death). To go further and assess our progress methodically, we needed a quantitative way to compare the different conditions tested. Accordingly, we switched to developing and using our Q-Warg workflow.

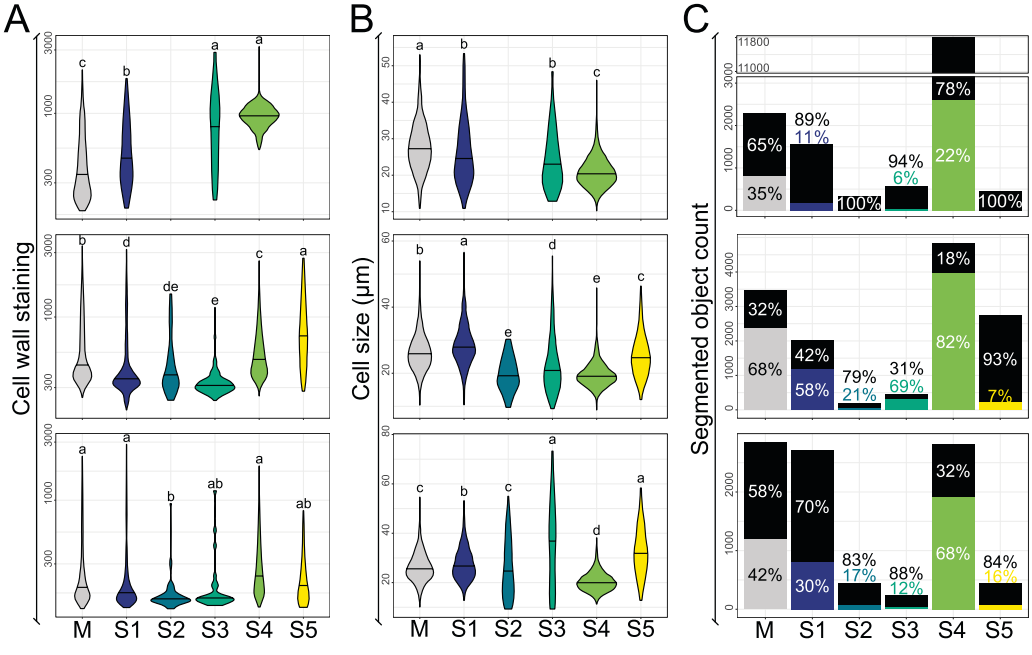

D

M	S1	S2	S3	S4	S5
Mannitol 0,4M Glucose 0,05M	Mannitol 0,4M Sucrose 0,025M	Trehalose 0,4M Glucose 0,05M	Trehalose 0,4M Sucrose 0,025M	Mannitol 0,25M Glucose 1M	Mannitol 0,25M Sucrose 0,5M

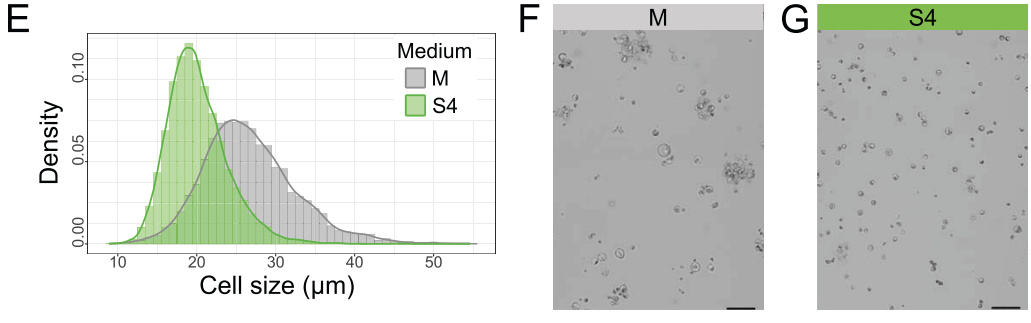

FIGURE 2 | Screening for the effect sugar composition in the medium to improve the CW recovery. (A–C) Plots from data processed with the Q-Warg pipeline on the effect of sugar composition in the medium for cell wall recovery, cell size, and viability, 4 days after protoplasting. Each plot corresponds to one replicate ($n = 3$). Note that in Replicate 1, no living cells was observed among the segmented objects; therefore, no quantification of CW staining intensity nor size is shown. (A) Cell wall mean intensity after staining with Calcofluor. (B) Cell size (diameter in µm). (C) Viability plots displaying the number of segmented objects (including debris, dead cells, or living cells). On violin plots, letters describe the statistically significant differences between populations determined by one-way ANOVA followed by Tuckey's HSD test ($p < 0{,}05$). In bar plots, each bar shows the total number of segmented objects and the proportion of objects negative for viability staining (in black) and living cells (in color). Chi-squared test of independence (significant if $p < 0.05$) was performed, followed by pairwise comparisons using the pairwise.prop.test function with Bonferroni correction for multiple testing. Results are in Data S1 (pages Fig 2_viability-stats). (D) Table with the tested media composition. All media contain Gamborg B5, MES, 1-µM NAA, and the corresponding sugars. (E) Cell size distribution for M and S4 media from the three replicates shown in B. (F–G) Four-day-old protoplast suspension in brightfield. Scale bar 100 µm. (F) Medium M, cells are forming aggregates. (G) Medium S4, cells are dispersed.

From all parameters that were previously reported to have an impact on the protoplasting and the CW recovery (Tables S1 and S2), we decided to focus on two main aspects: sugars (Sx media; Figure 2) and hormones (Hx media; Figure S1). Sugars have two different roles: keeping the osmolarity of the medium (mannitol and trehalose; Kuki, Yokoyama, et al. 2020) and feeding the cells (glucose and sucrose). In the starting protocol, 1-naphthalene acetic acid (NAA) was used as an auxin source. We also tested the effect of 2,4-dichlorophenoxyacetic acid (2,4-D) and indole-3-acetic acid (IAA) on the CW recovery (Figure S1).

We found a high impact of the type of sugars used on the viability of the cells (Figure 2D). For the three replicates, Media S2, S3, and S5 showed a low number or no living cells. Both S2 and S3 contained trehalose instead of mannitol, which did not seem to help our cells recover their CW. Media S1 and S5 both contained sucrose and displayed either a low number of living cells and/or low CW staining intensity mean compared to the reference Medium M (Figure 2B). Interestingly, Medium S4 provided comparable results in CW staining as Medium M. Note, however, that the differences in apparent CW staining intensity could also be due to the differences in callose deposition rather than true CW recovery. Moreover, the number of living cells after 4 days in culture was higher. Additionally, the cells were, on average, smaller and more homogeneous in size than those in Medium M (Figure 2C,E). The smaller size may also explain why the cells in Medium S4 recover their CW more efficiently, as they need fewer CW components to be secreted by the cells to recover the CW. In addition to the quantitative data showing that Medium S4 was a good candidate, the cell suspension in Medium S4 showed well-isolated cells, while in Medium M, more clumps/aggregates were present.

The results of the auxin screening were less clear. In our hands, the source of auxin did not seem to have any major impact on the CW recovery at the concentrations we tested when using our base medium (Figure S1B). Nevertheless, Medium H1 seemed to promote CW recovery a bit more than Medium M, suggesting that using a higher concentration of NAA could help the protoplasts recover their CW. Zhang et al. (2024) showed that a higher concentration of auxin enhanced the CW recovery. We then screened several concentrations of NAA (0–30 μM and 5-μM increment), this time using Medium S4 as base, to check if we could further increase CW recovery in our medium (Figure S1E). For both 5 and 10 μM, a significant increase in CW recovery was observed. As the proportion of living cells was higher with 5 μM of NAA, we chose to work with this concentration (Figure S1E).

Ultimately, with this approach using the Q-Warg pipeline, we successfully improved our medium for CW recovery on the protoplasts extracted from Arabidopsis-habituated root cell culture maintained at Umeå Plant Science Center (UPSC). Starting with the Medium M, we found that the Medium S4 led to a 1.61- to 3.22-fold increase in the total number of living cells, up to a 2.12-fold increase in CW staining mean intensity, and more homogeneous cell sizes (from 26.7 ± 5.89 μm for M to 20.1 ± 3.82 μm for S4). Note that the size variability might be partially reduced because of the higher osmotic pressure exerted on the cells in Medium S4. Building on Medium S4, increasing the NAA concentration from 1 to 5 μM resulted in a 1.12-fold increase in the total number of living cells and a 1.08-fold increase in cell wall staining mean intensity, while cell size and homogeneity remained similar (from 19.9 ± 4.71 to 19.1 ± 3.92 μm). With this, we propose an improved medium for our use case, based on Medium S4 and containing 5-μM NAA that we name CRRUM (CW recovery root cells UPSC medium).

Note that we performed the original sugar and hormone screen with three independent biological replicates to assess the robustness of the pipeline as a screening approach. The three biological replicates, while showing some differences, are largely in accordance with each other. We thus believe that our workflow can also be used as a robust and high-throughput screening tool by first testing various media and conditions and then using replicates for a subset of more promising media to confirm and refine choices in medium optimization.

2.3 | Further Selection of Single Plant Cells With Recovered CWs

Despite our efforts to improve CW recovery under our lab conditions, we have yet to identify a medium that reproducibly enables close to 100% of the cells to fully recover their CW. Furthermore, with the Q-Warg pipeline, we quantify fluorescent signal from CW staining, which highlights the wide disparity in CW recovery. There is no clear bimodal distribution of cells with and without recovered CWs. Not all cells seem to recover their wall at the same pace. This raises the following question: At which point do we consider the CW as "recovered"? Furthermore, while our workflow effectively characterizes these properties, it does not allow the selection of cells with recovered walls for further use.

One possibility to overcome this limitation is to sort cells with FACS based on cell size and fluorescence staining intensity. Before sorting, the cell suspension was stained for viability and CW recovery assessment. The sorted cell suspension contained only isolated cells that were positive for both viability and CW staining (Figure S2). However, during sorting, the cells are exposed to high pressure and friction forces, which may be harmful and could reduce yield. This method is suitable if a large population of cells meets the sorting requirements and the loss of some cells does not significantly affect the outcomes. Using FACS also implies the availability of suitable equipment, ideally sorting to be done in sterile conditions, and requires specific skills that may not be widely accessible in many plant biology labs.

One key function of the CW is to balance turgor pressure coming from the cytoplasm. After CW removal, protoplasts are initially kept in an iso-osmotic medium to avoid bursting before the CW is recovered. In turn, it can be argued that a non-biased binary (yes/no) estimation of CW recovery would be whether or not a cell can sustain its own turgor pressure when it is placed back in pure water or in the normal cell culture growth medium (Figure 3C). A sudden change of medium osmolarity could both provide a binary estimate of CW recovery when tested through our quantitative workflow and serve as a

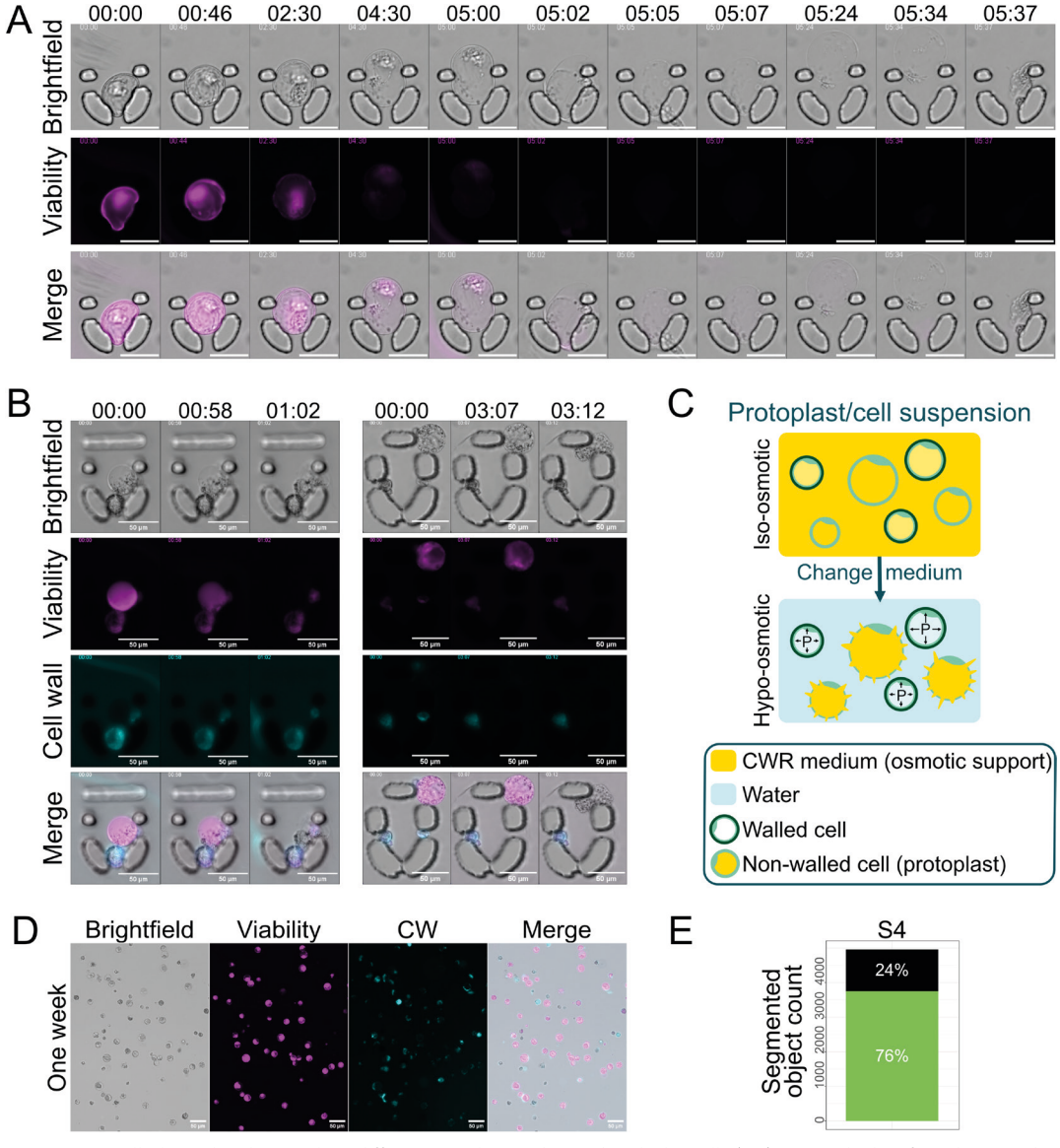

FIGURE 3 | Cell selection based on osmolarity differences in culture medium and single plant cells. (A,B) Osmotic shock performed on SPC 4 days after protoplasting. MilliQ water is flowing inside the chip from Time 0. The change in osmolarity makes the cells inflate and burst. The viability signal shows that the cell was alive at the start of the experiment. Note that the decrease in signal does not entirely correspond to the death of the cell as FDA stays fluorescent after conversion by cellular enzymes. In this case, the decrease of the signal is partially due to the bleaching of fluorescence. Complete movies in Videos S1–S3. (A) Opened trap. (B) Closed traps. Cell walls were stained with Calcofluor. (C) Scheme representing the osmotic shock strategy: The protoplast culture contains both walled and nonwalled cells. The nonwalled cells (protoplasts) are more susceptible to changes in medium osmolarity. In a hypo-osmotic medium, only walled cells will survive. (D) Single plant cells cultured into Medium S4 for 1 week. Cells are stained with FDA for viability and Calcofluor for CW. Imaged in microfluidic taped channels. (E) Quantification of living cells after 1 week of culture in S4.

means to eliminate (burst) cells with nonrecovered CW from a population. As a proof of concept, we first exposed the cell suspension (4 days after protoplasting in Medium S4) to pure water. To monitor the effect on individual cells, we used a microfluidic chip containing U-shaped traps (Sakai et al. 2019). This allowed us to keep the cells trapped in a fixed field of

view for live imaging while allowing a dynamic change of the liquid medium. Switching from Medium S4 to pure water led most of the observed cells to inflate and burst within a few minutes (Figure 3A,B). Observations using both viability and CW staining (Figure 3B) further suggest that cells with a qualitatively well-recovered wall (clear fluorescent signal) do not burst upon change of medium while protoplasts that do not appear to have CW staining burst. It is also likely that smaller walled cells showed a stronger resistance to the osmotic shock as a similar increase in turgor pressure would lead to higher stress in the CW of larger cells (Sapala et al. 2018; Figure 3B). These preliminary observations indicate that our hypo-osmotic shock approach could be useful at a larger scale. We then turned to look at the effect on large-scale cell populations and characterized the effect with the Q-Warg workflow. Pure water appeared to be too much of an osmotic shock, which may even lead to bursting of walled cells (Figure 3A,B). We used two media that contained less osmotic support than extraction or cultivation media for protoplasts to perform the osmotic shock: CRRUM without mannitol (CRRUM-noM) and the initial cell culture medium MS 3%. The cells were transferred after 4 days in culture in CRRUM into their new medium. Quickly all the cells in MS 3% died, suggesting that this medium transition had a negative effect on cell survival regardless of their CW recovery status (Figure S3C). In CRRUM-noM, we observed a quick inflation of the cells that can be attributed to the decreased osmotic pressure (Figure S3A). There was also a strong reduction in the number of cell-like objects counted and in the percentage of objects considered as living cells. Surprisingly, while we could expect the remaining living cells to be primarily strongly stained for CW, our quantification revealed the opposite trend, with cells having on average lower CW staining than the cell population kept in medium with osmotic support (Figure S3B). However, the comparison of CW staining intensity should be made carefully as the difference in medium osmolarity could affect staining capacity. Furthermore, apparently bright cell wall staining as reported by Calcofluor staining could also result from callose deposition. Thus, they may not correlate with properly regenerated cell walls displaying mechanical integrity able to sustain turgor pressure. Interestingly, after the osmotic shock, the CW fluorescence intensity average signal increased over cultivation time (3 days) while this trend is not seen in the medium with maintained osmotic support (Figure S3C). This could suggest that the remaining cells with mild cell wall signal, increasing over time, were those with "true" cell wall regeneration rather than bright callose patches. Thus, while in the current experiment we did not obtain the expected effect of binary selection of cells with recovered walls, the osmotic shock approach could still be a promising approach to select cells undergoing proper cell wall regeneration (Seyama and Kondo 2012). Furthermore, because we see an increasing trend in average cell wall staining after osmotic shock but not when cells are kept in the same medium, our results suggest that this approach may have the added benefit of further promoting CW recovery over time as suggested in other methods (Sakai et al. 2019). Note however that another explanation could be that the increased turgor pressure in the remaining living cells after the osmotic shock induces a stress response leading to the increased secretion of callose rather than cellulose.

2.4 | Assessment of Isolated Cell Viability

To assess the behavior and viability of SPCs over a long time, we used a small 3D printed microscope: Openflexure (Collins et al. 2020). Cells were plated on a glass-bottom Petri dish with a poly-lysine coating to maintain them in place. Using this DIY setup, the cells were maintained and imaged every 15 min for about 5 days. We could observe movement inside the cytoplasm of the cells, showing that they were still alive (Movie S1). In parallel, cells were kept in S4 for a week in the dark, after which they were stained to assess their viability and cell wall recovery. Notably, 74% of the segmented objects were computed as living cells (positive FDA signal and high circularity index), indicating that they could survive for a long time as single cells (Figure 3D,E). Interestingly, cells did not seem to divide in both setups, which gives us a large time window to use SPC in further experiments. To pursue divisions and calli development, cells might require other nutrients and/or hormones.

2.5 | Screening for CW Recovery in Media Aimed to Enhance Cell Division

First, to test the reusability of the Q-Warg pipeline, a trial run has been conducted in other hands in a different lab with different biological materials: at the Laboratory of Biochemistry, Wageningen University, using PSB-D cell culture derived from stem explants of *Arabidopsis thaliana* Landsberg erecta (Ler) ecotype. Unlike the previous results, imaging was done with a confocal microscope, showing the adaptability of the pipeline. We first conducted a similar screening of NAA concentration (ranging from 0 to 4 μM) within the initial Medium M during the first days of culture after protoplasting to assess cell viability. We could observe that in the absence of NAA, less than 30% of the segmented objects were living cells after 2 days of culture. By increasing the NAA concentration, we could note a positive effect on cell viability. After 2 days of culture, the more NAA was present in the medium, the larger the viable proportion of cells was (Figures 4A and S4). We also checked whether the CW recovery was increased at higher NAA concentrations, yet in those conditions, we could not observe a significant difference in CW recovery (Figure S4A).

In light of these results, we initiated a medium screening to determine the requirements for promoting micro-calli formation after protoplasting. Because cell divisions can only occur once the CW has been recovered, the first goal was to establish which parameters maintain a high viability and, second, promote CW recovery but using base media that contain hormones and nutrients aimed at enhancing cell division and regeneration. The screening was performed with three media over 3 days starting on the day of the protoplast extraction. In two tested media, "Murashige and Skoog with Minimal Organics" (MSMO) and "Protoplast Regeneration Medium" (PRM; Chupeau et al. 2013), kinetin, a form of cytokinin, was used to promote cell division when associated with auxin (respectively NAA or 2,4-D; Barciszewski et al. 2007). To compare with the previous results obtained with the root cell culture used in the beginning of this study, we also tested Medium M. Over this period of observation, we did not notice a significantly better medium for CW recovery.

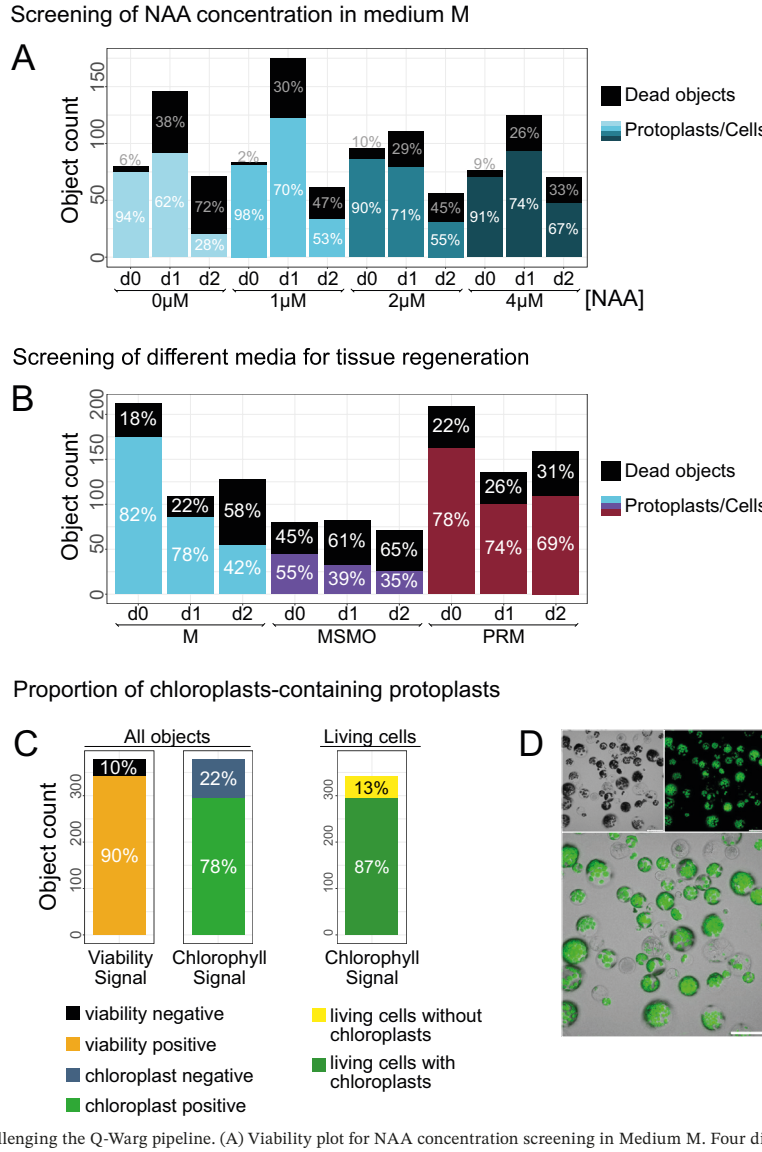

FIGURE 4 | Challenging the Q-Warg pipeline. (A) Viability plot for NAA concentration screening in Medium M. Four different concentrations of NAA have been tested. d0 corresponds to the protoplasting day. (B) Viability plot for medium screening. Three media for tissue regeneration were tested. d0 corresponds to the protoplasting day. (C,D) Protoplast extracted from *Arabidopsis thaliana* seedlings and imaged the day of extraction. (C) Left bar plot represents the proportion of living cells in yellow (90%). The middle bar shows the proportion of autofluorescent objects based on chlorophyll autofluorescence (78%). The right bar shows the proportion of chloroplast-containing cells among the living cells. (D) Protoplast suspension in brightfield (top left), autofluorescence of chlorophyll (top right), and merged image (bottom). Scale bar 50 µm. In plots, object count corresponds to the number of segmented objects (including debris, dead cells, or living cells). Each bar shows the total number of segmented objects and the proportion of objects negative for viability staining (in black) and living cells (in color). Protoplasts are issued from PSB-D cell culture. Chi-squared test of independence (significant if $p < 0.05$) was performed, followed by pairwise comparisons using the pairwise.prop.test function with Bonferroni correction for multiple testing. Results are in Data S1 (pages Fig 4_viability-stats).

Cells in M and MSMO showed a similar increase in CW signal, but viability decreased to about 40% of the segmented objects (Figure 4B). PRM medium did not show an improved CW recovery compared with M and MSMO (Figure S4B). However, the proportion of living cells after 2 days was maintained at 70% of the segmented objects, which made this medium promising. Future work will determine the best condition to achieve quick cell divisions to reach the micro-calli stage.

2.6 | Pipeline Versatility: Quantification of Chloroplast-Containing Cells

The Q-Warg pipeline is based on brightfield and fluorescence imaging and quantification and is not limited to viability and CW staining. The intensity quantification can in principle be done on any fluorescence marker or autofluorescence signal. To show the versatility of the pipeline, we quantified the proportion of chloroplast-containing protoplasts extracted from whole seedlings. Using the viability proportion plot, we first quantified the proportion of living cells in the suspension with the viability staining (FDA). Then inside this population of living cells, we used the workflow to quantify the number of cells containing chloroplasts (Figure 4C,D). To do this, instead of taking the fluorescence coming from a viability staining as input, we used the autofluorescence of chloroplasts. The plot given by the pipeline is then used to report the cells or objects with chloroplasts versus those without, based on their autofluorescence. In this experiment, among the objects segmented by the pipeline, 90% were viable protoplasts, and 78% presented an autofluorescence signal from chloroplasts. Using these data and the unique IDs of cells analyzed through the pipeline, we then calculated that 87% of the living cells extracted from those seedlings contain chloroplasts (Figure 4C "Living cells").

3 | Conclusion and Perspectives

In this work, we introduced the Q-Warg pipeline, an imaging and image processing-based workflow aimed at making studies of protoplast culture, viability, and CW recovery more accessible, quantitative, and standardized. We further applied it in several use cases to show its usefulness in different configurations, demonstrating its robustness and versatility.

Our initial aim when developing this pipeline was to create a tool that we could confidently use to assess our progresses when optimizing CW recovery media for the obtention of "single plants cells." Thus, in this work, we report the steps taken in this direction by testing the quantitative effect of changing a subset of the CW recovery medium composition, namely, the sugars and auxins used, and finding an improved medium. However, given the number of parameters that may influence protoplast culture and CW recovery (Table S1) and the range of possible values to be tested for each parameter, there is a virtually infinite number of media combinations to be tested. This is obviously impossible for practical reasons, but it is in principle possible to use design of experiment approaches to explore parameter spaces and define optimal settings without having to test every possible combination (Cano et al. 2012; Peng et al. 2022). We also believe that our workflow could further help in the future to streamline the media optimization process. The standardized nature of the pipeline also aimed to increase the reusability of the data. We provide a detailed user guide for the whole procedure (Method S2) and aimed to make the computational workflow user-friendly. We also strongly encourage future users to deposit their data in publicly accessible repository for future reuse. In practice, during the medium optimization process, it is more reasonable to test a restricted set of parameters, until reaching an acceptable result and moving on. Researchers have been doing this for several decades, but unfortunately those optimization steps are rarely reported, nor quantitatively measured, and there is no standardized format available. Instead, in vitro culture medium optimization is almost referred to as an art, only mastered by a few experts with decades of experience. We believe that the instinctive expertise acquired by such experts could be understood scientifically and be made available more broadly if we can generate enough standardized data on protoplast viability and regeneration and study them through advanced multivariate analyses or novel deep learning approaches. We could, for instance, imagine training a model with a large dataset gathering matching information on the parameters used in the media, types of tissues, varieties, species, growth conditions, and so on and matching quantification of viability and CW recovery. In turn, we may be able to interrogate the model to predict a set of media to test for further optimization, given a species, variety, tissues, and growth conditions of choice. This would effectively allow a much shorter time for medium refinement, by using complex knowledge from prior optimization experiments as a starting point for a subset of media to test. In parallel, the Q-Warg pipeline could be used for quantitative screening of large sets of mutants with improved or impaired protoplast viability or CW recovery to decipher the biological mechanisms regulating these processes.

The pipeline we developed here is also potentially highly versatile. Because of our original aim, we focused mainly on cell viability and CW recovery after protoplasting. However, the pipeline can also be used to explore other parameters. Here, we also used it to determine the percentage of chloroplast-containing cells inside a population of protoplasts extracted from seedlings. This workflow could also be used to check transformation efficiency with a fluorescent reporter or other parameters that can be observed quantitatively with fluorescent dyes or reporters at the cell level.

Encouraging open data practices and leveraging deep learning approaches, thanks to datasets acquired with such tools, could help make significant strides in unraveling the biological complexity of protoplasts, ultimately contributing to more robust and reproducible research outcomes and biotechnological applications.

4 | Methods

4.1 | Biological Material

4.1.1 | Root Cell Culture

The cell culture used in this study (unless stated otherwise) is derived from the root cells of *A. thaliana*, ecotype Colombia, and was previously reported (Pesquet, Korolev, et al. 2010). This cell

culture was habituated via prolonged culturing with decreasing exogenous hormones until it became able to grow and divide without exogenous hormones.

Prior to our set of experiments, the cell culture was re-screened for habituation (Ménard et al. 2017, 2024). Calli were grown on 1% plant agar (Duchefa) growth medium plates. One callus was used to start the new cell suspension to have a clonal culture. Growth medium MS 3% contains Murashige and Skoog medium including vitamins (M0222, Duchefa), 3% sucrose (VWR), and MES 20 mM. The pH is adjusted to 5.7 with KOH. Cells are growing in the dark under constant shaking (22°C and 120 rpm). The cell culture was maintained weekly by inoculating 72 mL of fresh MS 3% with 8 mL from the 1-week-old culture.

4.1.2 | PSB-D Culture

A. thaliana, ecotype Landsberg, cell suspension cultures (PSB-D) were donated by Geert de Jaeger (ABRC stock no. CCL84840) (Menges and Murray 2002; Van Leene et al. 2011). MSMO contains Murashige and Skoog Basal Salts with minimal organics 0.44% (Sigma-Aldrich) and sucrose 88 mM. The pH is adjusted to 5.7 with KOH. After autoclaving, 2.7-μM NAA and 0.23-μM kinetin were added. PSB-D cultures were grown in 50-mL MSMO (dark, 25°C, and 135 rpm) and were maintained weekly by taking 2.5 mL from the 1-week-old culture with 47.5 mL of fresh MSMO.

4.1.3 | Seedling Growth

A. thaliana, ecotype Columbia-0 (Col-0), seeds were sterilized by washing them with 70% ethanol, followed by a treatment with 0.8% NaOCl for 3 min. Seeds were washed five times with ultrapure water and were kept in water in the dark at 4°C for 2 days. Seeds were then sown on MS agar plates. MS agar plates contain half-strength Murashige and Skoog medium (Duchefa), 5-mM MES, and 0.8% plant agar (Duchefa). The pH was adjusted to 5.7 with KOH. The plates were vertically incubated at 22°C under a long day growth period (16-h light and 8-h dark).

4.2 | Protoplast Extraction

4.2.1 | Root Cell Culture

The protocol was adapted from Yoo et al. (2007) and is detailed in the protocol (Method S1). In brief, cells are incubated in an enzymatic solution for 4 h in the dark at 120 rpm and 24°C in nontreated six-well plates. Enzymatic digestion is stopped with W5, and the protoplast suspension is filtered through a 70-μm nylon basket before centrifugation and resuspension in culture medium. For all root cell culture protoplast extractions, the cell culture was 4 days old (4 days after refreshing medium).

4.2.2 | PSB-D Protoplast Extraction

PSB-D protoplasts are extracted similarly to root cell culture protoplasts, with the following adjustments. A 5-day-old PSB-D culture was used. The culture was incubated in the dark at 200 rpm and 25°C. Protoplasts were filtered through a 40-μm nylon basket. The final pellet was resuspended in 1 mL of the desired medium. Protoplast density was adjusted to $5.0*10^4$ cells/mL, and 200 μL of suspension was transferred to each well of an Ibidi μ-Slide (eight-well high, polymer coverslip, and uncoated). Slides were placed in a dark growth chamber at 22°C for 3 days.

4.2.3 | Seedling Protoplast Extraction

The protocol is detailed in Method S1. The protocol is adapted from Zhai et al. (2009) for protoplast extraction of 18-day-old seedlings with the following modifications. The protoplast suspension was filtered through a 40-μm nylon basket. W5+ was used instead of W5 to retrieve protoplasts within the sucrose gradient. W5+ differs from W5 by a higher KCl concentration (11 mM instead of 5 mM) and the inclusion of glucose (5.6 mM). Protoplast density was adjusted to $5.0*10^4$ cells/mL, and 200 μL of suspension was transferred to each well of an Ibidi μ-Slide (eight-well high, polymer coverslip, and uncoated). Seedling protoplasts were imaged directly after extraction.

4.3 | CW Recovery Medium

Initial medium for CW recovery, Medium M, contains Gamborg B5 (Gamborg's B-5 Basal Medium with minimal organics, G5893, Sigma-Aldrich), 0.4-M mannitol, 0.05-M glucose, 1-μM NAA, 20-mM MES filled up to the wanted volume with MilliQ water, and pH 5.7 adjusted with KOH. The different combinations of sugars and hormones that have been tested are reported in Figure 2A. The protoplasts were transferred directly after extraction in medium for CW recovery and kept in the dark at 22°C without shaking. After screening, the medium CRRUM was used for CW recovery with root cell culture: S4 with 5-μM NAA. For all changes of medium, the cell suspension was placed in Falcon 50-mL tubes and centrifuged at 200 g in a swing-rotor centrifuge for 3 min at room temperature. The supernatant was carefully removed by pipetting, and the new medium was added. Cells were resuspended by gently turning over the Falcon tube. The media used for CW recovery with the PSB-D cells were CRRUM, MSMO (previously described), and protoplast regeneration medium (PRM). PRM was modified from Chupeau et al. (2013) and contains half-strength Murashige and Skoog medium (Duchefa), 20-mM MES, 0.3-M mannitol, 0.2-M glucose, 4.5-μM 2,4-D, 0.46-μM kinetin filled up to the wanted volume with MilliQ water, and pH 5.7 adjusted with KOH.

4.4 | Microscopy Sample Preparation and Imaging

4.4.1 | Protoplasts Derived From Root Cell Culture

Viability was assessed by FDA (F1303 Thermofischer). Four minutes before imaging, FDA was added to the cell suspension to reach 8 μg/mL. For CW characterization, the cells were stained just before imaging with Calcofluor White (Calcofluor White Stain, Sigma-Aldrich) diluted 1:100 directly in the cell suspension. Double-stained cells were then loaded in an Ibidi channel chamber (μ-Slide VI 0.4 Bioinert) or an in-house

chamber. In-house chambers are composed of a microscopy slide on which strips of microfluidic tape (S5005DC, Adhesive Applications) are put to form channels and maintain a distance from the coverslip (see protocol file Method S1). Fluorescence imaging was done with a Leica DMi8 inverted brightfield and epifluorescence microscope with a motorized stage and navigator function. The microscope is equipped with a 10× objective lens (NA 0.32, air objective) and a Leica DFC9000GT camera mounted on a 1× C-mount adapter. Tile images made of 3 × 9 (27) individual images (12bits, 2048 × 2048 resolution for each image, and pixel size of 1.048 × 1.048 μm) were acquired with the Navigator function of the microscope using a 10% overlap. Tile images were merged with the LAS X software (Leica Microsystems, Germany). Before acquisition, autofocus is done on the brightfield channel. Three channels were acquired: brightfield, FDA signal excited with 460-nm LED, and emission detected above 515 nm (long pass filter) and Calcofluor signal excited with 365-nm LED and emission detected between 435 and 485 nm. The same procedure was used to quantify viability and CW recovery following osmotic shock (Figure S3).

4.4.2 | Protoplasts Derived From PSB-D and Seedlings

Protoplasts were imaged in Ibidi μ-Slide (eight-well high, polymer coverslip, and uncoated) with an inverted Nikon ECLIPSE Ti2 microscope equipped with a Nikon C2 confocal laser scanning head and a 40× (NA 0.95) dry objective. Five minutes before imaging, protoplasts were stained with 5-μg/mL FDA. PSB-D protoplasts were also stained with Calcofluor White (Calcofluor White Stain, Sigma-Aldrich) diluted 1:100. Calcofluor White/chloroplasts and FDA were excited sequentially using a 405- and 488-nm laser line, respectively. Calcofluor White/chloroplast fluorescence was detected using a dual-bandpass filter (C2 Filter Cube DAPI/Cy5 Dual, MHE46660) between 440 and 460 nm (Calcofluor White) and 680 and 720 nm (chloroplasts), and FDA fluorescence was detected between 500 and 550 nm (C2 Filter Cube 525/50595/40, MHE46770). With the 488-nm laser line, transmitted light was also collected. Z-stacks (512 × 512 pixels, pixel size 0.62 μm) were taken at 1-μm intervals of the bottom 12 μm of the cells. For Q-Warg analysis, maximum-intensity Z-projections were used for the fluorescence channels. For CellPose segmentation, we used the topmost plane of each z-stack, which corresponds approximately to a cross-sectional image of the middle of each cell.

4.5 | Computational Workflow

The analysis workflow is first based on (1) cell segmentation on the brightfield image using CellPose, (2) an ImageJ macro to extract quantitative information from the images, and (3) an R script to analyze and represent the quantitative data. The procedure described here can be downloaded from GitHub (https://github.com/VergerLab/Q-Warg) and Methods S3 and S4. The overall concept and procedure are described in the main text (Figure 1), and a detailed step-by-step description of the procedure is available in the user guide available in the GitHub repository and as Method S2.

4.5.1 | Cell Segmentation

Cell segmentation is done on the brightfield image with the generalist model cyto3 (Stringer and Pachitariu 2025). Used settings were default except for the cell diameter (40 pixels) and the flow threshold (0.2). The label image generated from the segmentation was saved as PNG. Details on how to use CellPose can be found in the Q-Warg user guide (Method S1).

4.5.2 | Quantification

We developed a batch processing ImageJ macro using Fiji (Schindelin et al. 2012) to extract quantitative information from segmented label images and the corresponding cell wall and viability fluorescence images (CWRegenerationQuantification.ijm; Method S3). The macro splits the multichannel image (brightfield, CW, and viability) and saves individual images as tif as well as brightfield images with cell segmentation (contours) overlap. The macro uses the ImageJ plugin MorpholibJ (Legland et al. 2016) to extract morphometric information (*Plugins>MorphoLibJ>Analyze>Analyze Regions*) on individual cells from the label image, as well as fluorescence intensity (*Plugins>MorphoLibJ>Analyze>Intensity Measurements 2D/3D*) on the CW and viability images for individual cells using the label image.

4.5.3 | Data Analysis

We developed an R script in a markdown notebook (QWARG.Rmd; Method S4) usable in RStudio (https://posit.co/download/rstudio-desktop/) to analyze the data issued from the quantification. Data tables generated by the CWRegenerationQuantification.ijm (additional File 4) macro were combined and organized to be treated all at once (tidyverse; Wickham et al. 2019). Automatic thresholding was computed to discriminate dead and living cells using the autothreshold library (Nolan et al. 2023) and applied in a shiny app using plotly to render interactive plots (shiny; Chang et al. 2024; Create Interactive Web Graphics via "plotly.js" [R package plotly version 4.10.4] 2024). The plots were done with the ggplot2 library. Another Shiny app helps check the results of the thresholding and cell segmentation by linking interactive plots (plotly) to the microscopy images (magick; Ooms 2024). All information about other libraries used can be found in the user guide (Method S2).

4.5.4 | Statistical Analysis

We performed statistical analysis within the R notebook using the agricolae library (de Mendiburu 2023). One-way analysis of variance (ANOVA) followed by Tukey's honestly significant difference (HSD) test was performed for multiple comparisons of means for CW staining intensity and cell size plots. Chi-squared test of independence (significant if $p < 0.05$) was performed, followed by pairwise comparisons using the pairwise.prop.test function with Bonferroni correction for multiple testing.

4.6 | Osmotic Shock in Microfluidic Chips

4.6.1 | Chip Fabrication

The microfluidic chips were fabricated according to the method detailed in Sakai et al. (2019). Starting from a SU8-on-silicon master mold (IPGG, Paris), a 9:1 PDMS (Silgard 184 Silicone Elastomer, Dow) mixture is poured on top of it, degassed for 2 hours in a vacuum chamber, and cured at 70°C overnight. The chips are then individually cut with a razor blade, and inlets and outlets are created using a biopsy puncher (1-mm diameter, pfm medical). PDMS chips are then rinsed with isopropanol and stuck to a glass bottom petri dish (WPI Fluorodish P35-100) in a cleanroom (Nanolab, Umeå) using an oxygen plasma cleaner (Plasma cleaning system ATTO, 0.35 mbar, 36 s).

4.6.2 | Chip Preparation

Before loading the cells, a flow of 96% EtOH was performed not only to sterilize the tubing (0.022 "ID × 0.042" OD, PTFE, Masterflex) and the chip but also to reduce the apparition of bubbles in the setup. Then, a filtered (0.2-μm filter) of pluronic F-127 0.02% solution in water was added overnight inside the chip. The pluronic solution was replaced with medium before loading the cells.

4.6.3 | Osmotic Shock

Four days post-extraction, the cell suspension was stained as explained previously with Calcofluor and FDA. The cells were loaded at 100 μL/min with a DIY syringe pump (Baas and Saggiomo 2021) until most of the traps contained a cell. MilliQ water was then pumped into the chip at 50 μL/min. Short-term brightfield timelapses of the chip are recorded with the Leica Dmi8 microscope.

4.6.4 | Timelapse Experiment

Protoplasts were cultured in FluoroDish (FD35, World Precision Instruments) coated with poly-lysine to maintain cells in place. FluoroDish glass bottom was covered by a solution of poly-L-lysine 0.1% (P8920, Sigma-Aldrich) for 5 min at room temperature. The liquid was removed as much as possible with a pipette and quickly dried with an air gun. The plates were dried in an oven at 60°C for 1 h. A 3D printed microscope Openflexure (high resolution version, Collins et al. 2020) was used to image the culture in brightfield, without staining. Images were taken every 15 min with white LED illumination for the duration of the experiments. Cells were cultured at room temperature (20°C–22°C).

4.7 | Fluorescence-Activated Cell Sorting

Before analysis and sorting, the cells were washed from the culture medium and put into W5 modified (W5m). The cell suspension was transferred into a 15-mL Falcon tube and centrifuged at 200rcf (swing out rotor centrifuge) for 5 min, RT. W5m contains only 2-mM calcium (instead of 125 mM) to avoid the precipitation with the sheath fluid (70% FACS Flow; BD Bioscience, San Jose, CA, USA) used during sorting and 0.1% BSA to prevent sticking of the cells to the plastic walls of the sorting plate.

The FACS BD Aria III equipped with four lasers: violet (405 nm), blue (488 nm), yellow green (561 nm), and red (633 nm) lasers (BD Biosciences, San Jose, CA, USA). BD FACSDiva software Version 7.0 was used for handling the cytometer and respective data analysis. For each condition, the nonstained sample was subjected to analysis as a negative control. Cell suspension was stained for 30 min with a 1:1000 dilution of CarboTrace 680 for CW staining and FDA (5-mg/mL stock solution, predilution: 1.6 μL for 1-mL medium, then add 1.6 μL of the predilution for 1-mL cell suspension).

Protoplast analysis and sorting: Filtered protoplast suspension through 70-μm Flowmi Cell strainer (SP Bel-Art, Wayne, NJ, USA) was loaded in the cell sorter (room temperature, mild agitation of 100 rpm) and forced through the cuvette in a single-file stream, where laser lights intercepted the stream at the sample interrogation point. After passing through the cuvette, the stream entered the integrated 100-μm nozzle tip, where the drop drive broke the stream into the droplets for sorting. The forward scatter (FSC) of light was initially filtered through a 1.5 neutral density filter and then perceived by a photodiode detector with a 488/10 bandpass filter. Light scatter information was collected to identify the protoplast population and to design sorting strategy (Figure S2).

Different protoplast populations based on fluorescent properties given by used fluorophores were sorted for microscopy analysis into 500 μL of CWR medium in a 24-well plate. To remove the debris, all events smaller than 16 μm were disregarded. The cells were sorted based on their viability (FDA staining) and their CW staining (CarboTrace 680). We used CarboTrace 680 instead of Calcofluor for CW staining to limit the toxicity applied to the cells. To identify and subsequently exclude doublets (the droplets containing more than one protoplast), the ratio of fluorescence signal width to the respective area was measured (Suda et al. 2007).

Author Contributions

The authors take full responsibility for this article.

Acknowledgments

We thank Åsa Strand and Xu Jin for providing the root cell culture material and initial technical help. We thank Adrien Heymans for helping with the statistical part of the R script. We thank Pauline Durand and Cyril Grandjean, Antoine Chevallier and Isaty Melogno, and Mateusz Majda and Lukas Hoermayer for the discussions about protoplast extraction and culture optimization. We thank Remko Offringa and Loïc Talide for giving us feedback on the manuscript. We thank the facilities and technical assistance of the Umeå Plant Science Center (UPSC), the microscopy facility, and the growth facility. We thank the NanoLab (Physics Department, Umeå University) for the technical resources for microfluidic chips fabrication. This work benefited from the technical contribution of the joint service unit CNRS UAR 3750 (Paris, France) at IPGG. This work was supported by grants from the Swedish Research Council (VR, 2020-03974), Novo Nordisk Foundation (NNF21OC0067282), Åforsk Foundation (20-502), Knut and Alice Wallenberg Foundation (KAW 2022.0029) to S.V. R.F. is financially supported by the TopSector TKI Horticulture and Starting Materials, the Netherlands, through the

project TU202312. J.S. and P.S. are funded by the European Research Council project Catch, project number 101000981. I.A. and V.S. were supported by grants from the Swedish Research Council (VR 2021-04938) and Kempestiftelserna (SMK21-0041). This work was also supported by Umeå Plant Science Center with grants from the Knut and Alice Wallenberg Foundation (KAW 2016.0352 and KAW 2020.0240), the Swedish Governmental Agency for Innovation Systems (VINNOVA 2016-00504), and Bio4Energy, a Strategic Research Environment supported through the Swedish Government's Strategic Research Area initiative.

Conflicts of Interest

The authors declare no conflicts of interest.

Data Availability Statement

All the raw data generated for this study, along with the processed data and quantification, have been deposited at Zenodo and are publicly available as of the date of publication (10.5281/zenodo.14971281).

The code for the Q-Warg workflow is publicly available on github (github.com/VergerLab/Q-Warg), and the specific version used for this study has been archived at Zenodo and is publicly available as of the date of publication at (10.5281/zenodo.14973382).

Requests for further information and resources should be directed to and will be fulfilled by the corresponding author, Stephane Verger: stephane.verger@umu.se.

References

Anderson, C. T., and J. J. Kieber. 2020. "Dynamic Construction, Perception, and Remodeling of Plant Cell Walls." *Annual Review of Plant Biology* 71 (Volume 71, 2020): 39–69. https://doi.org/10.1146/annurev-arplant-081519-035846.

Anderson, C. T., and J. Pelloux. 2025. "The Dynamics, Degradation, and Afterlives of Pectins: Influences on Cell Wall Assembly and Structure, Plant Development and Physiology, Agronomy, and Biotechnology." *Annual Review of Plant Biology* 76: 85–113. https://doi.org/10.1146/annurev-arplant-083023-034055.

Antoniadi, I., V. Skalický, G. Sun, et al. 2022. "Fluorescence Activated Cell Sorting – A Selective Tool for Plant Cell Isolation and Analysis." *Cytometry. Part A: Journal of the International Society for Analytical Cytology* 101, no. 9: 725–736. Available at:. https://doi.org/10.1002/cyto.a.24461.

Atakhani, A., L. Bogdziewiez, and S. Verger. 2022. "Characterising the Mechanics of Cell–Cell Adhesion in Plants." *Quantitative Plant Biology* 3: e2. https://doi.org/10.1017/qpb.2021.16.

Baas, S., and V. Saggiomo. 2021. "Ender3 3D Printer Kit Transformed Into Open, Programmable Syringe Pump Set." *HardwareX* 10: e00219. https://doi.org/10.1016/j.ohx.2021.e00219.

Barciszewski, J., F. Massino, and B. F. C. Clark. 2007. "Kinetin—A Multiactive Molecule." *International Journal of Biological Macromolecules* 40, no. 3: 182–192. https://doi.org/10.1016/j.ijbiomac.2006.06.024.

Besten, M., M. Hendriksz, L. Michels, et al. 2025. "CarboTag: A Modular Approach for Live and Functional Imaging of Plant Cell Walls." *Nature Methods* 22: 1081–1090. https://doi.org/10.1038/s41592-025-02677-4.

Bidhendi, A. J., and A. Geitmann. 2016. "Relating the Mechanics of the Primary Plant Cell Wall to Morphogenesis." *Journal of Experimental Botany* 67, no. 2: 449–461. https://doi.org/10.1093/jxb/erv535.

Cano, E. L., J. M. Moguerza, and A. Redchuk. 2012. "Design of Experiments With R." In *Six Sigma With R: Statistical Engineering for Process Improvement*, edited by E. L. Cano, J. M. Moguerza, and A. Redchuk, 197–215. New York, NY: Springer New York. https://doi.org/10.1007/978-1-4614-3652-2_11.

Chang, W. J. Cheng, J. J. Allaire, Y. Xie, and J. McPherson 2024 'Shiny: Web Application Framework for R'. https://cran.r-project.org/web/packages/shiny/ (Accessed: 19 February 2025).

Chupeau, M.-C., F. Granier, O. Pichon, J. P. Renou, V. Gaudin, and Y. Chupeau. 2013. "Characterization of the Early Events Leading to Totipotency in an Arabidopsis Protoplast Liquid Culture by Temporal Transcript Profiling." *Plant Cell* 25, no. 7: 2444–2463. https://doi.org/10.1105/tpc.113.109538.

Collins, J. T., J. Knapper, J. Stirling, et al. 2020. "Robotic Microscopy for Everyone: The OpenFlexure Microscope." *Biomedical Optics Express* 11, no. 5: 2447–2460. https://doi.org/10.1364/BOE.385729.

Cosgrove, D. J. 2024. "Structure and Growth of Plant Cell Walls." *Nature Reviews Molecular Cell Biology* 25, no. 5: 340–358. https://doi.org/10.1038/s41580-023-00691-y.

Create Interactive Web Graphics via 'plotly.js' [R package plotly version 4.10.4] 2024. Comprehensive R Archive Network (CRAN). https://CRAN.R-project.org/package=plotly (Accessed: 19 February 2025).

Damm, B., and L. Willmitzer. 1988. "Regeneration of Fertile Plants From Protoplasts of Different *Arabidopsis thaliana* Genotypes." *Molecular and General Genetics MGG* 213, no. 1: 15–20. https://doi.org/10.1007/BF00333392.

de Mendiburu, F. 2023. 'agricolae: Statistical Procedures for Agricultural Research'. Accessed: 19 February 2025 https://cran.r-project.org/web/packages/agricolae/index.html.

Eine Methode zur Isolierung lebender Protoplasten/von John Af Klercker 1892. *Accessed: 6 February 2025* http://sammlungen.ub.uni-frankfurt.de/botanik/4449859.

Fruleux, A., S. Verger, and A. Boudaoud. 2019. "Feeling Stressed or Strained? A Biophysical Model for Cell Wall Mechanosensing in Plants." *Frontiers in Plant Science* 10: 757. https://doi.org/10.3389/fpls.2019.00757.

Gilliard, G., E. Huby, S. Cordelier, M. Ongena, S. Dhondt-Cordelier, and M. Deleu. 2021. "Protoplast: A Valuable Toolbox to Investigate Plant Stress Perception and Response." *Frontiers in Plant Science* 12: 749581. https://doi.org/10.3389/fpls.2021.749581.

He, Q., Y. E, and R. Li. 2025 "Protoplast Cell-Wall Regeneration: Unlocking New Potential for Genetic Improvement and Tree Breeding." *Plant, Cell and Environment* 48, no. 8: 5786–5788. https://doi.org/10.1111/pce.15537.

Hoffmann, N., S. King, A. L. Samuels, and H. E. McFarlane. 2021. "Subcellular Coordination of Plant Cell Wall Synthesis." *Developmental Cell* 56, no. 7: 933–948. https://doi.org/10.1016/j.devcel.2021.03.004.

Huh, H., D. Jayachandran, J. Sun, et al. 2025. "Time-Resolved Tracking of Cellulose Biosynthesis and Assembly During Cell Wall Regeneration in Live *Arabidopsis* Protoplasts." *Science Advances* 11, no. 12: eads6312. https://doi.org/10.1126/sciadv.ads6312.

Jayachandran, D., P. Smith, M. Irfan, et al. 2023. "Engineering and Characterization of Carbohydrate-Binding Modules for Imaging Cellulose Fibrils Biosynthesis in Plant Protoplasts." *Biotechnology and Bioengineering* 120, no. 8: 2253–2268. https://doi.org/10.1002/bit.28484.

Jeong, Y. Y., H. Y. Lee, S. W. Kim, Y. S. Noh, and P. J. Seo. 2021. "Optimization of Protoplast Regeneration in the Model Plant *Arabidopsis thaliana*." *Plant Methods* 17, no. 1: 21. https://doi.org/10.1186/s13007-021-00720-x.

Jiang, F., J. Zhu, and H.-L. Liu. 2013. "Protoplasts: A Useful Research System for Plant Cell Biology, Especially Dedifferentiation." *Protoplasma* 250, no. 6: 1231–1238. https://doi.org/10.1007/s00709-013-0513-z.

Krasteva, G., V. Georgiev, and A. Pavlov. 2021. "Recent Applications of Plant Cell Culture Technology in Cosmetics and Foods." *Engineering in Life Sciences* 21, no. 3–4: 68–76. https://doi.org/10.1002/elsc.202000078.

Kuki, H., T. Higaki, R. Yokoyama, et al. 2017. "Quantitative Confocal Imaging Method for Analyzing Cellulose Dynamics During Cell Wall Regeneration in *Arabidopsis* Mesophyll Protoplasts." *Plant Direct* 1, no. 6: e00021. https://doi.org/10.1002/pld3.21.

Kuki, H., R. Yokoyama, T. Kuroha, and K. Nishitani. 2020. "Xyloglucan Is Not Essential for the Formation and Integrity of the Cellulose Network in the Primary Cell Wall Regenerated From Arabidopsis Protoplasts." *Plants* 9, no. 5: 629. https://doi.org/10.3390/plants9050629.

Kumari, I. 2019. "A Simple Procedure for Isolation, Culture of Protoplast and Plant Regeneration." In *In Vitro Plant Breeding Towards Novel Agronomic Traits*, edited by M. Kumar et al., 263–273. Springer Singapore. https://doi.org/10.1007/978-981-32-9824-8_14.

Laforest, L. C., and S. S. Nadakuduti. 2022. "Advances in Delivery Mechanisms of CRISPR Gene-Editing Reagents in Plants." *Frontiers in Genome Editing* 4: 830178. https://doi.org/10.3389/fgeed.2022.830178.

Legland, D., I. Arganda-Carreras, and P. Andrey. 2016. "MorphoLibJ: Integrated Library and Plugins for Mathematical Morphology With ImageJ." *Bioinformatics* 32, no. 22: 3532–3534. https://doi.org/10.1093/bioinformatics/btw413.

Leszczuk, A., P. Kalaitzis, J. Kulik, and A. Zdunek. 2023. "Review: Structure and Modifications of Arabinogalactan Proteins (AGPs)." *BMC Plant Biology* 23, no. 1: 45. https://doi.org/10.1186/s12870-023-04066-5.

Masson, J., and J. Paszkowski. 1992. "The Culture Response of *Arabidopsis thaliana* Protoplasts Is Determined by the Growth Conditions of Donor Plants." *Plant Journal* 2, no. 5: 829–833. https://doi.org/10.1111/j.1365-313X.1992.tb00153.x.

Matsuo, S., A. Takenaga, T. Seyama, and T. Kondo. 2014. "Secretion of a Bundle of (1→3)-β-Glucan Hollow Fibrils From Protoplasts of Callus Suspension Under a Ca2+−Rich and Acidic Stressed Condition." *Holzforschung* 68, no. 1: 69–73. https://doi.org/10.1515/hf-2013-0010.

McKenna, J. F., A. F. Tolmie, and J. Runions. 2014. "Across the Great Divide: The Plant Cell Surface Continuum." *Current Opinion in Plant Biology* 22: 132–140. https://doi.org/10.1016/j.pbi.2014.11.004.

Ménard, D., H. Serk, R. Decou, and E. Pesquet. 2017. "Establishment and Utilization of Habituated Cell Suspension Cultures for Hormone-Inducible Xylogenesis." In *Xylem: Methods and Protocols*, edited by M. de Lucas and J. P. Etchhells, 37–57. Springer. https://doi.org/10.1007/978-1-4939-6722-3_4.

Ménard, D., H. Serk, R. Decou, and E. Pesquet. 2024. "Inducible Pluripotent Suspension Cell Cultures (iPSCs) to Study Plant Cell Differentiation." In *Xylem: Methods and Protocols*, edited by J. Agusti, 171–200. Springer US. https://doi.org/10.1007/978-1-0716-3477-6_13.

Menges, M., and J. A. H. Murray. 2002. "Synchronous Arabidopsis Suspension Cultures for Analysis of Cell-Cycle Gene Activity." *Plant Journal* 30, no. 2: 203–212. https://doi.org/10.1046/j.1365-313X.2002.01274.x.

Mukundan, N. S., K. Satyamoorthy, and V. S. Babu. 2025. "Advancing Plant Protoplasts: Innovative Techniques and Future Prospects." *Plant Biotechnology Reports* [Preprint]. https://doi.org/10.1007/s11816-025-00957-1.

Nagata, T., and I. Takebe. 1970. "Cell Wall Regeneration and Cell Division in Isolated Tobacco Mesophyll Protoplasts." *Planta* 92, no. 4: 301–308.

Nolan, R., L. Alvarez, S. Padilla-Parra, and G. Landini. 2023. 'autothresholdr: An R Port of the "ImageJ" Plugin "Auto Threshold"'. https://cran.r-project.org/web/packages/autothresholdr/index.html (Accessed: 19 February 2025).

Oda, Y., S. Asatsuma, H. Nakasone, and K. Matsuoka. 2020. "Sucrose Starvation Induces the Degradation of Proteins in Trans-Golgi Network and Secretory Vesicle Cluster in Tobacco BY-2 Cells." *Bioscience, Biotechnology, and Biochemistry* 84, no. 8: 1652–1666. https://doi.org/10.1080/09168451.2020.1756736.

Ooms, J. 2024. 'magick: Advanced Graphics and Image-Processing in R'. Accessed: 19 February 2025 https://cran.r-project.org/web/packages/magick/index.html.

Paredez, A. R., C. R. Somerville, and D. W. Ehrhardt. 2006. "Visualization of Cellulose Synthase Demonstrates Functional Association With Microtubules." *Science* 312, no. 5779: 1491–1495. https://doi.org/10.1126/science.1126551.

Park, Y. B., and D. J. Cosgrove. 2012. "A Revised Architecture of Primary Cell Walls Based on Biomechanical Changes Induced by Substrate-Specific Endoglucanases." *Plant Physiology* 158, no. 4: 1933–1943. https://doi.org/10.1104/pp.111.192880.

Pasternak, T., K. Lystvan, A. Betekhtin, and R. Hasterok. 2020. "From Single Cell to Plants: Mesophyll Protoplasts as a Versatile System for Investigating Plant Cell Reprogramming." *International Journal of Molecular Sciences* 21, no. 12: 4195. https://doi.org/10.3390/ijms21124195.

Pasternak, T., I. A. Paponov, and S. Kondratenko. 2021. "Optimizing Protocols for *Arabidopsis* Shoot and Root Protoplast Cultivation." *Plants* 10, no. 2: 375. https://doi.org/10.3390/plants10020375.

Peng, L., X. Gao, L. Wang, et al. 2022. "Design of Experiment Techniques for the Optimization of Chromatographic Analysis Conditions: A Review." *Electrophoresis* 43, no. 18–19: 1882–1898. https://doi.org/10.1002/elps.202200072.

Pesquet, E., A. V. Korolev, G. Calder, and C. W. Lloyd. 2010. "The Microtubule-Associated Protein AtMAP70-5 Regulates Secondary Wall Patterning in *Arabidopsis* Wood Cells." *Current Biology* 20, no. 8: 744–749. https://doi.org/10.1016/j.cub.2010.02.057.

Pesquet, E., A. Wagner, and J. H. Grabber. 2019. "Cell Culture Systems: Invaluable Tools to Investigate Lignin Formation and Cell Wall Properties." *Current Opinion in Biotechnology* 56: 215–222. https://doi.org/10.1016/j.copbio.2019.02.001.

Purushotham, P., R. Ho, and J. Zimmer. 2020. "Architecture of a Catalytically Active Homotrimeric Plant Cellulose Synthase Complex." *Science* 369, no. 6507: 1089–1094. https://doi.org/10.1126/science.abb2978.

Reed, K. M., and B. O. R. Bargmann. 2021. "Protoplast Regeneration and Its Use in New Plant Breeding Technologies." *Frontiers in Genome Editing* 3: 734951. https://doi.org/10.3389/fgeed.2021.734951.

Reyna-Llorens, I., M. Ferro-Costa, and S. J. Burgess. 2023. "Plant Protoplasts in the Age of Synthetic Biology." *Journal of Experimental Botany* 74, no. 13: 3821–3832. https://doi.org/10.1093/jxb/erad172.

Sakai, K., F. Charlot, T. le Saux, et al. 2019. "Design of a Comprehensive Microfluidic and Microscopic Toolbox for the Ultra-Wide Spatio-Temporal Study of Plant Protoplasts Development and Physiology." *Plant Methods* 15, no. 1: 79. https://doi.org/10.1186/s13007-019-0459-z.

Sakamoto, Y., A. Kawamura, T. Suzuki, et al. 2022. "Transcriptional Activation of Auxin Biosynthesis Drives Developmental Reprogramming of Differentiated Cells." *Plant Cell* 34, no. 11: 4348–4365. https://doi.org/10.1093/plcell/koac218.

Sapala, A., A. Runions, A. L. Routier-Kierzkowska, et al. 2018. "Why Plants Make Puzzle Cells, and How Their Shape Emerges." *eLife* 7: e32794. https://doi.org/10.7554/eLife.32794.

Sasamoto, H., S. Ogita, N. Hayashi, Y. Wakita, S. Yokota, and N. Yoshizawa. 2003. "Development of Novel Elongated Fiber-Structure in Protoplast Cultures of *Betula platyphylia* and *Larix leptolepis*." *In Vitro*

Cellular and Developmental Biology - Plant 39, no. 2: 223–228. https://doi.org/10.1079/IVP2002388.

Schindelin, J., I. Arganda-Carreras, E. Frise, et al. 2012. "Fiji: An Open-Source Platform for Biological-Image Analysis." *Nature Methods* 9, no. 7: 676–682. https://doi.org/10.1038/nmeth.2019.

Schirawski, J., S. Planchais, and A.-L. Haenni. 2000. "An Improved Protocol for the Preparation of Protoplasts From an Established *Arabidopsis thaliana* Cell Suspension Culture and Infection With RNA of Turnip Yellow Mosaic Tymovirus: A Simple and Reliable Method." *Journal of Virological Methods* 86, no. 1: 85–94. https://doi.org/10.1016/S0166-0934(99)00173-1.

Seyama, T., and T. Kondo. 2012. "Morphological Responses of *Betula* Protoplasts in Fiber Spinning." *Holzforschung* 66, no. 3: 407–411. https://doi.org/10.1515/hf.2011.158.

Stringer, C., and M. Pachitariu. 2025. "Cellpose3: One-Click Image Restoration for Improved Cellular Segmentation." *Nature Methods* 22: 592–599. https://doi.org/10.1038/s41592-025-02595-5.

Suda, J., P. Kron, B. C. Husband, and P. Trávníček. 2007. "Flow Cytometry and Ploidy: Applications in Plant Systematics, Ecology and Evolutionary Biology." In *Flow Cytometry With Plant Cells*, 103–130. John Wiley & Sons, Ltd. https://doi.org/10.1002/9783527610921.ch5.

Tagawa, S., and T. Kondo. 2018. "Secretion of a Callose Hollow Fiber From Herbaceous Plant Protoplasts Induced by Inhibition of Cell Wall Formation." *Journal of Wood Science* 64, no. 5: 467–476. https://doi.org/10.1007/s10086-018-1726-8.

Tagawa, S., Y. Yamagishi, U. Watanabe, R. Funada, and T. Kondo. 2019. "Dynamics of Structural Polysaccharides Deposition on the Plasma-Membrane Surface of Plant Protoplasts During Cell Wall Regeneration." *Journal of Wood Science* 65, no. 1: 47. https://doi.org/10.1186/s10086-019-1826-0.

Tan, L., S. Eberhard, S. Pattathil, et al. 2013. "An Arabidopsis Cell Wall Proteoglycan Consists of Pectin and Arabinoxylan Covalently Linked to an Arabinogalactan Protein[W]." *Plant Cell* 25, no. 1: 270–287. https://doi.org/10.1105/tpc.112.107334.

Van Leene, J., D. Eeckhout, G. Persiau, et al. 2011. "Isolation of Transcription Factor Complexes From Arabidopsis Cell Suspension Cultures by Tandem Affinity Purification." In *Plant Transcription Factors: Methods and Protocols*, edited by L. Yuan and S. E. Perry, 195–218. Humana Press. https://doi.org/10.1007/978-1-61779-154-3_11.

Verma, A., M. Verma, and A. Singh. 2020. "Chapter 14 – Animal Tissue Culture Principles and Applications." In *Animal Biotechnology*, edited by A. S. Verma and A. Singh, Second ed., 269–293. Academic Press. https://doi.org/10.1016/B978-0-12-811710-1.00012-4.

Wickham, H., M. Averick, J. Bryan, et al. 2019. "Welcome to the Tidyverse." *Journal of Open Source Software* 4, no. 43: 1686. https://doi.org/10.21105/joss.01686.

Wu, F.-H., S. C. Shen, L. Y. Lee, S. H. Lee, M. T. Chan, and C. S. Lin. 2009. "Tape-Arabidopsis Sandwich - A Simpler Arabidopsis Protoplast Isolation Method." *Plant Methods* 5, no. 1: 16. https://doi.org/10.1186/1746-4811-5-16.

Xu, Y., R. Li, H. Luo, et al. 2022. "Protoplasts: Small Cells With Big Roles in Plant Biology." *Trends in Plant Science* 27, no. 8: 828–829. https://doi.org/10.1016/j.tplants.2022.03.010.

Yokoyama, R., H. Kuki, T. Kuroha, and K. Nishitani. 2016. "Arabidopsis Regenerating Protoplast: A Powerful Model System for Combining the Proteomics of Cell Wall Proteins and the Visualization of Cell Wall Dynamics." *Proteomes* 4, no. 4: 34. https://doi.org/10.3390/proteomes4040034.

Yokoyama, R., N. Shinohara, R. Asaoka, H. Narukawa, and K. Nishitani. 2014. "The Biosynthesis and Function of Polysaccharide Components of the Plant Cell Wall." In *Plant Cell Wall Patterning and Cell Shape*, 1–34. John Wiley & Sons, Ltd. https://doi.org/10.1002/9781118647363.ch1.

Yoo, S.-D., Y.-H. Cho, and J. Sheen. 2007. "Arabidopsis Mesophyll Protoplasts: A Versatile Cell System for Transient Gene Expression Analysis." *Nature Protocols* 2, no. 7: 1565–1572. https://doi.org/10.1038/nprot.2007.199.

Yue, J.-J., J. L. Yuan, F. H. Wu, et al. 2021. "Protoplasts: From Isolation to CRISPR/Cas Genome Editing Application." *Frontiers in Genome Editing* 3: 717017. https://doi.org/10.3389/fgeed.2021.717017.

Zhai, Z., H. Jung, and O. K. Vatamaniuk. 2009. "Isolation of Protoplasts From Tissues of 14-Day-Old Seedlings of *Arabidopsis thaliana*." *Journal of Visualized Experiments : JoVE* 30: 1149. https://doi.org/10.3791/1149.

Zhang, S., T. Zhang, S. Wang, Z. Han, X. Duan, and J. Wang. 2024. "Phenotyping of Single Plant Cells on a Microfluidic Cytometry Platform With Fluorescent, Mechanical, and Electrical Modules." *Analyst* 149, no. 17: 4436–4442. https://doi.org/10.1039/d4an00682h.

Supporting Information

Additional supporting information can be found online in the Supporting Information section.

Acta Universitatis Agriculturae Sueciae

Doctoral Thesis No. 2025:75

Cell adhesion is fundamental for plant growth and development. Yet, the molecular actors involved in cell-cell adhesion or plasma membrane to cell wall adhesion are not well defined due to the lack of tools existing to quantify these interactions. This thesis work aims to reduce this knowledge gap by developing methodologies to quantify and characterize plant cell adhesion.

Léa Bogdziewiez received her graduate education at the Department of Forest Genetics and Plant Physiology, Swedish University of Agricultural Sciences, Sweden. She completed her Master in Immunology and Inflammation at Strasbourg University, France.

Acta Universitatis Agriculturae Suecicae presents doctoral theses from the Swedish University of Agricultural Sciences (SLU).

SLU generates knowledge for the sustainable use of biological natural resources. Research, education, extension, as well as environmental monitoring and assessment are used to achieve this goal.

ISSN 1652-6880
ISBN (print version) 978-91-8124-059-7
ISBN (electronic version) 978-91-8124-105-1